

TABLE OF CONTENTS

	Page
INTRODUCTION	1
CHAPTER 1 LITERATURE REVIEW	3
1.1 Floods and future trends.....	3
1.2 Hydrological modelling	4
1.2.1 Calibration and validation process.....	5
1.3 Global and regional climate modelling.....	7
1.3.1 Climate projections: general trends	11
1.3.2 Sources of uncertainty.....	13
1.4 Regional studies: Quebec.....	14
1.5 Research objectives.....	16
CHAPTER 2 STUDY AREA AND DATA.....	17
2.1 Study area.....	17
2.2 Observed data.....	18
2.3 Climate simulation data	19
2.3.1 Regional climate model (RCM).....	20
CHAPTER 3 METHODS	21
3.1 Overview.....	21
3.2 Climate data comparison.....	22
3.3 Hydrological modelling	24
3.3.1 Hydrological models.....	25
3.3.2 Calibration and validation.....	25
3.3.3 Streamflow simulations	26
3.3.3.1 Return Periods.....	28
CHAPTER 4 RESULTS	29
4.1 Climate simulations intercomparison	29
4.1.1 Spatial resolution	29
4.1.1.1 Temperature	29
4.1.1.2 Precipitation	34
4.2 Hydrological modelling performance	38
4.2.1 HSAMI and MOHYSE calibration and validation results.....	38
4.2.1.1 Spatial distribution of hydrological modelling performance	40
4.2.1.2 Hydrological model parameter sets	43
4.3 Climate model driven streamflow simulations	45
4.3.1 Spatial resolutions.....	45
4.3.2 Hydrological model parameter sets	48
CHAPTER 5 DISCUSSION	51
5.1 Impact of spatial resolution climate outputs	51

5.2	Climate model-driven hydrological streamflow simulations.....	54
5.2.1	Generation of the climate model-driven hydrological streamflows	54
5.2.2	Spatial resolution effects on climate model-driven hydrological streamflows	55
5.2.3	Flood indicators	56
5.3	Hydrological models structure and parameters impacts	56
5.4	Regional climate model configuration.....	57
5.5	Streamflow simulations and catchment size	60
5.6	Limitations	62
	CONCLUSION.....	65
	RECOMMENDATIONS.....	69
APPENDIX I	REGIONAL CLIMATE MODEL DOMAINS	71
APPENDIX II	CLIMATE SIMULATIONS INTERCOMPARISON: DRIVERS	73
APPENDIX III	STREAMFLOW SIMULATIONS AND CATCHMENT SIZE	75
	LIST OF BIBLIOGRAPHICAL REFERENCES.....	83

LIST OF TABLES

		Page
Table 1.1	Trends for the 2050 horizon for southern Quebec.....	15
Table 2.1	Description of the CRCM climate datasets used in this study.....	19
Table 3.1	Summary of CRCM4 and CRCM5 climate datasets comparisons.....	22
Table 3.2	Summary of the objective functions for the hydrological model's calibration.....	26

LIST OF FIGURES

		Page
Figure 1.1	Hydrological modelling calibration process	6
Figure 1.2	Mean summer maximum temperature for the reference period 1970–1999 from observations (E-OBS v5.0 0.5°(Haylock et al., 2008)) and a range of AOGCMs in the CMIP3 database. Taken from Hawkins et al. (2013, p. 20).....	9
Figure 1.3	Regional climate model configuration.....	10
Figure 1.4	Cascade of uncertainty	14
Figure 2.1	Location and mean annual precipitation (mm) of the 50 watersheds used in this study.....	17
Figure 3.1	Overview of this project’s research methodology	21
Figure 4.1	Annual daily mean temperature (°C) bias between simulations issued from CRCM4 for the summer (JJA) and fall (SON) seasons for the period 1961-1990.The upper panels (a) show the comparisons for the datasets driven by CGCM. The lower panels (b) show the comparisons for the datasets driven by ERA40c	30
Figure 4.2	Annual daily mean bias of temperature (°C) between simulations issued from CRCM5 for the summer (JJA) and fall (SON) seasons for the period 1981-2010.The upper panels (a) show the comparisons for the datasets with 12 km and 24 km resolution. The lower panels (b) show the comparisons for the datasets with 12 km and 48 km resolution.....	31
Figure 4.3	Ratio of annual seasonal mean temperature variances between simulations issued from CRCM4 for the summer (JJA) and fall (SON) seasons for the period 1961-1990.The upper panels (a) show the comparisons for the datasets driven by CGCM. The lower panels (b) show the comparisons for the datasets driven by ERA40c	32
Figure 4.4	Ratio of annual seasonal mean temperature variances between simulations issued from CRCM5 for the summer (JJA) and fall (SON) seasons for the period 1981-2010. The upper panels (a) show the comparisons for the datasets with 12 km and 24 km resolution. The lower panels (b) show the comparisons for the datasets with 12 km and 48 km resolution.....	33

Figure 4.5 Annual daily mean relative precipitation biases (%) between simulations issued from CRCM4 for the summer (JJA) and fall (SON) seasons for the period 1961-1990. The upper panels (a) show the comparisons for the datasets driven by CGCM. The lower panels (b) show the comparisons for the datasets driven by ERA40c34

Figure 4.6 Annual daily mean relative biases (%) of precipitation between simulations issued from CRCM5 for the summer (JJA) and fall (SON) seasons for the period 1981-2010. The upper panels (a) show the comparisons for the datasets with 12 km and 24 km resolution. The lower panels (b) show the comparisons for the datasets with 12 km and 48 km resolution.....35

Figure 4.7 Ratio of annual seasonal mean temperature variances between simulations issued from CRCM4 for the summer (JJA) and fall (SON) seasons for the period 1961-1990. The upper panels (a) show the comparisons for the datasets driven by CGCM. The lower panels (b) show the comparisons for the datasets driven by ERA40c36

Figure 4.8 Ratio of annual seasonal mean temperature variances between simulations issued from CRCM5 for the summer (JJA) and fall (SON) seasons for the period 1981-2010. The upper panels (a) show the comparisons for the datasets with 12 km and 24 km resolution. The lower panels (b) show the comparisons for the datasets with 12 km and 48 km resolution.....37

Figure 4.9 KGE values on the calibration and validation years. Panel a) presents the objective function-1, b) the objective function-2 and c) presents the objective function-3. KGE values for all the year (left panel) and June to October (right panel) are shown for both models and each objective function.....39

Figure 4.10 Map of the KGE values on the validation years with the OF-1 over the fifty watersheds. The upper panels (a) present the performances over the full time series and the lower panels (b) present the performances during summer-fall months (June-October).....40

Figure 4.11 Map of the KGE values on the validation years with the OF-2 over the fifty watersheds. The upper panels (a) present the performances over the full time series and the lower panels (b) present the performances during summer-fall months (June-October).....41

Figure 4.12 Map of the KGE values on the validation years with the OF-2 over the fifty watersheds. The upper panels (a) present the performances over the full time series and the lower panels (b) present the performances during summer-fall months (June-October).....42

Figure 4.13	KGE values of the 50 watersheds for the different calibration approaches on the calibration years. The upper panels (a) present the KGE values for the full-time series and the lower panels (b) present the values for the summer-fall months.....	43
Figure 4.14	KGE values of the 50 watersheds for the different calibration approaches on the validation years. The upper panels (a) present the KGE values for the full-time series and the lower panels (b) present the values for the summer-fall months.....	44
Figure 4.15	Seasonal KGE values of the comparisons between streamflows generated with climate outputs at different resolutions. The upper panels (a) present the results obtained with OF-1, the middle panels (b) present the results obtained with OF-2 and the lower panels (c) present the results obtained with OF-3	45
Figure 4.16	Seasonal relative bias values of the comparisons between streamflows generated with climate outputs at different resolutions. The upper panels (a) present the results obtained with OF-1, the middle panels (b) present the results obtained with OF-2 and the lower panels (c) present the results obtained with OF-3.....	46
Figure 4.17	Relative biases (%) between the return periods (2, 5, 10 and 20-year) of the different generated streamflows. The upper panels (a) present the results obtained with OF-1, the middle panels (b) present the results obtained with OF-2 and the lower panels (c) present the results obtained with OF-3.....	47
Figure 4.18	KGE values between generated streamflows with different calibration approaches. The upper panels (a) present the results obtained on the full-time series evaluations and the lower panels (b) present the results obtained on the summer-fall months.....	48
Figure 4.19	Relative biases (%) between generated streamflows with different calibration approaches. The upper panels (a) present the results obtained on the full-time series evaluations and the lower panels (b) present the results obtained on the summer-fall months.....	49
Figure 4.20	Relative biases (%) between return periods of the generated streamflows with different calibration approaches. The first panels (a) present the comparisons of 2-year return periods, the second panels (b) the comparisons of 5-year return periods, the third panels (c) the comparisons of 10-year return periods and the fourth panels (d) the comparisons of the 20-year return periods	50

Figure 5.1 Annual daily mean bias of temperature (°C) between simulations issued from CRCM4 for the summer (JJA) and fall (SON) seasons for the period 1981-2010. The upper panels (a) show the comparisons for the 15 km resolution datasets with different drivers. The lower panels (b) show the driver comparison for the 45km resolution datasets.....58

Figure 5.2 Annual daily mean relative biases (%) of precipitation (mm) between simulations issued from CRCM4 for the summer (JJA) and fall (SON) seasons for the period 1961-1990. The upper panels (a) show the comparisons for the 15km resolution datasets. The lower panels (b) show the comparison for the 45km resolution datasets.....59

Figure 5.3 Relative biases (%) between the return periods (2, 5, 10 and 20-year) of the generated streamflows with CRCM5 outputs at different resolutions grouped by small (s) and large (L) watersheds for the OF-2. The first panels (a) present the comparisons of 2-year return periods, the second panels (b) the comparisons of 5-year return periods, the third panels (c) the comparisons of 10-year return periods and the fourth panels (d) the comparisons of the 20-year return periods61

LIST OF ABBREVIATIONS

AOGCMs	Atmosphere-Ocean General Circulation Models
AR5	Fifth Assessment Report of the Intergovernmental Panel on Climate Change
BDH	Banque de Données Hydriques
CEHQ	Centre d'Expertise Hydrique du Québec
CGCM	Canadian General Circulation Model
CMAES	Covariance Matrix Adaptation Evolution Strategy
CMIP	Coordinated Modelling Intercomparison Project
CORDEX	Coordinated Regional Downscaling Experiment
CRCM	Canadian Regional Climate Model
CV	Coefficient of Variation
DJF	December January February
ED	Euclidean Distance
ERA-40c	European Retrospective Analysis 40 years
ERA-Interim	European Retrospective Analysis Interim
ESMs	Earth System Models
GCMs	General Circulation Models
HSAMI	A lumped conceptual rainfall-runoff model developed by Hydro-Québec
IPPC SREX	IPCC Special Report on Managing the Risks of Extreme Events and Disasters to Advance Climate Change Adaptation
JJA	June July August
KGE	Kling Gupta Efficiency
LAMs	Limited Area Models

MDDELCC	Ministère du Développement Durable, de l'Environnement et de la Lutte contre les Changements Climatiques
MAM	March April May
MOHYSE	MOdèle HYdrologique Simplifié à l'Extrême
NA	North American domain
OF	Objective Function
QC	Quebec domain
RCMs	Regional Climate Models
RCP	Representative Concentration Pathways
SON	September October November
WDR	World Disasters Report

INTRODUCTION

Earth's atmosphere has been going through changes without precedents in human records. During the last thirty years, the global mean surface temperature has consecutively been warmer decade after decade (IPCC, 2013b; McGuffie & Henderson-Sellers, 2001). These observed alterations in the climate system and their potential impacts on different aspects of our society emphasized the need to comprehend and evaluate these changes now in order to prepare actions for the future.

The Fifth Assessment Report (AR5) of the Intergovernmental Panel on Climate Change has emphasized the importance of further research on the potential impacts of changes on extreme climate events due to its possible higher impact on society and ecosystems compared to changes in mean climate (Hartmann et al., 2013; IPCC, 2013c). The impact of climate change has been perceived in processes within the hydrological cycle, different studies implied that changes in climate might have been already affecting hydrological events by modifying the intensity and distribution of precipitation as well as the surface and underground runoff (Bates et al., 2008; IPCC, 2012; Kron & Berz, 2007).

Flooding is a constant problem that causes large social, economic and environmental losses around the world. The World Disasters Report (WDR, 2016) pointed out that floods cause more losses than the combination of all other natural hazards. Changes in hydrological regimes can also have impacts on the management of water resources such as hydro-based electricity production. Quebec, province of Canada, possesses significant water resources and they are of great importance as ninety six percent of the province's electricity consumption is obtained by hydroelectric power stations (CEHQ, 2015; Clavet-Gaumont et al., 2013). As a result of these great potential impacts, the number of studies evaluating the potential effect of climate change on extreme hydrological events has increased dramatically. Hydrological modelling and streamflow forecasting thus play an important role in the global and regional economy and in many aspects of social development (Grey & Sadoff, 2007).

The climate change impacts on hydrology are usually evaluated using the climate model outputs as inputs for the hydrological models. Lately, numerous General Circulation Models (GCMs) have been developed and downscaled with higher-resolution Regional Climate Models (RCMs) that can improve the process representation of climate variables such as precipitation (Teutschbein & Seibert, 2010). Therefore, researchers have thrived to improve climate model's spatial resolution as it is thought that the finer scales will allow for a better representation of the hydrological processes for studies at the catchment scale.

The increase in spatial resolution also increases the climate model and hydrological model simulation times, which raises the need to evaluate how increasing resolution in climate modelling, impacts the hydrological streamflow simulations. In other words, it is necessary to analyse what are the effects of the higher climate model resolution on the simulation of hydrological extremes such as floods. Thus, to address this issue, this study aims to analyse the spatial resolution impact of the Canadian Regional Climate Model (CRCM) spatial resolution on the hydrological modelling of rainfall-driven floods in southern Quebec.

CHAPTER 1

LITERATURE REVIEW

1.1 Floods and future trends

Floods are defined by the Special Report on “Managing the Risks of Extreme Events and Disasters to Advance Climate Change Adaptation” of the Intergovernmental Panel on Climate Change (IPCC SREX) as: “*the overflowing of the normal confines of a stream or other body of water or the accumulation of water over areas that are not normally submerged. Floods include river (fluvial) floods, flash floods, urban floods, pluvial floods, sewer floods, coastal floods, and glacial lake outburst floods*” (IPCC, 2012; Kundzewicz et al., 2013). Climatic and non-climatic factors can influence a flood occurrence, for instance processes such as heavy precipitation, long-lasting precipitation, snowmelt, land use changes or a dam failure, making the assessment of flood causes a complex and difficult task (Bates et al., 2008; Field, 2012).

The change in climate due to global warming is evident, and there is great certainty that will continue to affect the hydrological cycle (Arsenault et al., 2013; J. Hansen et al., 2016; IPCC, 2013b; Mareuil et al., 2007; Troin et al., 2016). The observed global warming has been related with numerous elements of the hydrological systems such as changes in precipitation intensity and extremes, alteration on the melting of snow and ice, increases in water vapour, evaporation and runoff variations (Bates et al., 2008; Coppola et al., 2016; Vormoor et al., 2016; Wehner et al., 2017)

The hydrologic system has not only been affected in mean conditions but also in the occurrence of extreme events such as floods bringing potential consequences to vulnerable regions (Riboust & Brissette, 2015). Therefore, it has become essential to assess the impacts of climate change on the hydrologic cycle and any modification to the risks related to flood events.

Efforts have been made recently to examine the impacts of climate change on flood intensity and occurrence at different regional scales around the world. For example, Dankers and Feyen (2008) and Lehner et al. (2006) carried out continental scale studies over Europe. Smaller scale studies have also been explored with national flood analyses such as the study by Veijalainen et al. (2010) over Finland. However, the projected flood trends at those scales were unclear, underlining the need for a more coherent assessment at local scales (Hall et al., 2014). Thus, studies at catchment scale have considerably increased in numbers over the last years (Chen et al., 2011; Graham et al., 2007; Kundzewicz et al., 2014; Minville et al., 2008; Riboust & Brissette, 2015). These case studies usually estimate climate change impacts by feeding GCM or RCM climate projections with hydrological models to produce estimates of future streamflow and analysing the uncertainties involved. However, due to the limited amount of evidence and considerable uncertainties involved, there is still low confidence in projections of future changes on flood magnitude and frequency (Kundzewicz et al., 2014).

Floods vary in space and time, complicating their detection and attribution (Wehner et al., 2017). For this reason, higher spatial resolution of forcing data is expected to increase the coherency in the assessment of these phenomena. This highlights the importance to further research on the effects of increasing spatial resolutions of climate simulations on the hydrological modelling of floods.

1.2 Hydrological modelling

Currently there is an abundant variety of hydrological models, which are based on approximations of the hydrological system processes and provide an estimate of the streamflow within a watershed (Beven, 2011; Singh & Woolhiser, 2002). The different ways of simplifying systems have shaped different types of models. There are mainly two types, deterministic models and stochastic models (Te Chow, 1988).

The deterministic model is characterized because it does not consider randomness, so a given simulation always produces the same results. Deterministic models use parameters in order to represent hydrological processes. These hydrological models are also called conceptual when non-physically based elements are included (Singh & Woolhiser, 2002). At the same time, within the deterministic models, there are the lumped models and spatially distributed models. Lumped models consider mean values throughout the catchment treating it as a single unit while distributed model consider the spatial variability of the variables (Beven, 2011; Pechlivanidis et al., 2011). The stochastic model, unlike the deterministic, considers partial randomness, that is, it produces predictions. In some cases, the randomness of hydrological processes in a model is high, so it is considered completely random, in which case the model is called probabilistic (Beven, 2011; Te Chow, 1988). For the scope of this project, two deterministic lumped conceptual models were selected.

1.2.1 Calibration and validation process

As mentioned previously, models use parameters to describe some processes of the hydrological cycle. The model calibration process consists of the selection of the most suitable parameter values to best represent the behaviour of the catchment (Moore & Doherty, 2005; Pechlivanidis et al., 2011). Optimization algorithms are used to adjust the parameter sets so that the hydrological model outputs better fit the historical observations of the basin. The simulated and observed datasets are compared through the use of an objective function, a metric that allows evaluating the model performance in regards to the observations, which is then validated using a non-calibrated period of the catchment (Duan et al., 1994; Moriasi et al., 2007). The schematic representation of the hydrological modelling calibration process is presented in Figure 1.1.

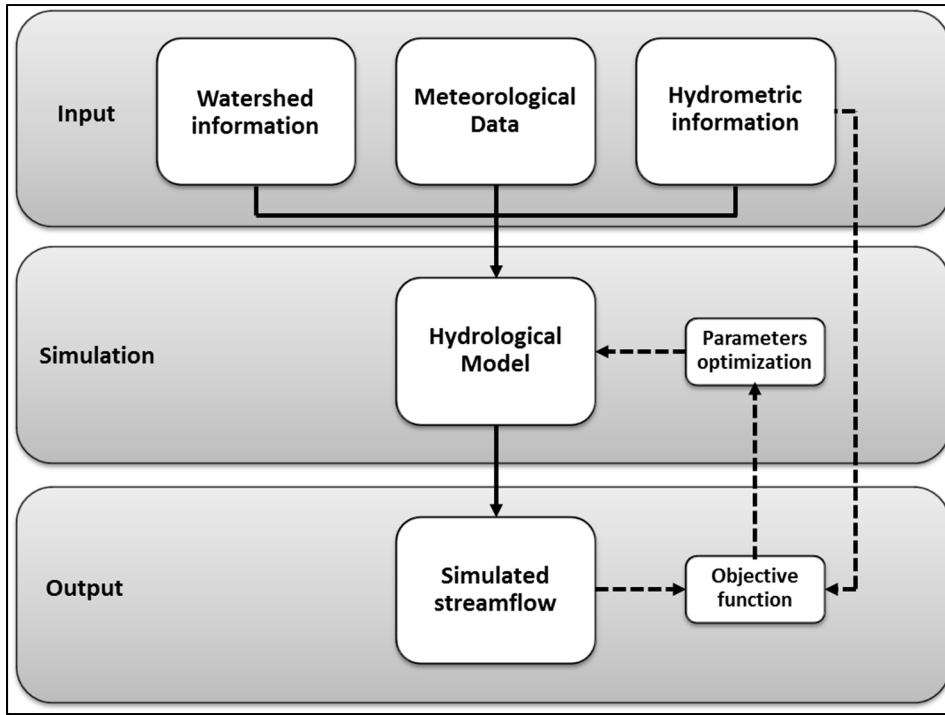


Figure 1.1 Hydrological modelling calibration process

One of the most commonly used objective functions in hydrological model calibration is the Nash-Sutcliffe efficiency metric (Nash & Sutcliffe, 1970), which is a quadratic error type function. More recently, Gupta et al. (2009) proposed a derivative of the Nash-Sutcliffe efficiency metric, the Kling-Gupta Efficiency criteria (KGE), in which components of bias, variance and correlation are distinct. The KGE was later modified by Kling et al. (2012), as shown in the equations 1.1-1.4. The KGE describes the difference between unity and the Euclidian distance (ED) from the ideal point in a three-dimensional space and is calculated as follows:

$$KGE = 1 - ED \quad (1.1)$$

$$ED = \sqrt{(r - 1)^2 + (\beta - 1)^2 + (\gamma - 1)^2} \quad (1.2)$$

$$\beta = \frac{\mu_s}{\mu_o} \quad (1.3)$$

$$\gamma = \frac{CV_s}{CV_o} = \frac{\sigma_s/\mu_s}{\sigma_o/\mu_o} \quad (1.4)$$

Where r represents the correlation coefficient between observed and simulated streamflows, β represents the bias ratio and γ represents the variability ratio. The μ represents the mean streamflow, CV is the variation coefficient and σ represents the standard deviation of the streamflow. The “o” subscript represents the observed data and the “s” subscript represents the simulated data.

The KGE criterion has been shown to overcome the problems related to the use of functions based on the mean squared error such as the runoff peaks and variability underestimation (Gupta et al., 2009). Along with it, the KGE increasing popularity in the literature (Beck et al., 2016; Huang et al., 2016; Oyerinde et al., 2017; Thirel et al., 2015), warrants its use in this study.

1.3 Global and regional climate modelling

The climate system, as described by Schneider (1992), is mainly composed of five components (1) the atmosphere; (2) the hydrosphere (oceans); (3) the cryosphere (ice and snow); (4) the terrestrial and marine biospheres and (5) the land surface. These components jointly interact defining the climate of the atmosphere through several complex processes. The threats of global warming have encouraged researchers to improve our collective understanding of these interactions by developing climate models.

These complex models consist in mathematical simulations of the climate system performed by algorithms in powerful computers, facilitating our understanding of its processes, and to be able to make estimates of the future climate (Randall et al., 2007; Trenberth, 1992). Climate modelling has become an independent discipline since the first attempt at weather forecasting published by Richardson (1922), who is considered as the father of climate modelling (McGuffie & Henderson-Sellers, 2001).

Climate models differ by their complexity. Nowadays, the most complex models available are the atmosphere-ocean general circulation models (AOGCMs) and the earth system models (ESMs) integrating physical climate, biosphere and chemical processes interactions, to provide the most accurate representations of the climate system (Heavens et al., 2013; IPCC, 2013a). GCM horizontal resolution normally ranges from 150 to 250 km with numerous vertical layers (10 to 20) in the atmosphere and can have up to 30 layers in the oceans, which is considered coarse to the scale needed for regional studies (Solomon et al., 2007; Teutschbein & Seibert, 2010). In more recent years, the scientific community has come together to join efforts and create common projects, such as the Coordinated Modelling Intercomparison Project (CMIP) phase 3 (Meehl et al., 2007) and, the most recent phase, the CMIP5 (Taylor et al., 2011) to collect and compare the developed climate models around the world. The groups participating in the CMIP5 produce simulations with more than 50 GCMs with high-spatial resolutions, such as the MRI-AGCM3-2S model with a 0.188° ($\approx 20\text{km}$) grid resolution (Mizuta et al., 2012) and the MIROC4h model with a 0.5625° ($\approx 60\text{km}$) grid resolution (Sakamoto et al., 2012).

The use of GCM outputs for simulation in hydrological studies is considered inadequate in terms of spatial and temporal resolution for regional hydrological impact studies at the catchment scale (Diaz-Nieto & Wilby, 2005). One of the main reasons is the inaccuracy in the precipitation simulations. The intensity, frequency and distribution of the precipitation data is not well represented by the GCMs mainly due to its coarse resolutions which is inappropriate and insufficient for regional hydrological studies (Hostetler, 1994; Randall et al., 2007; Teutschbein & Seibert, 2010).

The coarse resolution impact can be clearly observed in Figure 1.2, where mean temperature datasets with different spatial resolutions issued from AOGCMs are compared with observed data. It is observed that the selected AOGCMs have different spatial resolutions between them.

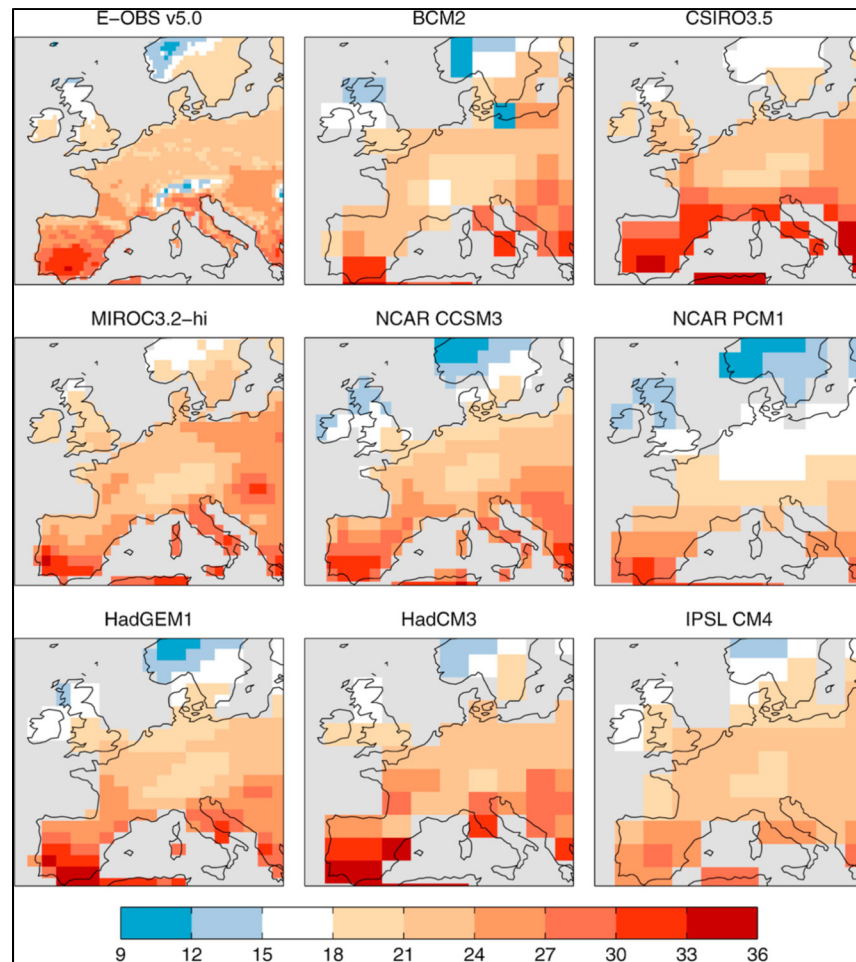


Figure 1.2 Mean summer maximum temperature for the reference period 1970–1999 from observations (E-OBS v5.0 0.5°(Haylock et al., 2008)) and a range of AOGCMs in the CMIP3 database. Taken from Hawkins et al. (2013, p. 20)

However, all of them have larger grid cells than the observed data in the upper left corner which clearly differs in intensity and distribution with the coarser datasets (Hawkins et al., 2013).

In the simulation of the water cycle, finer resolution is particularly necessary mainly because its variables are highly influenced by their spatial distribution (Music & Caya, 2009). Therefore, the demand for higher resolution in climate simulations has increased, so accurate and reliable climate impact and adaptation studies can be performed. Consequently,

downscaling procedures have become essential in order to provide an adequate resolution of climate simulations for hydrological studies at a regional scale (Chen et al., 2011; Prudhomme et al., 2002; Teutschbein & Seibert, 2010). The downscaling methods are the most used approaches in impact studies, mainly because with these techniques, it is possible to overcome differences in spatial and temporal scale between climate and hydrological models, and also to overcome biases present in climate model outputs (Riboust & Brissette, 2015).

Downscaling methods are mainly categorized as statistical or dynamic. Statistical downscaling produces future scenarios using statistical relationships between large-scale climate variables and regional characteristics identified from recent climate records. This process involves various techniques such as multiple regressions, stochastic generators and neural networks, which are used to establish the statistical relationships between observed local conditions and simulated climate variables (Diaz-Nieto & Wilby, 2005; Wilby et al., 1998). More recently, bias correction methods based on model output statistics have been used more and more frequently (Jakob Themeßl et al., 2011).

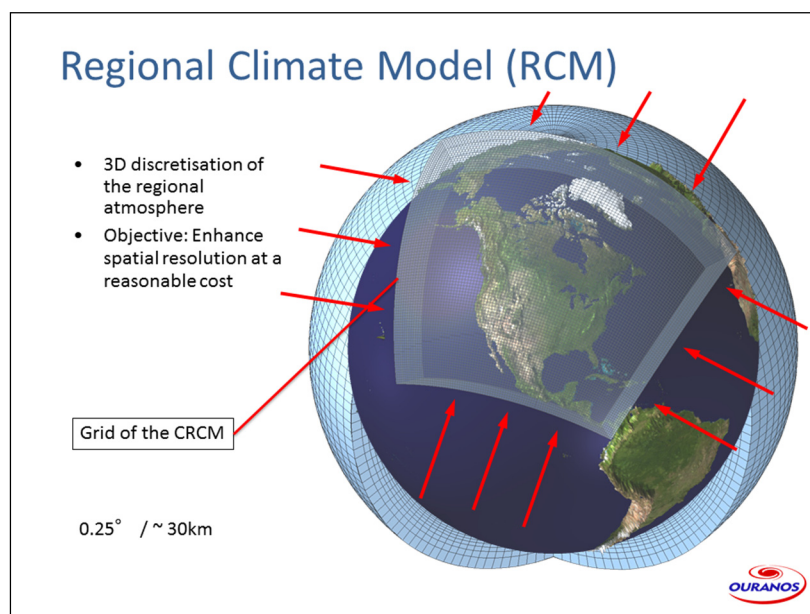


Figure 1.3 Regional climate model configuration
Taken with the permission of Marco Braun (2017) Ouranos

Dynamic downscaling is based on climate models at fine resolution (from 10 km to 50 km) describing the atmospheric processes nested within GCM's outputs. These are commonly named Limited Area Models (LAMs) or Regional Climate Models (RCMs) (R. Jones et al., 1995; Laprise, 2008). These models provide a more physically realistic representation of the regional climate at finer resolutions. RCMs, as shown in Figure 1.3, are provided with data from a driving model at the RCM boundaries of the domain to simulate. The driving model can be a GCM or another fine resolution gridded data product such as reanalysis datasets (Charron, 2014). Reanalysis data is high-resolution data which combines observations and climate simulations to produce recent past simulations that better represent the state of the atmosphere (Bengtsson & Shukla, 1988; Carter et al., 2007).

Consequently, large computational resources are required to perform these simulations. Nonetheless, the need for more accurate regional climate simulations has driven the creation of international initiatives such as the Coordinated Regional Downscaling Experiment (CORDEX) project (Giorgi & Gutowski, 2015). This programme creates a framework to generate an ensemble of regional-local scale climate projections for more adequate impact and adaptation studies (Giorgi et al., 2009). The CORDEX project assembles RCMs used around the world with a variety of domains, drivers and resolutions.

1.3.1 Climate projections: general trends

Due to the worldwide-observed climate change impacts, what will happen in the future is a fundamental issue for the modern society. Thus, climate models are used to simulate plausible scenarios and generate projections of the future (AghaKouchak et al., 2012).

Over the years, scientists have shown more confidence in the fact that the rising trend in the greenhouse gas concentrations will increase the global temperatures, yet there is lower confidence of how the climate will change at a regional scale (Giorgi et al., 2001). It is at the regional scale, such as that of a river catchment, that climate change will be noticed. Therefore, to generate predictions of climate change at these scales, it is necessary to use a

number of plausible future climates referred to as climate scenarios (Carter et al., 2007). The most recent generation of scenarios is the Representative Concentration Pathways (RCP), used for the ensemble of climate models in the CMIP5. Four RCPs were identified by the research community to address the new developments and thus allow climate models to represent the range of the latest climate policies (IPCC, 2013c; Moss et al., 2010). One mitigation scenario (RCP2.6), two stabilization scenarios (RCP4.5 and RCP6) and one scenario with very high greenhouse gas emissions (RCP8.5) are used to attempt to cover the largest range of plausible emissions (IPCC, 2013c). These four scenarios are represented by future radiative forcings (2.6, 4.5, 6 and 8.5), which describes the change on the atmosphere radiation balance (incoming and outgoing) caused by plausible changes in its constituents (Moss et al., 2010).

Climate scenarios are then used to produce climate projections, which attempt to represent the possible evolution of the different components within the climate system influenced by the different RCPs (Charron, 2014; Moss et al., 2010). However, it is important to note that climate scenarios are neither predictions nor forecasts. A climate scenario is only a plausible description of how the future could behave over long time scales, i.e. decades or centuries, according to stated assumptions regarding future trends in greenhouse gases emissions, changes in land use and population growth (IPCC, 2013c). For this reason, it is important to mention that the future remains uncertain, as the different scenarios are constructed on multiple assumptions that may or may not happen in the future.

The warming climate has affected the water cycle in different ways. The AR5 assembled observed evidence of these impacts. Observations with different measurement devices (i.e. stations, radiosondes, satellites, etc.) indicate increases of water vapour in the troposphere since the 1970s. Precipitation is harder to measure; however, decreasing snowfalls, increasing winter temperatures and significant seasonal reductions of snow cover have been observed (Stocker et al., 2013). Thus, along with these trends, future changes in the water cycle are expected to occur.

Projections of future changes suggest that increases in global precipitation and tropospheric water vapour are expected during the 21st century. However, in a much warmer world, these changes are projected to be highly variable depending on the region and the season (IPCC, 2013b). Likewise, the global runoff projections remain highly uncertain due to the complexity of the interactions between different processes within the water cycle (Stocker et al., 2013).

1.3.2 Sources of uncertainty

Uncertainty has become one of the most important subjects in the studies of climate change. There are numerous sources of uncertainties in the process of hydrological modelling and climate change impact assessments (Prudhomme et al., 2003). This process has been studied during the last decade and is referred to as the “cascade of uncertainty” (Schneider, 1983; Wilby & Dessai, 2010) or the “uncertainty explosion” (Henderson-Sellers, 1993; R. N. Jones, 2000).

Different studies have identified sources of uncertainty and it has been agreed upon that the most important sources are the greenhouse emission scenarios, global climate model structure, downscaling method, impact (or catchment) model and the natural climate variability uncertainty (Falloon et al., 2014; Poulin et al., 2011; Wilby, 2005). Figure 1.4 shows the “cascade of uncertainty” which clearly illustrates the growth of the envelope of uncertainty from various sources starting with the uncertain future society to the accumulated uncertainty at the end to obtain adaptation responses.

The climate model is generally considered the most important source of uncertainty. Therefore, recent studies have analyzed other sources of uncertainty related to the GCM and RCM configurations. For example, P. Roy et al. (2014) showed that the largest source of uncertainty on simulation of precipitation extremes came from the model selection and domain size followed by the member selection during the summer months.

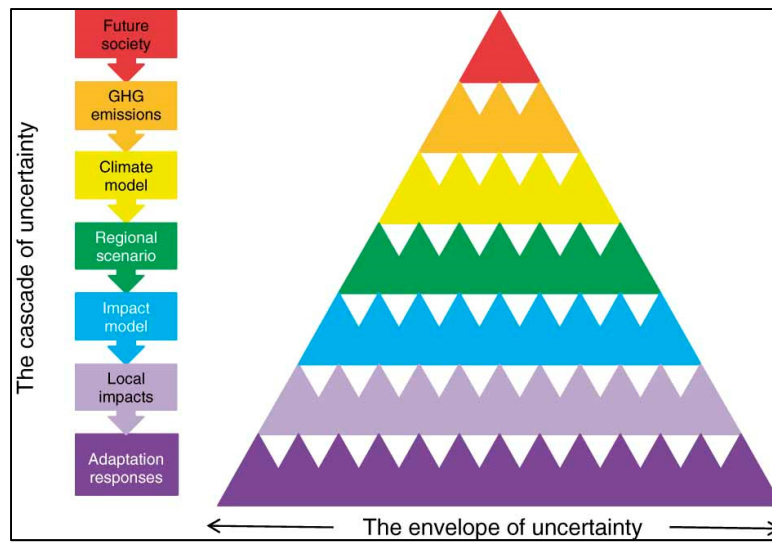


Figure 1.4 Cascade of uncertainty
Taken from Wilby and Dessai (2010, p. 181)

It is seen that many sources of uncertainty can be included in the modelling chain. Therefore, the research community keeps working to identify and quantify the types of uncertainty that are the most important for each particular impact study (Hawkins et al., 2013).

1.4 Regional studies: Quebec

Water resources are of great importance in the province of Quebec, thus regional hydrological impact studies have been performed to analyse future projections of the hydrologic regime. Catchment-scale studies have been assessed in past and recent years in different regions of the province. Examples of such studies are presented by Minville et al. (2008), Minville et al. (2009), Chen et al. (2011), Arsenault et al. (2013), Troin et al. (2016) and Trudel et al. (2017) where RCMs outputs were used as inputs for climate change impact and uncertainty assessments.

More specifically, high flows have been investigated in different studies over the region. For example, L. Roy et al. (2001) assessed the impact of climate change on seasonal floods of the Châteauguay River Basin. Canadian GCM simulations coupled with a hydrological model were used to assess the floods for different return periods. The results indicated

potential augmentations of streamflow. Larger increases on this trend were showed when longer return periods were considered. Quilbé et al. (2008) evaluated the effects of climate change in the Chaudière River suggesting future increases on winter flows and decreases in spring flows as other authors have also implied (Boyer et al., 2010; L.-G. Fortin et al., 2007; Mareuil et al., 2007; Minville et al., 2008).

Local initiatives have emerged to provide an ample and homogeneous assessment of hydrological projections. The Hydroclimatic Atlas of Southern Quebec is a project involving various experts providing reliable hydrological projections over selected catchments in the province. The latest version of the Hydroclimatic Atlas of Southern Quebec (CEHQ, 2015) presented the following main trends expected on the water regimes for southern Quebec for the 2050 horizon (see table 1.1).

Table 1.1 Trends for the 2050 horizon for southern Quebec.
Taken from the Hydroclimatic Atlas of Southern Quebec (CEHQ, 2015, p. V)

Trends for the 2050 horizon	Confidence
Spring high flow will come earlier	High
Spring high flow volume will be lower in southernmost Quebec	Moderate
The spring high flow peak will be lower in southernmost Quebec	Moderate
The summer and autumn high flow peak will be higher throughout large areas of southern Quebec	Moderate
Summer low flow will be more severe and last longer	High
Winter low flow will be less severe	High
Summer mean flow will be lower	High
Annual mean flow will be higher in the north of southern Quebec and lower to the south.	Moderate

These trends were also confirmed in a larger study of hydrological projection over numerous catchments in the province (Guay et al., 2015). Higher winter flows and lower summer flows with earlier spring floods are expected. The height of snow cover along with the number of days with snow on the ground are likely to decrease in the south while more snow in a shorter season is expected in the north. However more research is still required as improved and finer climate datasets and approaches are constantly updated since they are expected to yield better representations of the climate system. Studies have analyzed the effects of the spatial resolution on the regional climate model outputs showing evidences of the gain, generally named “added value”, on the use of higher spatial resolutions on the Canadian RCM (Curry et al., 2016a; Lucas-Picher et al., 2016).

The spatial resolution increase also requires an increase in the climate model simulation times, which raises the need to evaluate how the spatial resolution in climate modelling impacts the hydrological streamflow simulations. In other words, it is necessary to analyse the effects of the higher climate model resolution on the simulation of hydrological extremes such as floods.

1.5 Research objectives

The main objective of this project is to analyse the impact of spatial resolution of different climate simulations issued from two different versions of the Canadian Regional Climate Model (CRCM) on the hydrological modelling of summer and fall floods in southern Quebec. In order to address the main objective, the following specific objectives will be investigated:

1. Evaluate the impact of increasing spatial resolution on temperature and precipitation climate model outputs.
2. Study the impact of the different hydrological models structure on summer and fall flood simulations.
3. Study the impact of hydrological model parameter set on summer and fall flood simulations.

CHAPTER 2

STUDY AREA AND DATA

2.1 Study area

This study was carried out over 50 watersheds located in southern and central Quebec (see Figure 2.1). This region covers a significant part of the integrated water resources management zones defined by the Ministère du Développement Durable, de l'Environnement et de la Lutte contre les Changements Climatiques (MDDELCC, 2017) and is part of the study area used in the latest Hydroclimatic Atlas of Southern Quebec (CEHQ, 2015).

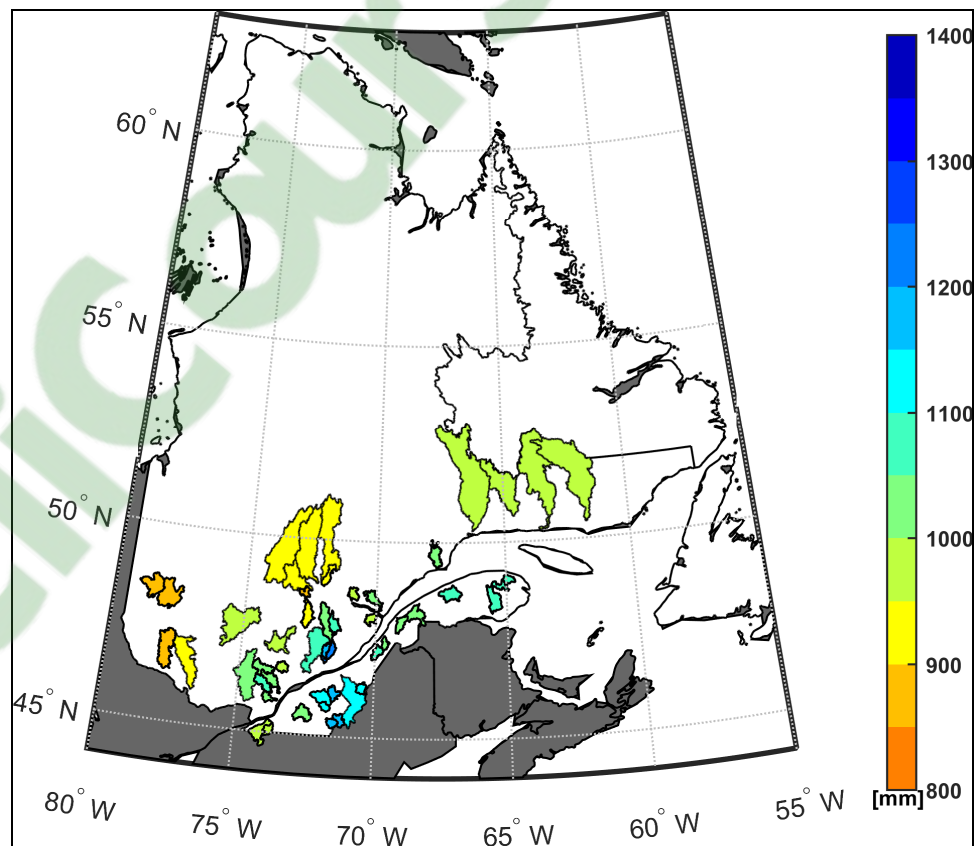


Figure 2.1 Location and mean annual precipitation (mm) of the 50 watersheds used in this study

The Figure 2.1 shows the location of the selected watersheds along with their mean annual precipitation. The watersheds were selected in order to accomplish the following criteria:

1. **Diversity of catchment area.** In order to account for the effects in regions with different characteristics, the watersheds have a diversity of catchment areas ranging from 512 km² to 18,983 km².
2. **Availability of data.** Due to data availability, the meteorological and hydrometric observed data have a period length of at least 12 years to have representative datasets to perform the calibration and validation of the hydrological models. These datasets were obtained between 1969 and 2010 depending on the available hydrometric and meteorological records for each watershed.
3. **Natural observed streamflow.** The hydrometric data of all the watersheds is based on natural observed streamflows or weakly influenced but not restored (i.e. an estimate of the natural flow that is regulated by a reservoir). This condition is essentially needed to avoid any impact on the hydrological modelling due to streamflow regulations

2.2 Observed data

For this project, observed historical records of meteorological data (minimum temperature, maximum temperature and precipitation) and streamflow were used.

The meteorological data was obtained from the Centre d'Expertise Hydrique du Québec (CEHQ) unit from the MDDELCC. As described in the "Plateforme de modélisation hydrologique du Québec méridional" (CEHQ, 2014), the meteorological database is derived from the simple kriging interpolation of observations from 971 stations operated by the MDDELCC and 21 stations operated by Rio Tinto. The interpolated dataset forms a grid of 0.1° (\approx 11 km) resolution covering the domain limited from 43° to 55° latitude and -60° to -80° longitude with daily values for the 1969-2010 period.

The hydrometric data were obtained from the Banque de Données Hydriques (BDH) of the Centre d'Expertise Hydrique du Québec (CEHQ) covering the same period of the meteorological data on a daily time step for the 50 hydrometric stations.

2.3 Climate simulation data

The climate model simulations datasets used for this project were issued from the fourth and fifth versions of the CRCM and were provided by the Ouranos Consortium on Regional Climatology and Adaptation. The climate datasets issued from CRCM4 (version 4) cover the 1961-1990 period and the datasets issued from CRCM5 cover the 1981-2010 period. Four climate simulations issued from the CRCM4 and three issued from the CRCM5, with a variety of drivers, domains and resolutions were used (Table 2.1).

Table 2.1 Description of the CRCM climate datasets used in this study

Acronym*	Version	Driver	Domain	Resolution
15 _{km} (CGCM, CRCM4) _{QC}	4.2.4	CGCM3.1v2	Quebec	15 km
45 _{km} (CGCM, CRCM4) _{AMNO}	4.2.3	CGCM3.1v2	North America	45 km
15 _{km} (ERA40c, CRCM4) _{QC}	4.2.4	ERA40C	Quebec	15 km
45 _{km} (ERA40c, CRCM4) _{AMNO}	4.2.3	ERA40C	North America	45 km
12 _{km} (ERAint75, CRCM5) _{QC}	5 v3331	ERA-Interim 75	Quebec	0.11° ≈ 12 km
24 _{km} (ERAint75, CRCM5) _{QC}	5 v3331	ERA-Interim 75	Quebec	0.22° ≈ 24 km
48 _{km} (ERAint75, CRCM5) _{QC}	5 v3331	ERA-Interim 75	Quebec	0.44° ≈ 48 km

*The acronym stands for: Resolution (Driver, RCM) Domain

2.3.1 Regional climate model (RCM)

In this work, two RCMs were used, the CRCM4 and the CRCM5. Even though they share continuous numbered versions, they are in fact two different climate models. The CRCM4 is a limited-area nested model developed at Université du Québec à Montréal (UQAM) based on the fully elastic nonhydrostatic Euler equations (Daniel Caya & Laprise, 1999; D. Caya et al., 1995; Music & Caya, 2007). The CRCM5 is based on a limited-area version of the Global Environment Multiscale (GEM) model used for Numerical Weather Prediction at Environment Canada and developed at the Centre pour l'Étude et la Simulation du Climat à l'Échelle Régionale (ESCIER Centre) at the UQAM (Côté et al., 1998; Martynov et al., 2013). The CRCM5 provides a more realistic representation of water and energy exchange between the land surface and atmosphere and has contributed to the CORDEX project over North America (Lucas-Picher et al., 2016).

In order to attain the main objective, seven different climate datasets issued from the CRCM4 and the CRCM5 were evaluated. From CRCM4, four datasets were used. They consist of two datasets driven by the Canadian General Circulation Model (CGCM) third generation (Scinocca et al., 2008) and two driven by the ERA-40c reanalysis (Uppala et al., 2005). For each driver, the climate model was run at 45km and 15km resolution. As observed in Table 2.1, the four CRCM4 datasets also have different domains; the simulations at 45km resolution were simulated over North American domain, while the simulations at 15km .resolutions were simulated over Quebec domain. The maps of the different domains are presented in the appendix I

The three CRCM5 datasets share more similarities. All CRCM5 datasets were driven by the ERA Interim (Dee et al., 2011) reanalysis and were simulated over Quebec domain. The only difference between these three simulations by CRCM5 is their different spatial resolutions of 0.44° (≈ 48 km), 0.22° (≈ 24 km) and 0.11° (≈ 12 km) respectively.

CHAPTER 3

METHODS

3.1 Overview

The general methodology of the present project is described in the following schematic representation presented in Figure 3.1.

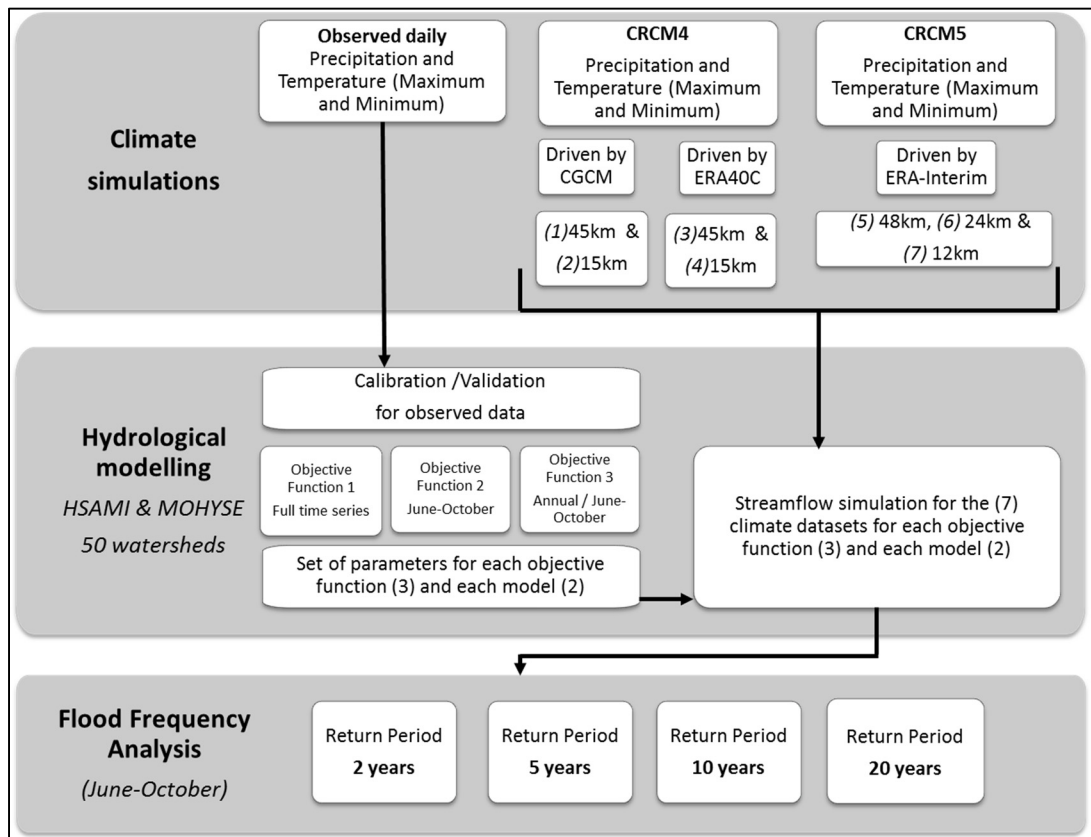


Figure 3.1 Overview of this project's research methodology

The overall methodology is divided in three main parts, (1) the climate simulations comparison, (2) the hydrological modelling by two different hydrological models and (3) the summer-fall floods analysis by the use of 2, 5, 10 and 20-year return periods as flood indicators.

3.2 Climate data comparison

This study aims to analyse the effects of spatial resolution on summer-fall floods simulation. Thus, in order to address the main objective, the first specific objective is to evaluate the impact of increasing spatial resolution on temperature and precipitation datasets as simulated by the different versions of the CRCM.

The evaluation of the effects of spatial resolution on the climate datasets is done by comparing the differences between two simulations with different resolutions. Where a given simulation named “X” and another simulation named “Y” are compared and presented as X/Y, where Y is the simulation used as the reference dataset. A summary of the comparisons used to evaluate the spatial resolution impact is presented in Table 3.

Table 3.1 Summary of CRCM4 and CRCM5 climate datasets comparisons

Acronym*	Version	Driver	Resolutions
15 _{km} (CGCM, CRCM4) _{QC} / 45 _{km} (CGCM, CRCM4) _{AMNO}	4.2.4	CGCM3.1v2	15 km / 45km
15 _{km} (ERA40c, CRCM4) _{QC} / 45 _{km} (ERA40c, CRCM4)	4.2.4	ERA40C	15 km / 45km
12 _{km} (ERAint75, CRCM5) _{QC} / 24 _{km} (ERAint75, CRCM5) _{QC}	5 v3331	ERA-Interim 75	12 km / 24 km
12 _{km} (ERAint75, CRCM5) _{QC} / 48 _{km} (ERAint75, CRCM5) _{QC}	5 v3331	ERA-Interim 75	12 km / 48 km

*The acronym stands for: simulation X / simulation Y

Performance statistics were computed to evaluate the mean and variability differences between the compared CRCM4 and CRCM5 climate simulations. The comparisons of temperature and precipitation datasets were evaluated using the following metrics.

Mean seasonal temperature and precipitation

The climate datasets comparison was performed using the mean seasonal values for the temperature and precipitation datasets. The mean seasonal temperature (\bar{T}) and the mean seasonal precipitation (\bar{P}) were calculated as follows:

$$\bar{T} = \frac{\sum_{i=1}^{N_y} \sum_{j=1}^{N_s} T_{ij}}{N_y N_s} \quad (3.1)$$

$$\bar{P} = \frac{\sum_{i=1}^{N_y} \sum_{j=1}^{N_s} P_{ij}}{N_y N_s} \quad (3.2)$$

where T_{ij} and P_{ij} are the daily values of temperature or precipitation, N_s is the number of days of the season and N_y is the number of years of the full time series. The leap year day is removed from the datasets.

Temperature seasonal bias

The temperature seasonal bias is calculated between the mean seasonal temperatures of a given dataset x named \bar{T}_x and the mean seasonal temperatures of a reference dataset y named \bar{T}_y as follows:

$$B_T = \bar{T}_x - \bar{T}_y \quad (3.3)$$

Precipitation seasonal relative bias

The precipitation seasonal relative bias is calculated between the mean seasonal precipitations of a given dataset x named \bar{P}_x and the mean seasonal precipitations of a reference dataset y named \bar{P}_y as follows:

$$B_{P_{rel}}(\%) = \frac{\bar{P}_x - \bar{P}_y}{\bar{P}_y} \cdot 100\% \quad (3.4)$$

Ratio of the seasonal variances

The variance (σ^2) describes the variability of the data in regards of the mean values of a determined dataset X (temperature or precipitation). The mean seasonal variance ($\overline{\sigma^2}$) is calculated as follows:

$$\overline{\sigma^2} = \frac{\sum_{i=1}^{N_y} \sum_{j=1}^{N_s} (X_{ij} - \bar{X}_i)^2}{N_y N_s} \quad (3.5)$$

where X_{ij} is the daily value, \bar{X}_i is the mean value of the season N_s for year i . These values are averaged by the number of years N_y of the full time series. The leap year day is also removed from the datasets. The ratio of the seasonal variances (temperature or precipitation) is calculated between the mean variance of a given dataset x named $\overline{\sigma_x^2}$ and the mean variance of a reference dataset y named $\overline{\sigma_y^2}$ as follows:

$$\text{Ratio of the variances} = \frac{\overline{\sigma_x^2}}{\overline{\sigma_y^2}} \quad (3.6)$$

These metrics were selected to quantify the differences between the climate simulations with different spatial resolutions to evaluate their impacts. Thus, no comparisons were made with actual historical observations.

3.3 Hydrological modelling

The hydrological modelling was performed by two lumped conceptual models with different structures and levels of complexity in order to study the impact of the hydrological model structure. These models have been largely used in research on the province of Quebec and were selected due to their availability and relatively short time of simulation.

3.3.1 Hydrological models

HSAMI model

The HSAMI hydrological model (V. Fortin, 2000), has been used by Hydro-Quebec over the province of Quebec during the last decades and has been applied in numerous studies (e.g. Arsenault et al., 2013; Chen et al., 2011; Minville et al., 2008; Poulin et al., 2011). HSAMI is a lumped conceptual model based on reservoirs that simulates the main processes of the hydrological cycle. To perform a simulation, the inputs required are the mean values of maximum and minimum temperatures over the selected area, precipitation (liquid and solid) and cloud cover fraction. The model has up to 23 calibration parameters, all of which were calibrated by the Covariance Matrix Adaptation Evolution Strategy (CMAES) (N. Hansen & Ostermeier, 1997) as recommended by Arsenault et al. (2014).

MOHYSE model

The MOHYSE model is a simpler lumped conceptual model that was developed by V. Fortin and Turcotte (2006). The model has been used in different studies in Canadian watersheds such as the studies presented by Arsenault (2015) and Velázquez et al. (2010). MOHYSE simulates the main hydrological processes and can be run on different time scales (from sub-daily to multiple days). The required input data are mean daily temperatures, total daily rain and snow. All of these values are averaged over the watershed since the model is lumped. This model has ten parameters, all of which were also calibrated with the CMAES algorithm.

3.3.2 Calibration and validation

The calibration of the hydrological models was performed on the odd years of the 1969-2010 period using three different objective functions since quantifying the impact of hydrological model parameter set is one of the specific aims of the project. The three objective functions are variations of the Kling-Gupta Efficiency criterion previously described in the equations 1.1 to 1.4.

The first objective function used for this project is the KGE over the calibration period. The second objective function is the KGE value over the summer-fall months (June to October) to give focus to those seasons which are of interest in this study. Finally, the third objective function consists of a custom criterion combining the KGE value of the interannual mean hydrograph and the KGE on the summer-fall months to focus on the summer-fall period and also to avoid sacrificing the rest of the hydrograph. Table 3 presents a summary of the three objective functions.

Table 3.2 Summary of the objective functions for the hydrological model's calibration

Acronym	Description
OF-1	KGE
OF-2	$KGE_{summer-fall}$
OF-3	$\frac{KGE_{interannual\ mean}}{2} + \frac{KGE_{summer-fall}}{2}$

This KGE criterion measures the goodness of fit between two datasets (observed and simulated streamflow in this case) ranging from $-\infty$ to 1, where a value of 1 indicates a perfect fit between the datasets, a value of 0 means a good fit on average values and negative values indicates worse fitting than using the mean as a predictor. The validation was then performed on the even years (not calibrated) for each watershed.

3.3.3 Streamflow simulations

After analyzing the CRCM climate outputs, the hydrological modelling was performed to evaluate the impacts of the climate simulations spatial resolution on the floods modelling. To address this issue, streamflow simulations driven by the seven CRCM climate datasets (temperature and precipitation) were generated and compared.

To generate the streamflow simulations, the hydrological models were firstly calibrated and validated with historical records of observed streamflows in order to evaluate their performance in summer-fall floods estimations for the three different objective functions. Thus, three different parameter sets were obtained for both hydrological models on each of the fifty watersheds. In this way, along with the main objective, the impacts of hydrological model structure (specific objective 2) and the impacts of model parameter set (specific objective 3) are also investigated by comparing the results of the hydrological models and the different calibration approaches.

Once the hydrological models are validated, the CRCM climate datasets are directly used as input for the hydrological models to produce the climate driven streamflow simulations. It is important to mention that no recalibration was performed to generate the climate driven streamflow simulations. This approach was fixed in order to avoid any influence on the extreme events magnitude and frequency due to the recalibrations, as they are expected to have a diminishing effect on the data's variability, a characteristic important to preserve in the analysis of extreme events such as floods. Thus, the parameter sets obtained in the calibration process were preserved to produce the different streamflow simulations to later be inter-compared. Therefore, seven (7) climate driven streamflows for both hydrological models (2) each calibrated on three (3) objective functions and fifty (50) watersheds were then generated.

The climate-driven streamflow simulation comparison was done following the same approach described for the climate datasets comparison. The comparisons were performed between two different climate driven streamflow simulations (as performed in the climate data comparison), where a given streamflow simulation "X" and another streamflow simulation "Y" are compared, using Y as the reference dataset (presented as X/Y). The climate driven streamflow simulations comparisons were made by using two performance statistics to measure the difference between two datasets: The seasonal KGE value described previously in the equations 1.1 to 1.4 and the seasonal relative bias (%) described in the equation 1.7.

3.3.3.1 Return Periods

The main objective of the study is to identify the effects of the spatial resolution on flood events. Thus, four flood indicators were defined to evaluate the spatial resolution impact: the 2-year, 5-year, 10-year and 20-year return period of summer-fall floods. The different climate datasets have a length of 30 years, thus, the four flood indicators were defined in function of the sample size. In this manner, the datasets have a valid sample size (30 values of annual summer-fall peak flows) to estimate representative distributions for each flood indicator. The four return periods were estimated from the simulated climate driven streamflows by a flood frequency analysis using the Gumbel distribution. This distribution is often used in hydrology to represent flood peaks distributions due to its commonly good approximations and simplicity of use (Chebana & Ouarda, 2011; Loaiciga & Leipnik, 1999; Marques et al., 2015; Yue et al., 1999).

The return periods are compared using the same approach that was described for the climate simulations and the streamflow simulations, where a given flood indicator “X” and another flood indicator “Y” are compared and presented as X/Y. The comparisons between the estimated return periods were done by using the relative bias (%) as an evaluation metric:

$$B_{rel}(\%) = \frac{X - Y}{Y} \cdot 100\% \quad (3.6)$$

where Y is the value used as a reference.

This metric was used to quantitatively evaluate the impact of the spatial resolution in the different estimated flood indicators estimated from the generated climate-driven summer-fall peak flows.

CHAPTER 4

RESULTS

The results are presented in three main sections. First, the comparisons between the climate simulations with different resolutions (temperature and precipitation) are presented. Second, the hydrological modelling performance is shown for calibration and validation years in regards of observed data over the fifty watersheds. Finally, the climate driven streamflow simulations are compared and analyzed by calculating the different performance statistics over the streamflow simulations and the flood indicators.

4.1 Climate simulations intercomparison

As presented in chapter 3, the first stage of the methodology consists in the analysis of the CRCM climate simulations. To that effect, four comparisons were done to evaluate the impact of spatial resolution over the province of Quebec: two comparisons for the climate outputs issued from the fourth version of the CRCM and two comparisons between simulations issued from the fifth version of the CRCM.

4.1.1 Spatial resolution

4.1.1.1 Temperature

Figures 4.1 and 4.2 present maps of the annual daily mean temperature (°C) bias between simulations with different resolutions issued from CRCM4 and CRCM5, respectively. Each figure shows the bias between two temperature simulations with different resolutions. No comparisons were done against observations. The maps show the bias for the summer (June, July and August) and fall (September, October and November) seasons over the province. The fifty watersheds of the study area are highlighted in black.

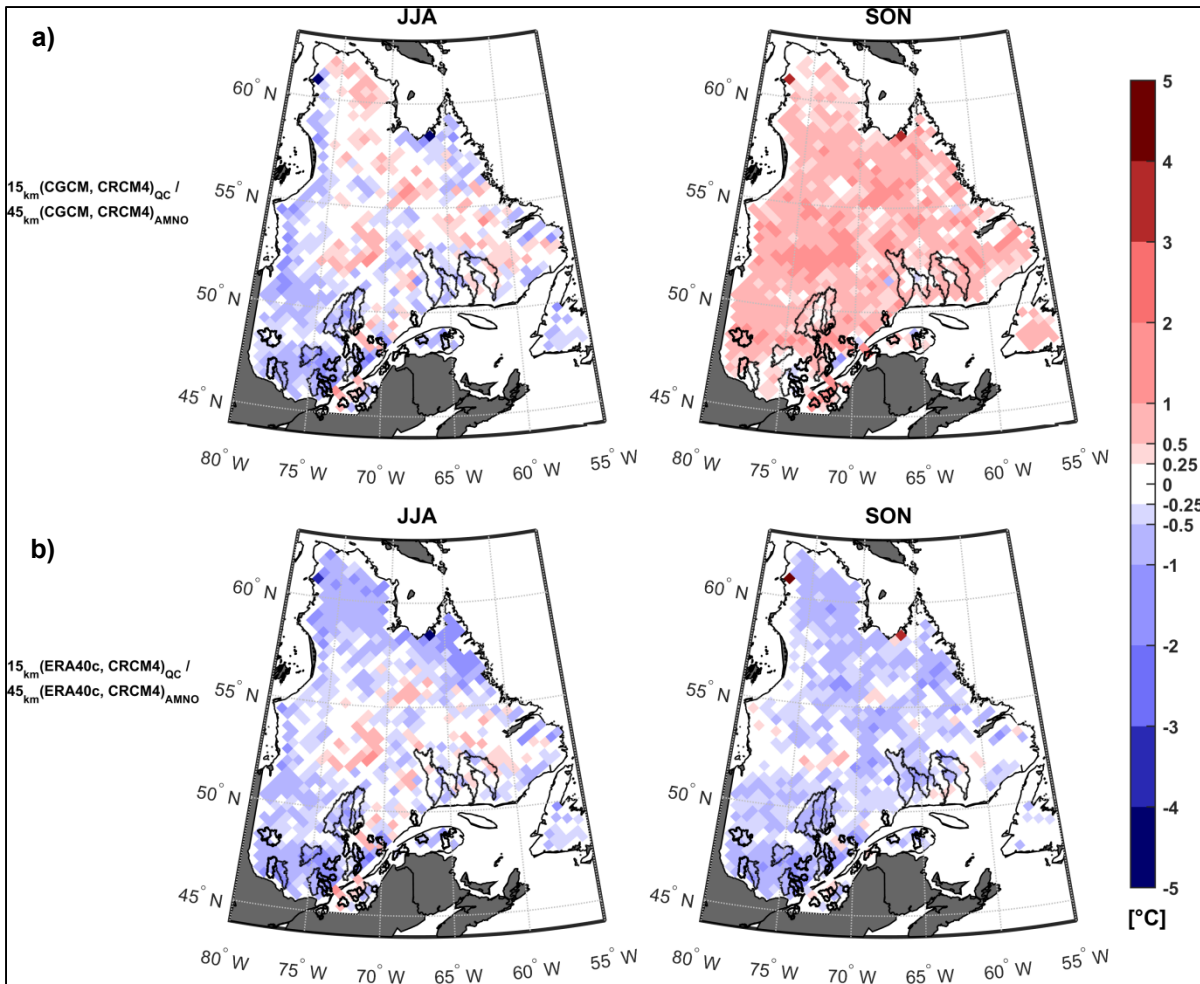


Figure 4.1 Annual daily mean temperature ($^{\circ}\text{C}$) bias between simulations issued from CRCM4 for the summer (JJA) and fall (SON) seasons for the period 1961-1990. The upper panels (a) show the comparisons for the datasets driven by CGCM. The lower panels (b) show the comparisons for the datasets driven by ERA40c

On the comparisons of temperature datasets issued from CRCM4 driven by CGCM (upper panel on Figure 4.1) a consistent hot bias is observed during the fall months. More variability is observed during the summer months with a bias varying between 2 and -2 degrees Celsius. On the other hand, the comparisons of the ERA40c-driven simulations show similar trends on the summer and fall seasons. A general cold bias is observed over the province with some hot spots on the center and southern regions of the province. This is true for both seasons with a slightly hotter bias observed during the summer months.

For the comparisons of temperature datasets issued from CRCM5 (see Figure 4.2), two comparisons are presented. The bias between the 12 km and 24 km resolution (top two panels) shows a consistent cold bias over the entire region during the fall months. Smaller and generally cold biases are observed during the summer with some hot biases observed close to the coastal areas. Similar trends are also observed for the 12 km and 48 km resolutions comparison (bottom two panels), yet, the range of bias is slightly larger, reaching values of up to 3 degrees Celsius difference.

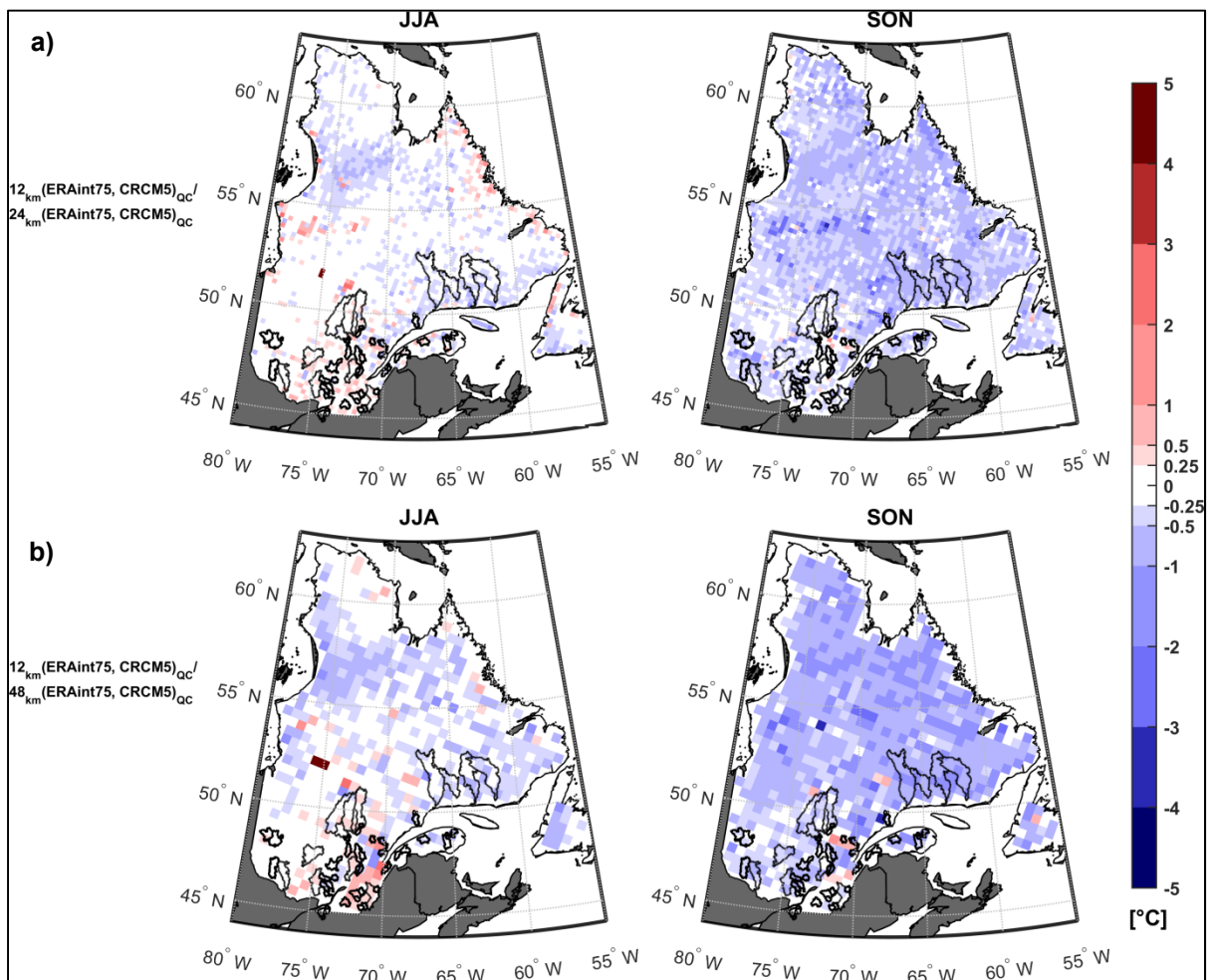


Figure 4.2 Annual daily mean bias of temperature ($^{\circ}\text{C}$) between simulations issued from CRCM5 for the summer (JJA) and fall (SON) seasons for the period 1981-2010. The upper panels (a) show the comparisons for the datasets with 12 km and 24 km resolution. The lower panels (b) show the comparisons for the datasets with 12 km and 48 km resolution

It can be observed in Figure 4.3 that the 15 km resolution datasets have larger variances than the 45 km resolution datasets in the northern parts of the province for both seasons and both drivers. Mean differences of 15 % are observed for the CGCM-driven comparison while differences of up to 50 % are shown for the ERA40c- driven comparisons. In the south (over the study region), the 15 km resolution presents smaller variances (around 5 to 15 % difference) than the 45 km resolution temperature variances. The CGCM-driven comparison shows larger differences during the fall and the ERA40c-driven comparison shows larger variance difference during the summer.

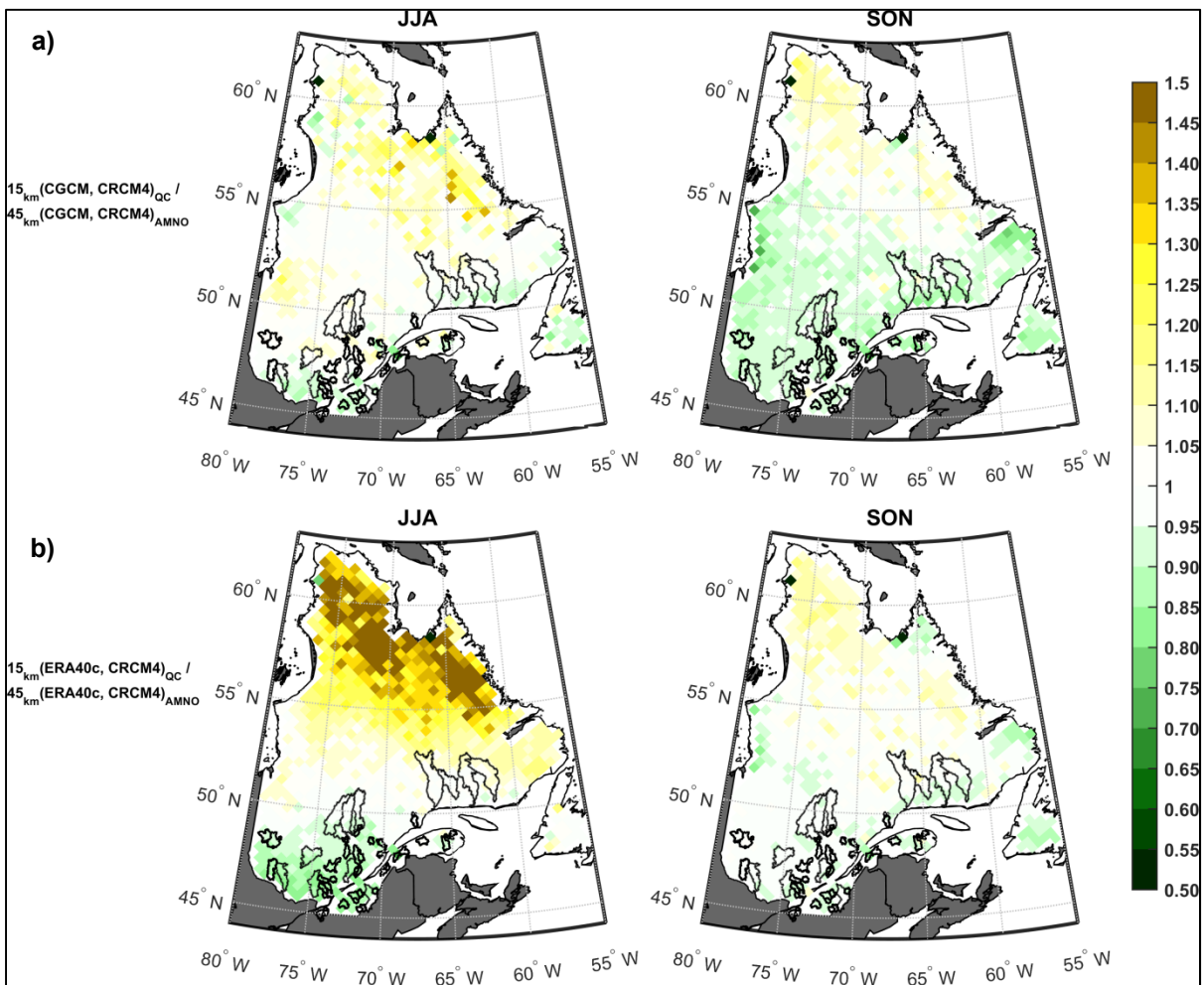


Figure 4.3 Ratio of annual seasonal mean temperature variances between simulations issued from CRCM4 for the summer (JJA) and fall (SON) seasons for the period 1961-1990. The upper panels (a) show the comparisons for the datasets driven by CGCM. The lower panels (b) show the comparisons for the datasets driven by ERA40c

Figure 4.4 shows similar trends for the results of the CRCM5 variance ratio comparisons for both seasons. A consistent larger variance is observed for the 12 km resolution temperature simulation during the fall months. Differences reaching up to 20 to 25 % are observed for the 12 km and 48 km resolution comparison, with smaller differences (5 to 15 %) for the 12 km and 24 km resolution comparison.

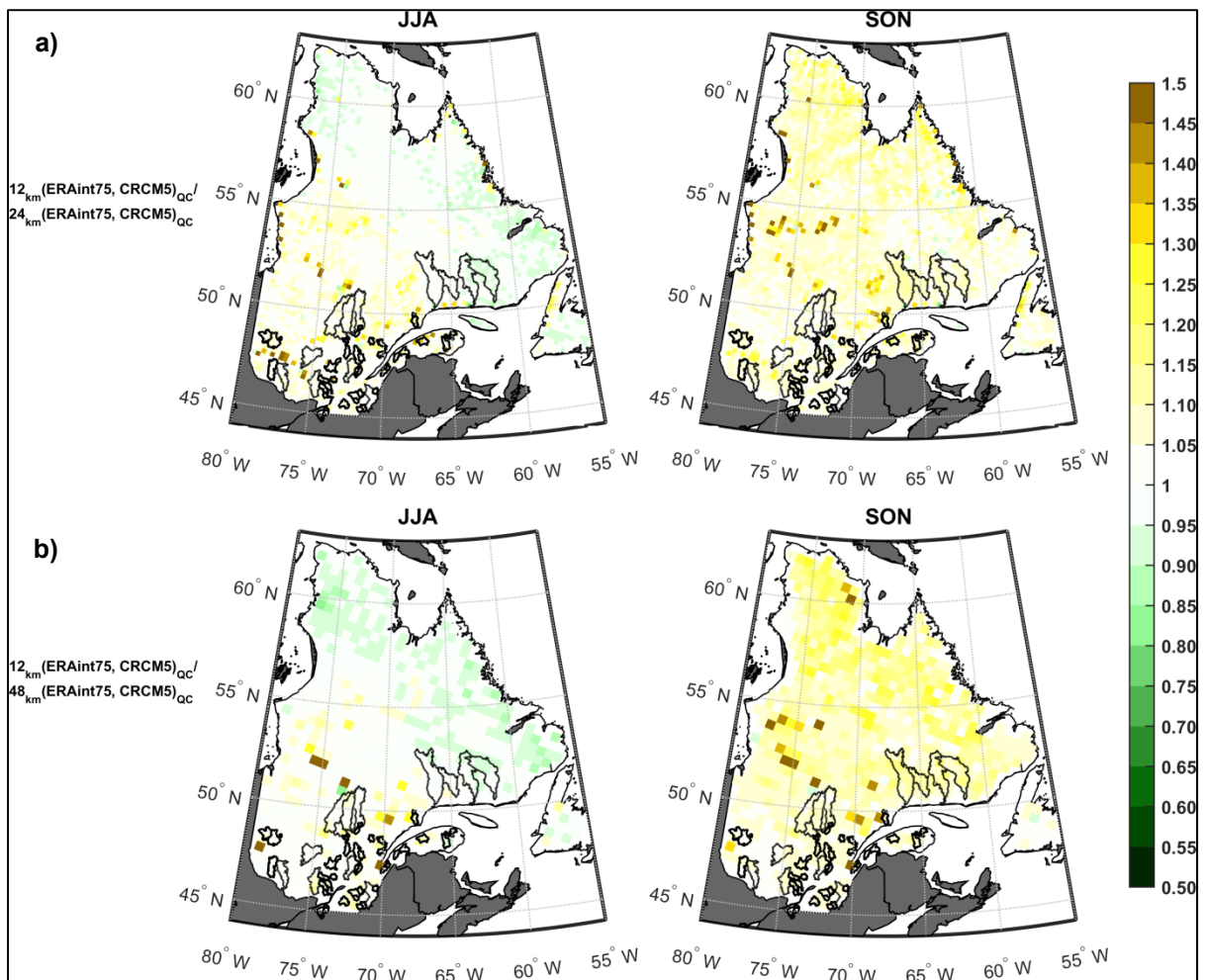


Figure 4.4 Ratio of annual seasonal mean temperature variances between simulations issued from CRCM5 for the summer (JJA) and fall (SON) seasons for the period 1981-2010. The upper panels (a) show the comparisons for the datasets with 12 km and 24 km resolution. The lower panels (b) show the comparisons for the datasets with 12 km and 48 km resolution

During summer, the 12 km simulations show smaller variances on the northeast and larger variances on the southwest when compared to the 24 km and 48 km resolutions. Yet, slightly

larger differences are observed between the 12 km simulation and the coarser (48 km) resolution temperature data.

4.1.1.2 Precipitation

Figures 4.5 and 4.6 present maps of the annual daily mean precipitation relative bias (%) between simulations with different resolutions issued from CRCM4 and CRCM5, respectively.

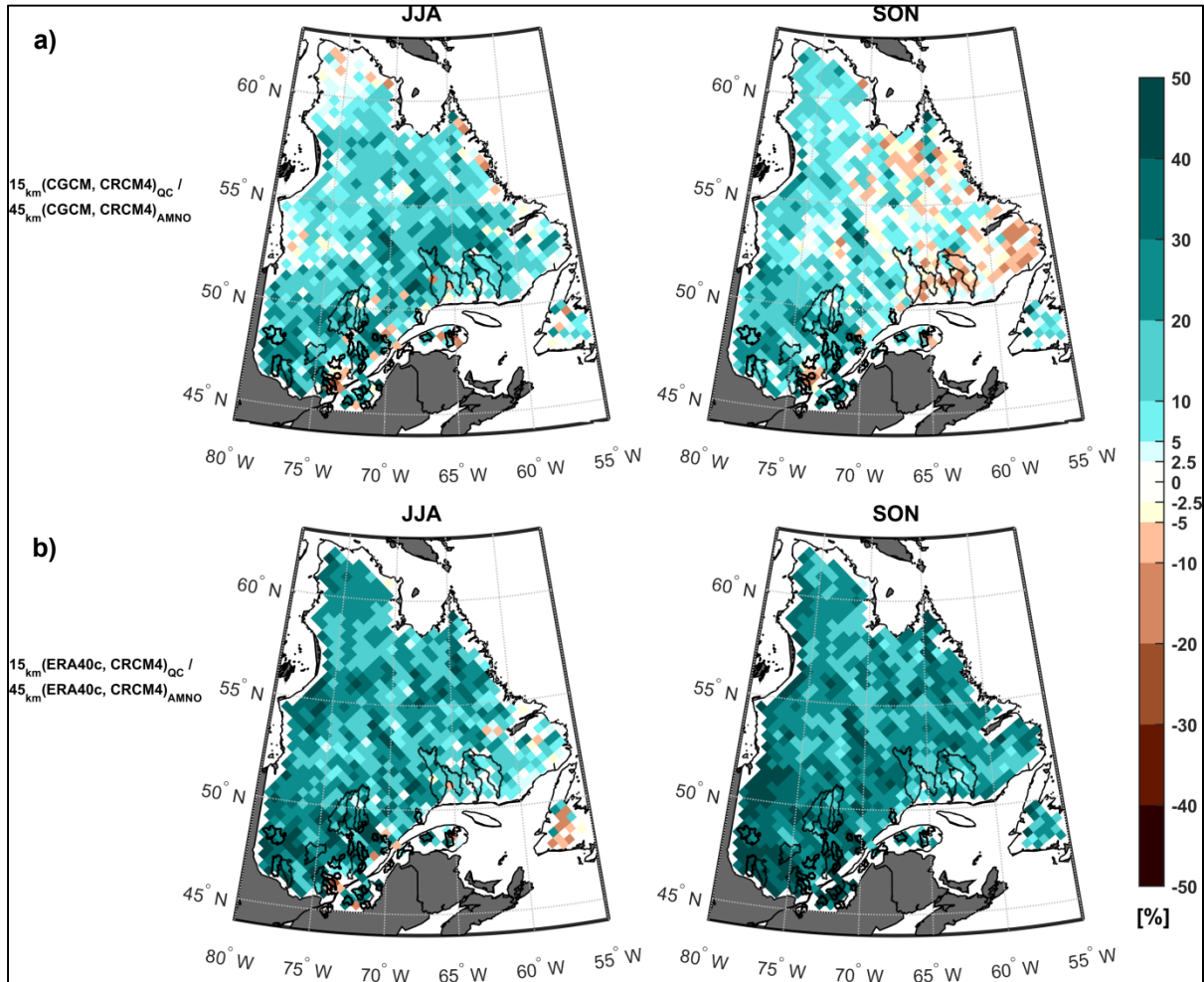


Figure 4.5 Annual daily mean relative precipitation biases (%) between simulations issued from CRCM4 for the summer (JJA) and fall (SON) seasons for the period 1961-1990. The upper panels (a) show the comparisons for the datasets driven by CGCM. The lower panels (b) show the comparisons for the datasets driven by ERA40c

In the CRCM4 precipitation comparisons (Figure 4.5), a consistent wet bias is observed over the entire province for both drivers. However, on the CGCM-driven simulations the wet relative biases are smaller. Also, differences are observed during the fall months of the CGCM-driven simulations whereas dryer relative biases are observed on the southeast side of the province, where the largest studied watersheds are located.

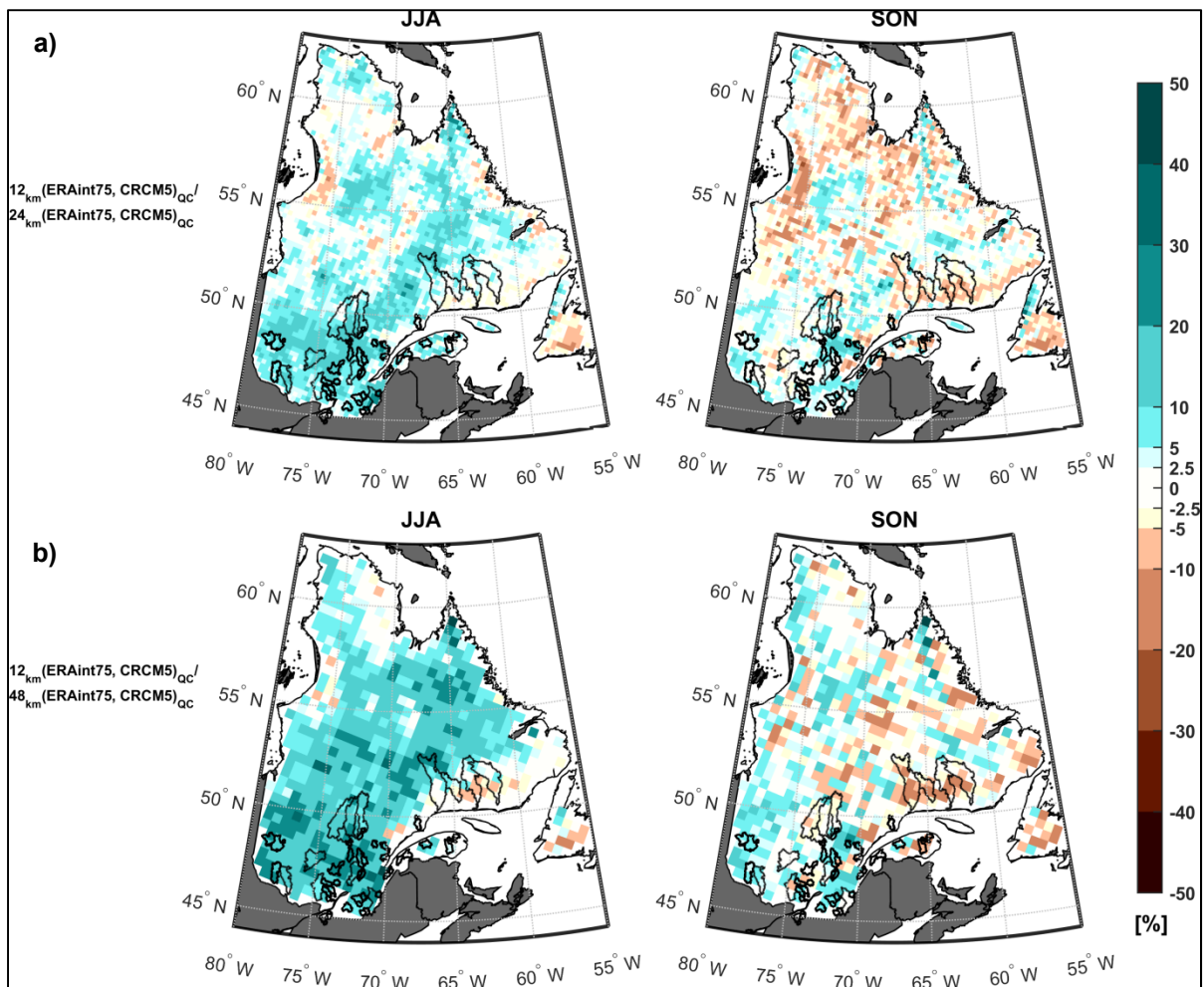


Figure 4.6 Annual daily mean relative biases (%) of precipitation between simulations issued from CRCM5 for the summer (JJA) and fall (SON) seasons for the period 1981-2010. The upper panels (a) show the comparisons for the datasets with 12 km and 24 km resolution. The lower panels (b) show the comparisons for the datasets with 12 km and 48 km resolution

Figure 4.6 presents the relative biases of the CRCM5 precipitation comparisons. Both comparisons show similar trends for the summer and fall months, where a general wet trend

is observed during the summer months. Meanwhile, wet and dry relative biases are observed during the fall. Overall, larger relative biases are observed between the 12 km resolution data and the 48 km resolution data (lower panels).

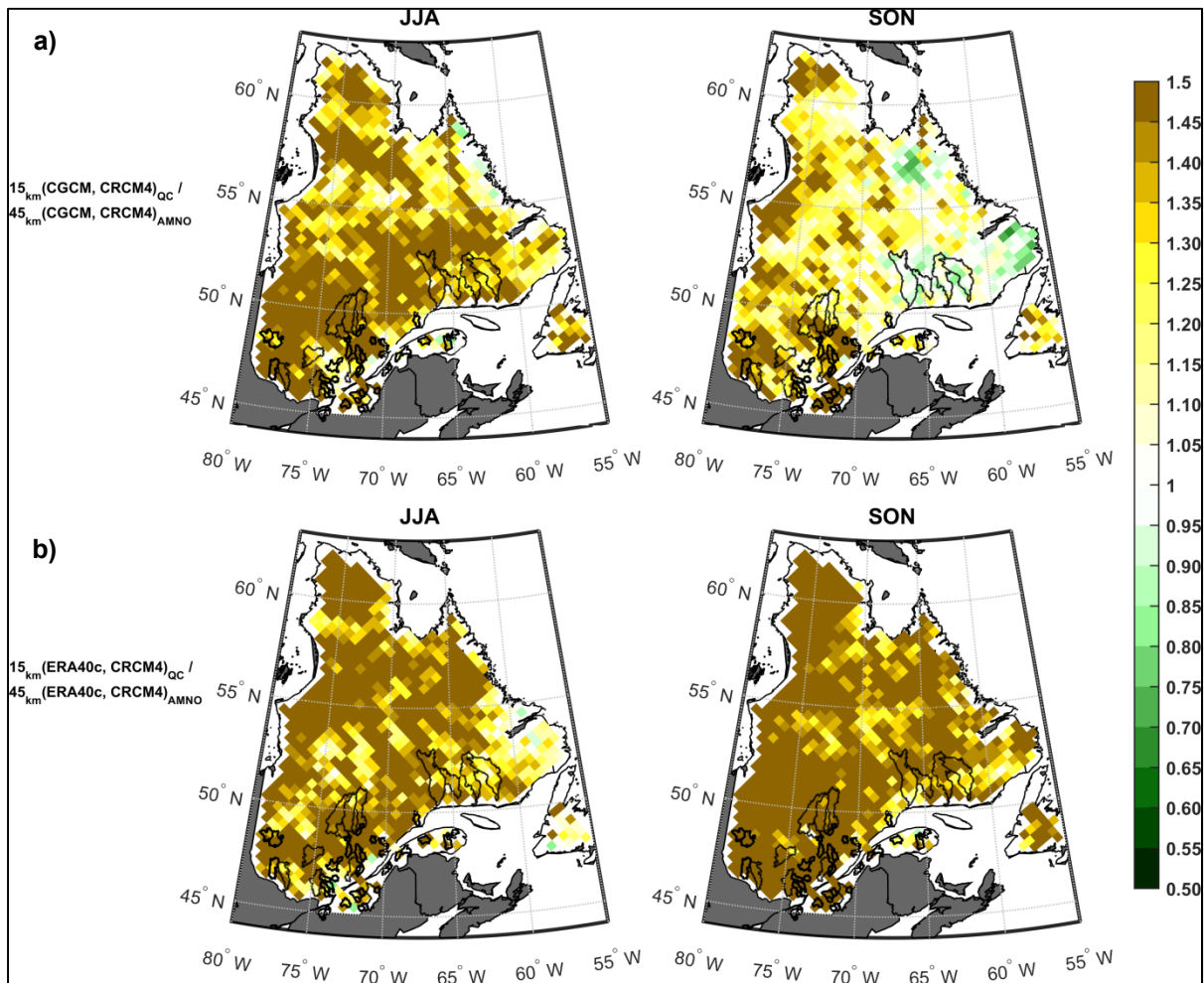


Figure 4.7 Ratio of annual seasonal mean temperature variances between simulations issued from CRCM4 for the summer (JJA) and fall (SON) seasons for the period 1961-1990. The upper panels (a) show the comparisons for the datasets driven by CGCM. The lower panels (b) show the comparisons for the datasets driven by ERA40c

Figures 4.7 and 4.8 present the maps of the ratio of seasonal mean precipitation variances between simulations with different resolutions issued from CRCM4 and CRCM5. The 15 km outputs of CRCM4 (Figure 4.7) have a larger variance (up to 50 %) than its 45 km counterpart for both seasons for both drivers.

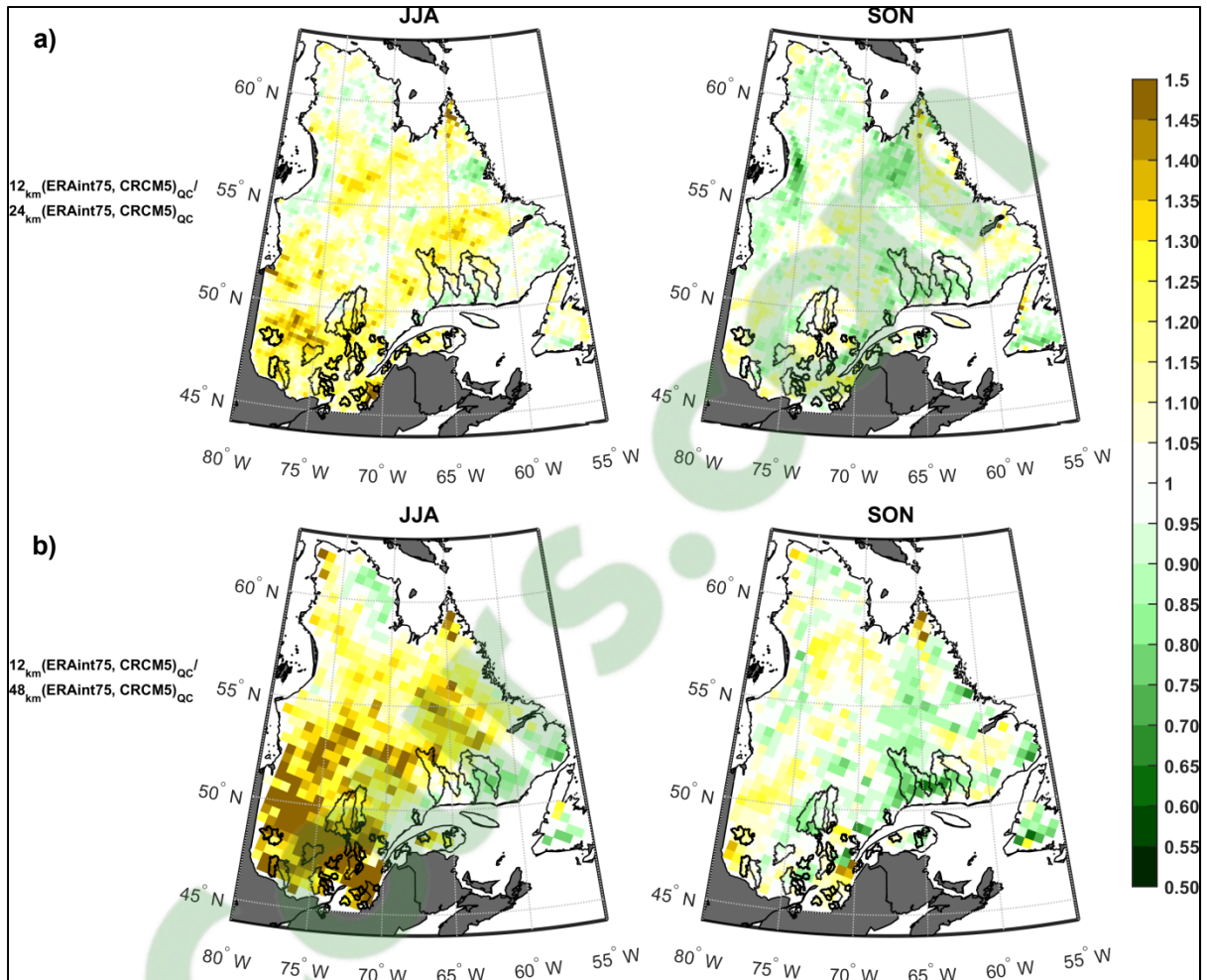


Figure 4.8 Ratio of annual seasonal mean temperature variances between simulations issued from CRCM5 for the summer (JJA) and fall (SON) seasons for the period 1981-2010. The upper panels (a) show the comparisons for the datasets with 12 km and 24 km resolution. The lower panels (b) show the comparisons for the datasets with 12 km and 48 km resolution

For CRCM5, the 12 km resolution presents larger variances in the south during summer months, yet the difference increases when comparing with the 48 km resolution simulation (for up to 50%). During the fall, smaller differences in variance are generally observed for both comparisons. Differences of variance are slightly larger between the 12 km and the 48 km resolution comparisons (lower panels) than between the 12 km and the 24 km resolution comparisons (upper panels) on the studied watersheds reaching differences of up to 10 and 25 %.

Differences were observed on the climate outputs intercomparisons obtained with CRCM4 and CRCM5 simulations. As previously presented in Table 2.1, the climate datasets have important differences. The CRCM4 datasets were simulated with different drivers (CGCM and ERA40c) and different domains (Quebec and North America). The CRCM5 datasets were simulated with same driver (ERA-Interim) and same domain (Quebec). The CRCM4 configuration differences are expected to also impact the streamflow simulations. For this reason, only the CRCM5 streamflow simulations will be presented in the following sections. This subject will be further discussed in chapter 5.

4.2 Hydrological modelling performance

This section presents the results obtained for the calibration and validation of the two hydrological models (HSAMI and MOHYSE). The results obtained with the three different calibration approaches described in chapter 3 are presented to validate hydrological models performance against observed data

4.2.1 HSAMI and MOHYSE calibration and validation results

The hydrological models calibration was performed during the odd years of the period 1969-2010. Then, the validation was performed over the even years of the same period. The number of years used for each of the 50 watersheds varies between them, according the data availability as mentioned in chapter 2.

Figure 4.9 presents the calibration and validation performances of the fifty watersheds for both hydrological models (MOHYSE and HSAMI) and the three different calibration approaches. The figure displays the distributions (boxplots) of the Kling-Gupta Efficiency values to evaluate the watersheds performance over the full time series and the performance during the summer-fall months (June to October). Accordingly, the boxplots are made with fifty values, one for each watershed. For the first calibration approach (Figure 4.9a), the two hydrological models perform similarly for both the calibration and validation periods. Yet,

both models have difficulties in representing streamflows during the summer-fall months with average KGE values of approximately 0.6. For the second objective function (b), models perform better during the periods from June to October. However, a decrease is observed in the KGE average values over the evaluation of the full time series for both hydrological models. For the third calibration approach (c) the KGE values distributions are similar for the evaluations over the full time series and the summer-fall months; however, slightly better performance values are observed for the evaluations over the entire year.

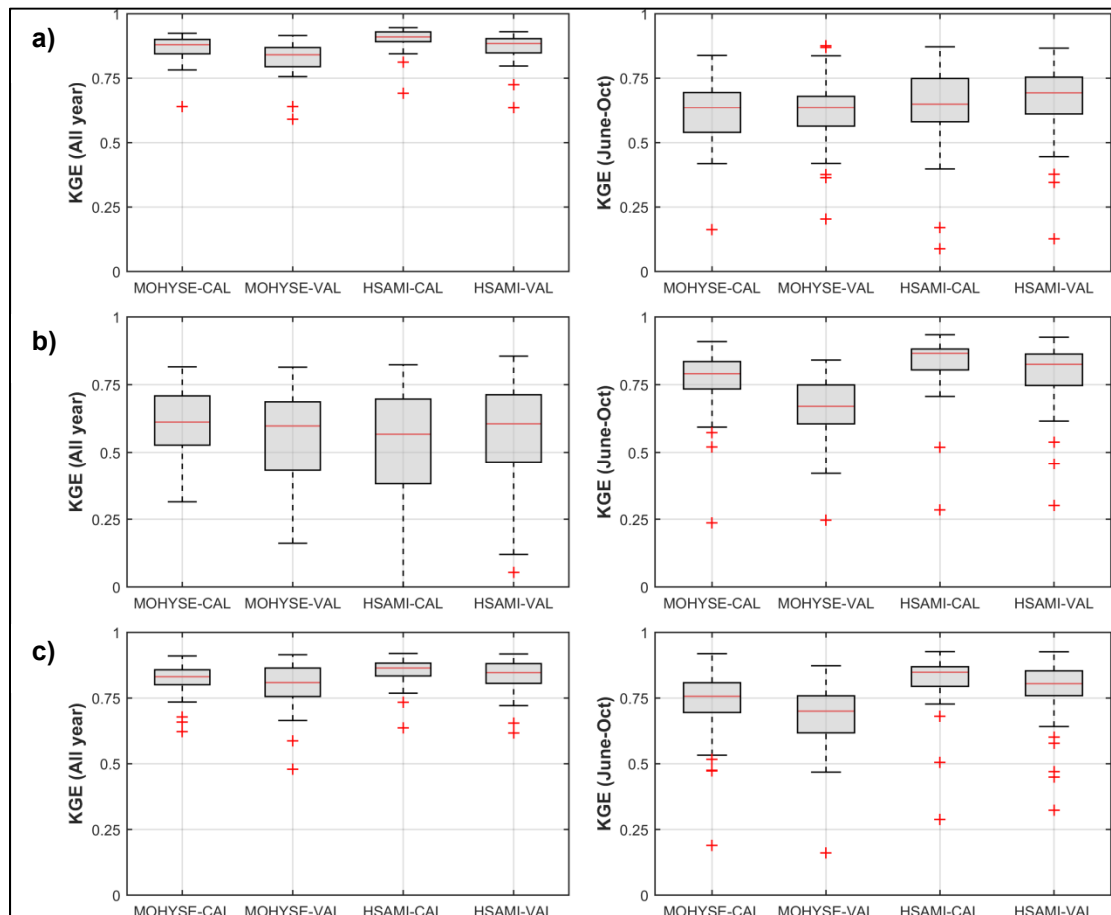


Figure 4.9 KGE values on the calibration and validation years. Panel a) presents the objective function-1, b) the objective function-2 and c) presents the objective function-3. KGE values for all the year (left panel) and June to October (right panel) are shown for both models and each objective function

Overall, the two hydrological models show good performance and similar tendencies when coupled with the different calibration approaches. However, HSAMI generally perform better than MOHYSE for both the calibration and validation periods.

4.2.1.1 Spatial distribution of hydrological modelling performance

In order to observe the spatial distribution of the hydrological modelling over the study area, the KGE values obtained during the validation periods are presented in the maps displayed in Figures 4.10, 4.11 and 4.12.

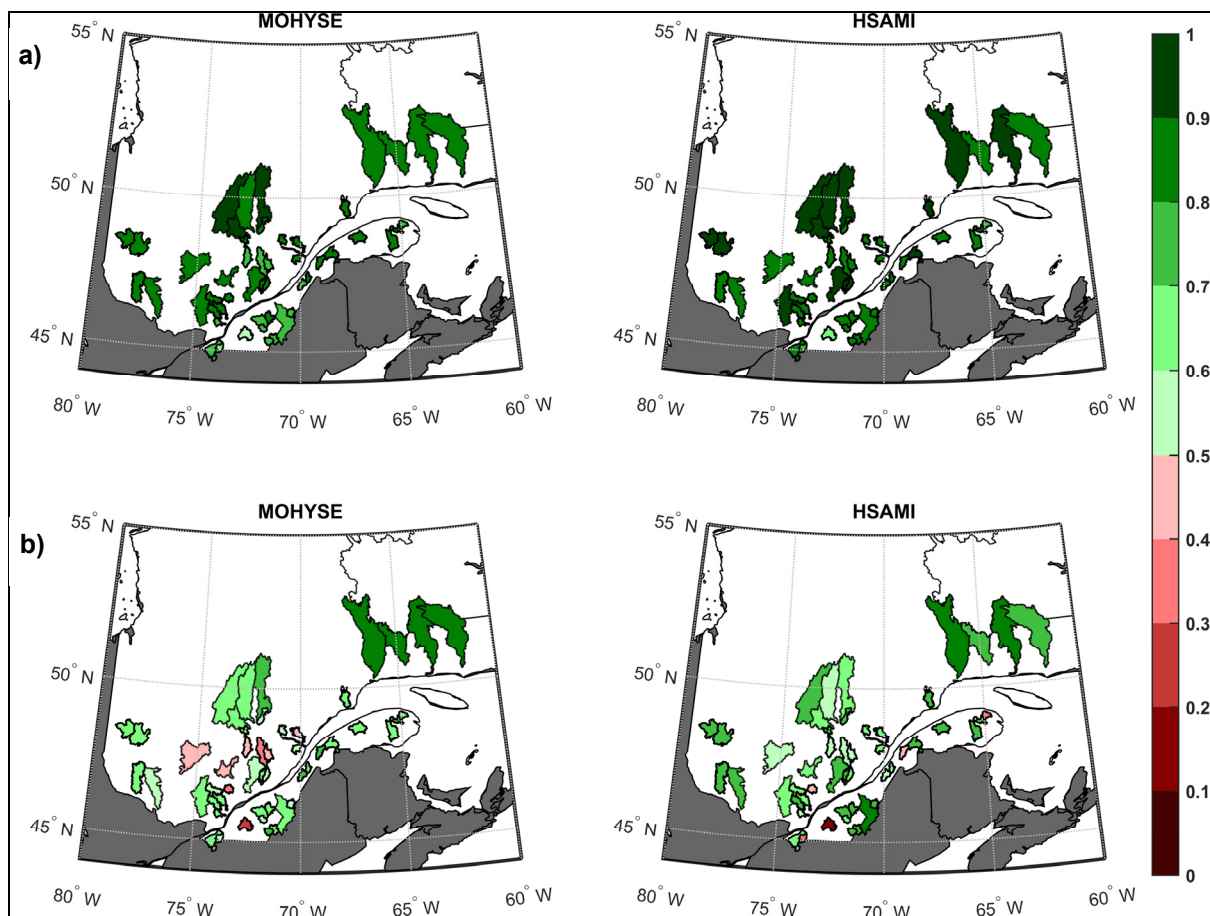


Figure 4.10 Map of the KGE values on the validation years with the OF-1 over the fifty watersheds. The upper panels (a) present the performances over the full time series and the lower panels (b) present the performances during summer-fall months (June-October)

Figure 4.10 illustrates the KGE performance values obtained for the objective function 1 (OF-1) that uses the KGE criteria over the full time series. The upper panel shows the evaluations over the full time series where a generally good performance is observed for both models with average values ranging between 0.8 and 0.9. However, HSAMI outperforms MOHYSE in most catchments. During the summer-fall months, similar performances are observed over the larger catchments for both models. However, differences are observed over the small watersheds, where MOHYSE presents more KGE values under 0.5 than HSAMI.

Figure 4.11 presents the performance results obtained with the OF-2, where the function targets the summer-fall months.

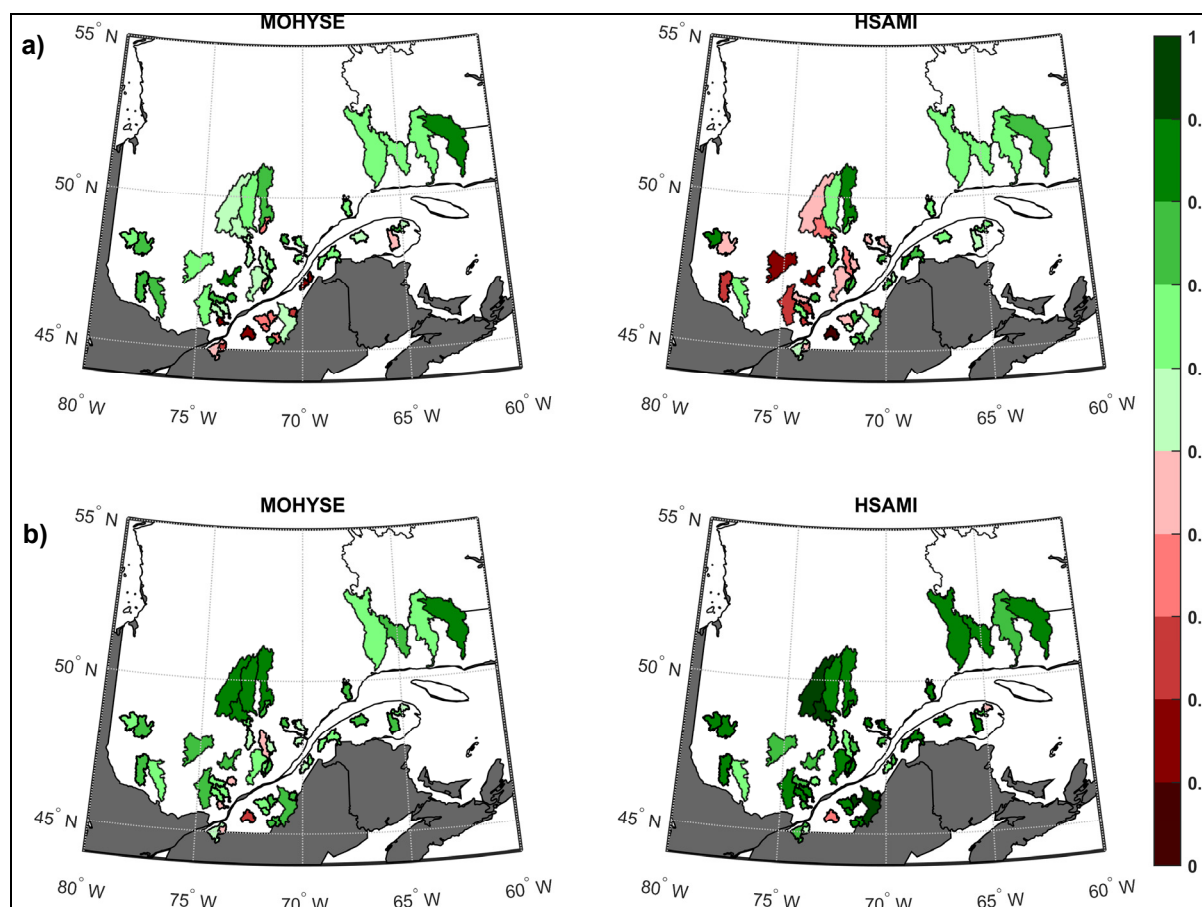


Figure 4.11 Map of the KGE values on the validation years with the OF-2 over the fifty watersheds. The upper panels (a) present the performances over the full time series and the lower panels (b) present the performances during summer-fall months (June-October)

The upper panels show that MOHYSE perform better than HSAMI on many watersheds over the full time series evaluations. Indeed HSAMI presents performance values ranging down to 0.1 on small or medium sized catchments. The contrary is observed on the lower panels where HSAMI generally perform better during the summer-fall months.

Figure 4.12 presents the KGE values obtained with the OF-3, where the custom function gives half the weight to the interannual KGE evaluation and the other half corresponds to the summer-fall performance.

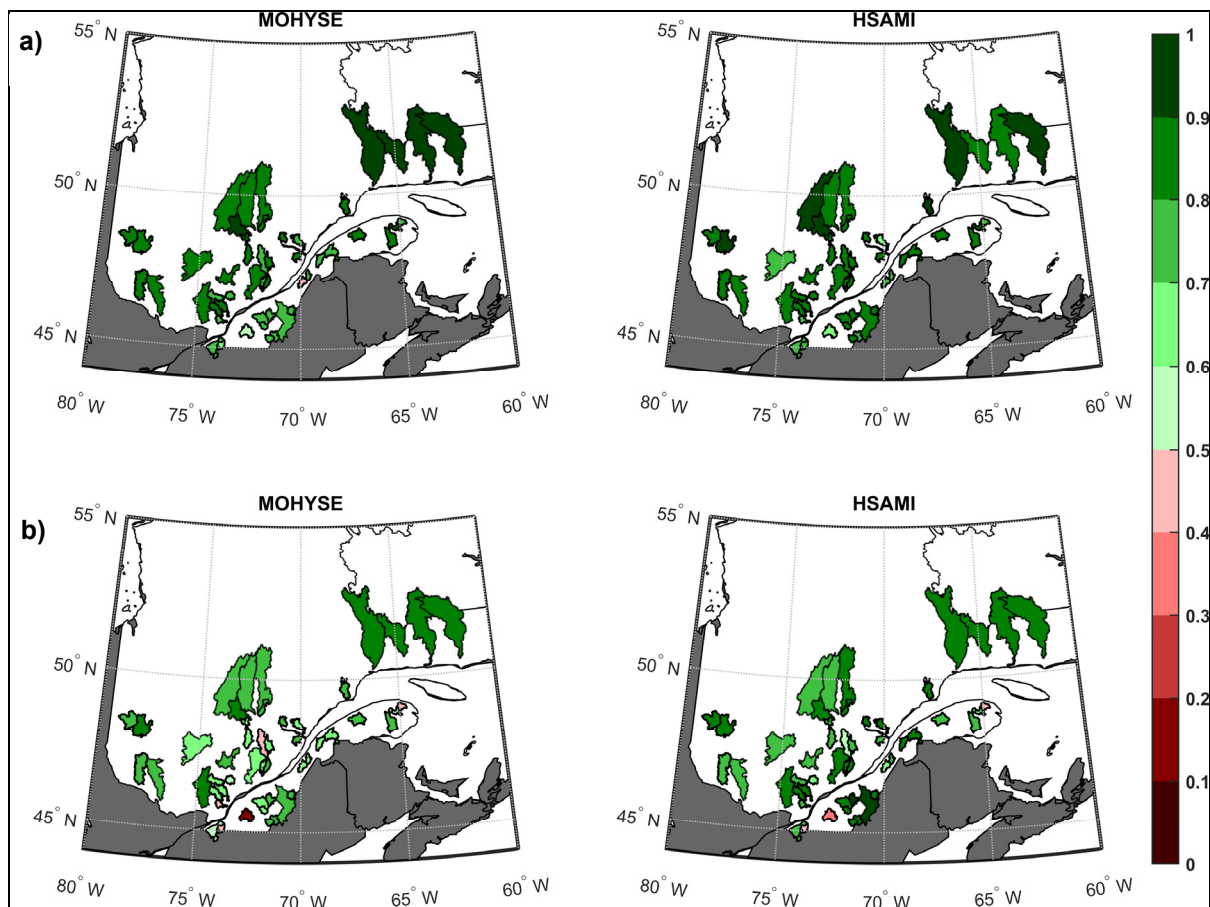


Figure 4.12 Map of the KGE values on the validation years with the OF-2 over the fifty watersheds. The upper panels (a) present the performances over the full time series and the lower panels (b) present the performances during summer-fall months (June-October)

The upper panels show that both models have good performances with average KGE values above 0.8. On the lower panels similar results are observed for both models, with average values generally between 0.7 and 0.8. A good performance is observed over the full time series and summer-fall series evaluations for both models. HSAMI slightly outperforms MOHYSE in some watersheds during the summer-fall months (see lower panels).

4.2.1.2 Hydrological model parameter sets

Figures 4.13 and 4.14 present the distributions of the KGE values obtained with the three different calibration approaches for the calibration and validation years respectively. The performances over the full time series and the summer-fall months are presented for both models. Figures 4.13 and 4.14 present the same results as Figure 4.9, but in a different manner emphasizing the choice of objective function.

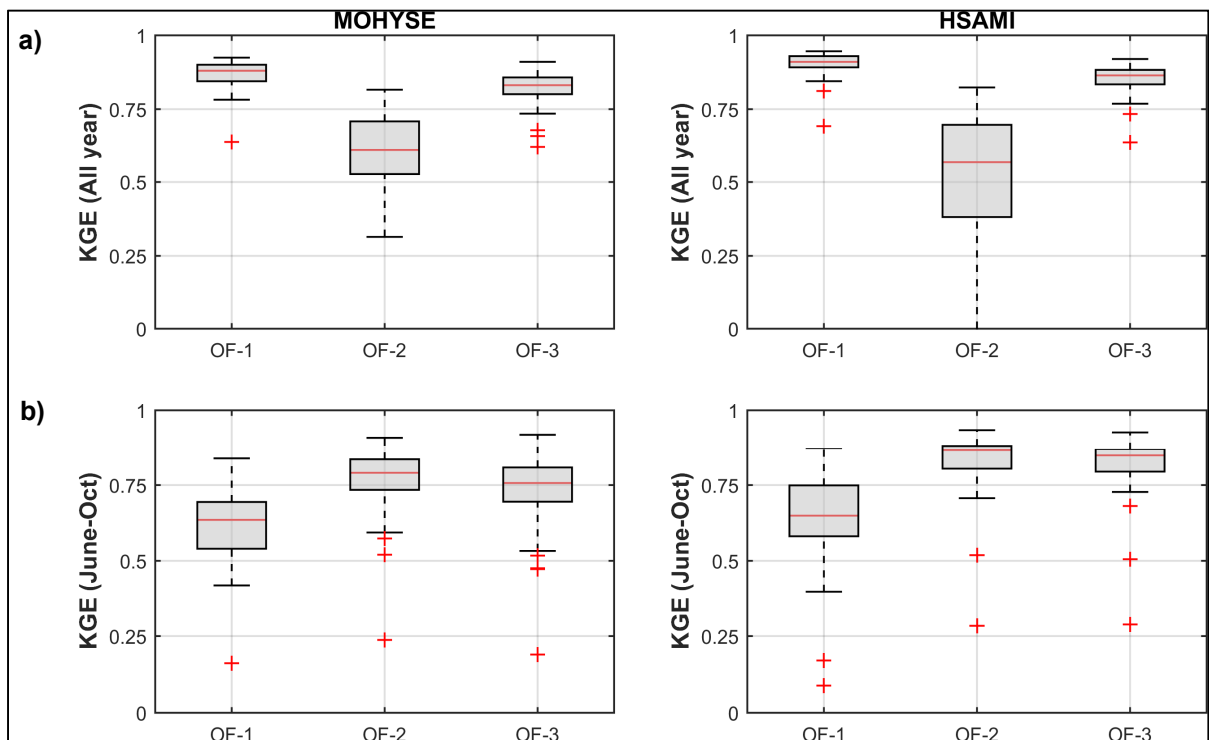


Figure 4.13 KGE values of the 50 watersheds for the different calibration approaches on the calibration years. The upper panels (a) present the KGE values for the full-time series and the lower panels (b) present the values for the summer-fall months

Over the calibration years (Figure 4.13a), both models perform well with either OF-1 or OF-3. Both models perform clearly worse using OF-2 to simulate the full time series, with HSAMI being worse than MOHYSE. The opposite behaviour is observed during the summer-fall months (Figure 4.13b). However, good performances are also observed with OF-3, while the worst results are observed with OF-1.

For the validation years (Figure 4.14) results are similar to the previously observed over the calibration years. On the evaluations on the full time series, OF-2 gives the worst results. For the summer-fall period, OF-2 performs well for both models. OF-3 presents good KGE values for both models.

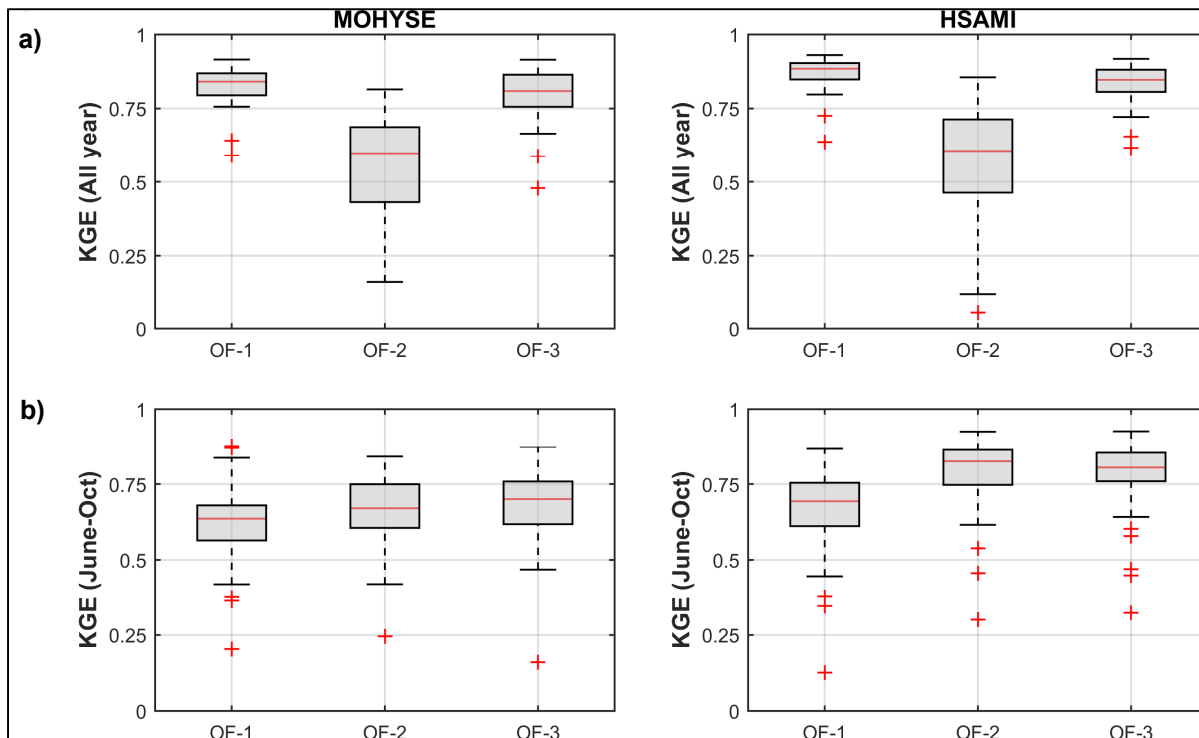


Figure 4.14 KGE values of the 50 watersheds for the different calibration approaches on the validation years. The upper panels (a) present the KGE values for the full-time series and the lower panels (b) present the values for the summer-fall months

In general, HSAMI outperforms MOHYSE in most of the cases, with a better mean KGE value and tighter interquartile range.

4.3 Climate model driven streamflow simulations

This section presents the comparisons between the streamflows generated with CRCM5 climate outputs. The KGE and the relative bias are presented for the different comparisons.

4.3.1 Spatial resolutions

Figures 4.15 and 4.16 show seasonal comparisons of streamflows simulated with climate data with different resolutions by using the KGE and the relative bias respectively.

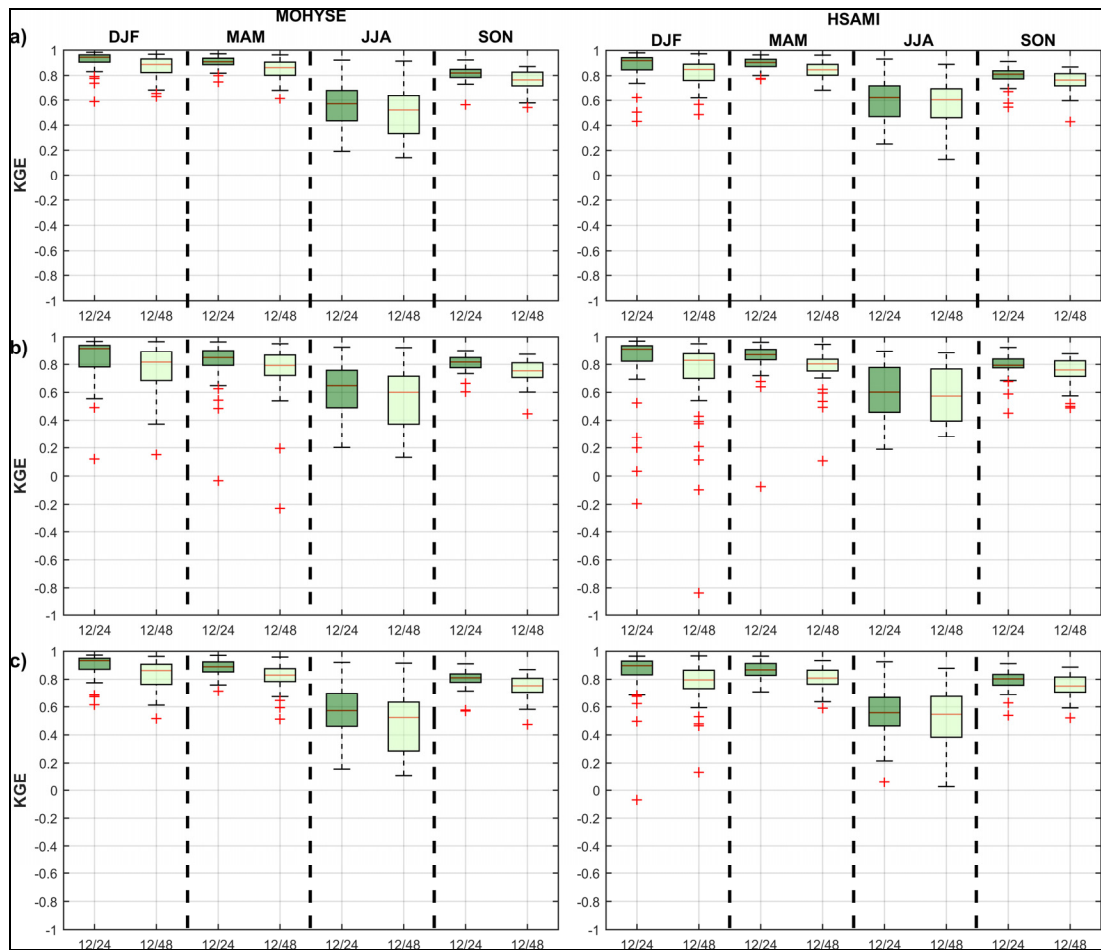


Figure 4.15 Seasonal KGE values of the comparisons between streamflows generated with climate outputs at different resolutions. The upper panels (a) present the results obtained with OF-1, the middle panels (b) present the results obtained with OF-2 and the lower panels (c) present the results obtained with OF-3

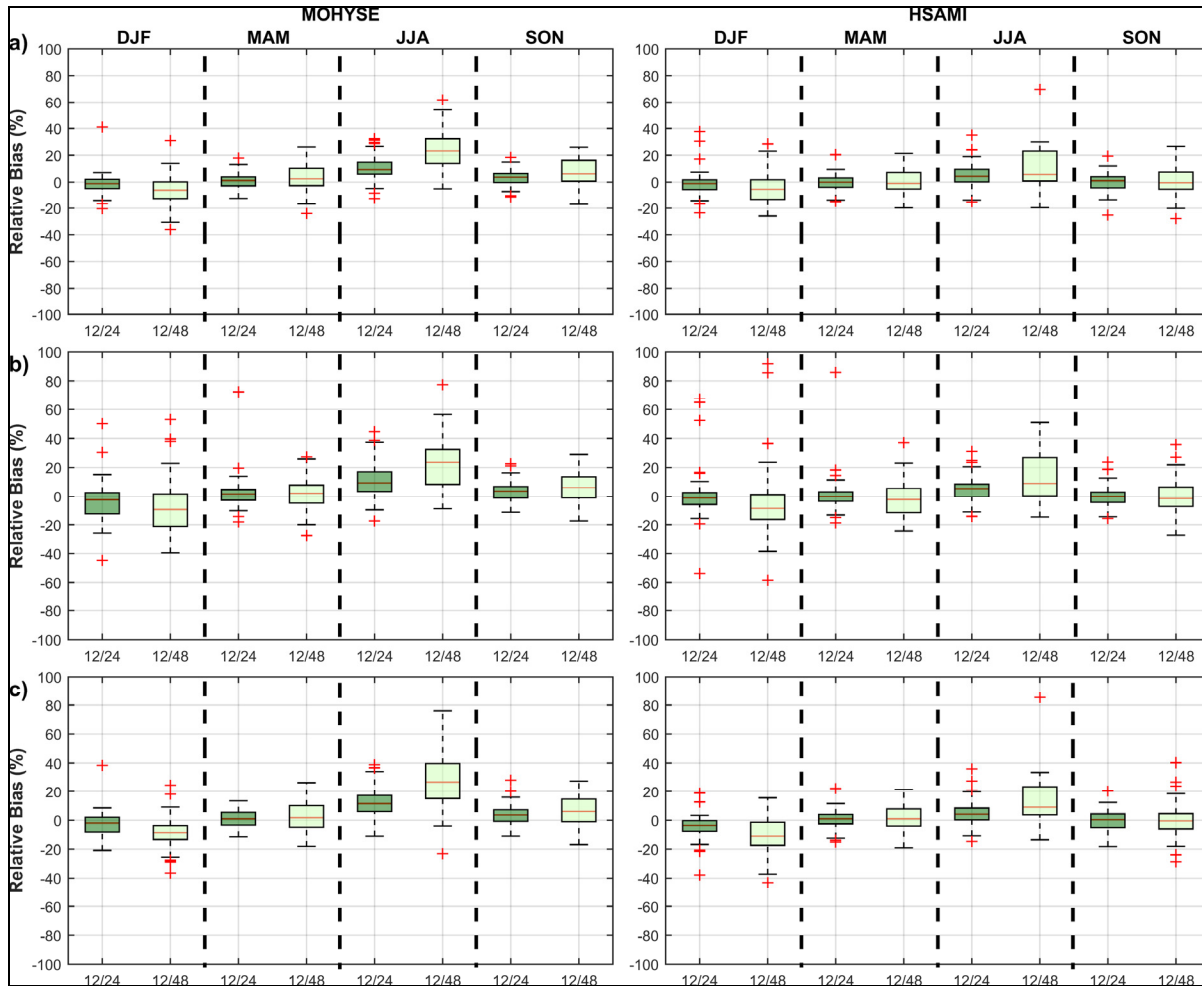


Figure 4.16 Seasonal relative bias values of the comparisons between streamflows generated with climate outputs at different resolutions. The upper panels (a) present the results obtained with OF-1, the middle panels (b) present the results obtained with OF-2 and the lower panels (c) present the results obtained with OF-3

Figure 4.15 shows the comparisons evaluated by using the KGE criterion. Smaller differences are observed between streamflows simulated with 12 km and 24 km resolutions than between the 12 km and the 48 km resolutions. These differences are observed for all seasons, with the largest differences observed during the summer months (June, July and August). This tendency is observed for both hydrological models and for the three calibration approaches.

On the seasonal relative bias distributions (Figure 4.16), similar trends are observed. Smaller relative biases are observed between the finer resolutions for the three calibration approaches. In other words, the larger the difference is in resolution, the larger the difference is for streamflows for both models and both indicators.

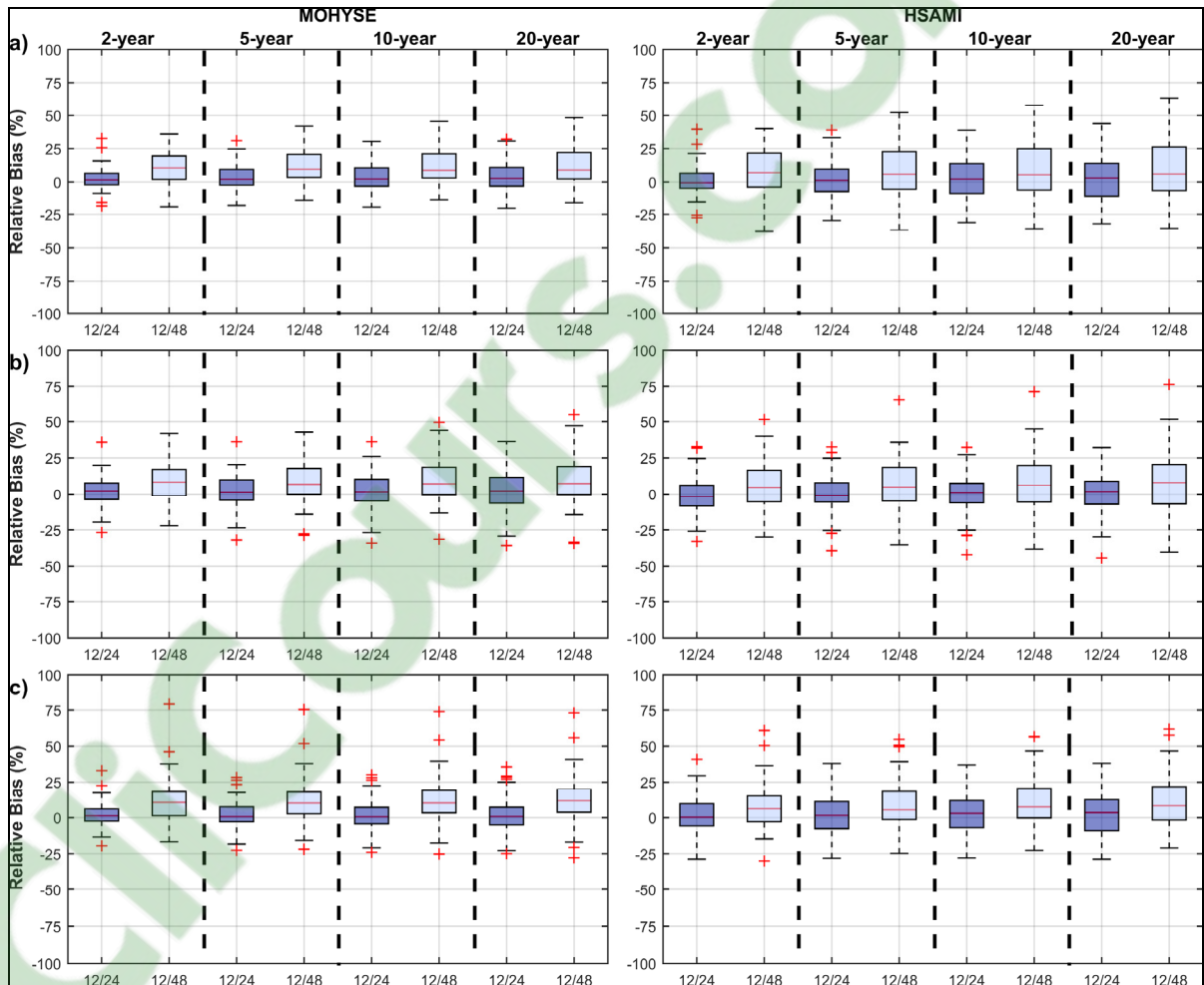


Figure 4.17 Relative biases (%) between the return periods (2, 5, 10 and 20-year) of the different generated streamflows. The upper panels (a) present the results obtained with OF-1, the middle panels (b) present the results obtained with OF-2 and the lower panels (c) present the results obtained with OF-3

Figure 4.17 shows the comparisons between flood indicators obtained from the generated summer-fall peak streamflows. Both hydrological models show an increase in the summer-fall floods return periods with increasing resolution. This tendency is observed for the three

different calibration approaches. Moreover, an increasing difference between floods is observed with increasing return periods.

4.3.2 Hydrological model parameter sets

In order to address the study of the hydrological models parameter sets, Figures 4.18 and 4.19 present the comparisons between streamflows simulated with the different calibration approaches. The comparisons are presented by using the KGE and the relative bias respectively.

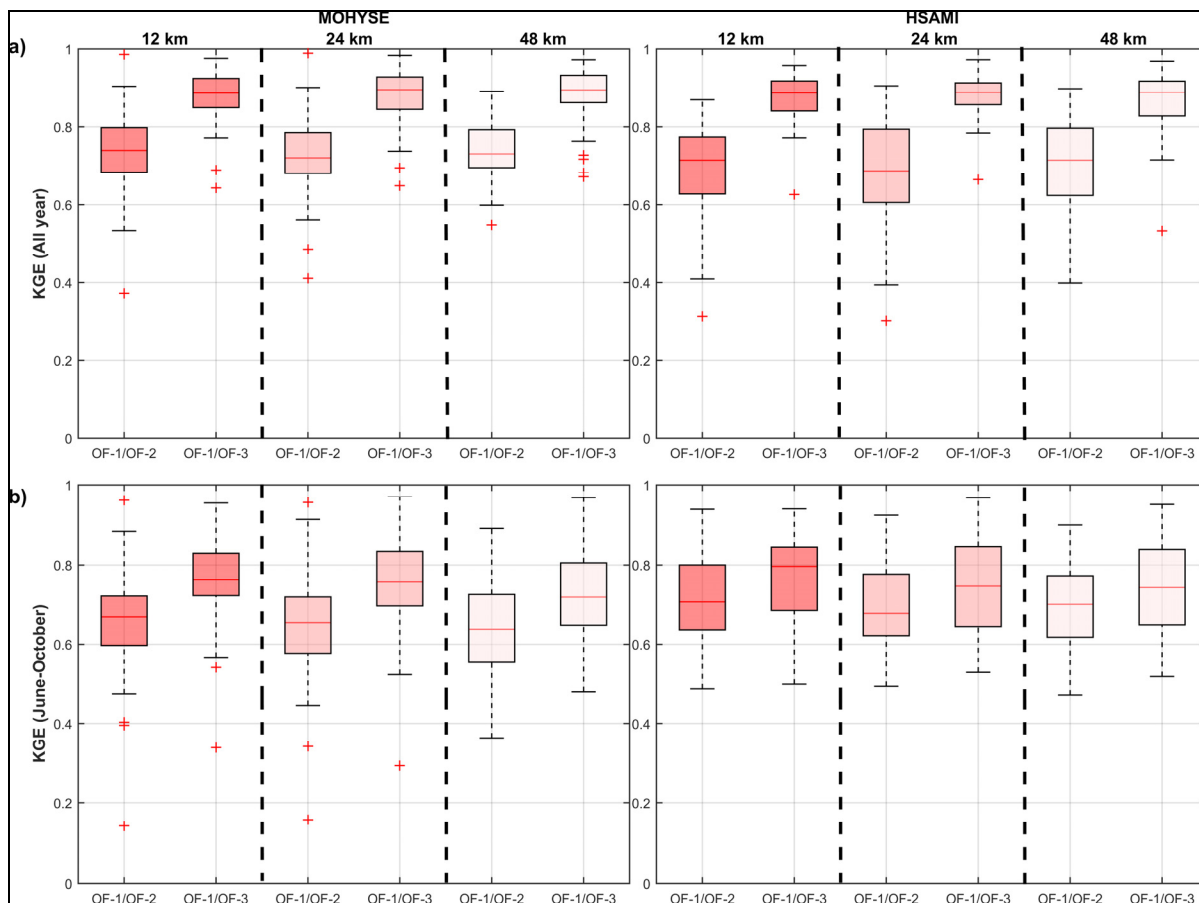


Figure 4.18 KGE values between generated streamflows with different calibration approaches. The upper panels (a) present the results obtained on the full-time series evaluations and the lower panels (b) present the results obtained on the summer-fall months

Figure 4.18 shows that both models are similarly impacted by the use of different calibration approaches. Both models preserve similar average values on the different distributions. On the other hand, MOHYSE shows a larger spread of results as larger distributions are observed on the different comparisons, and especially so during the summer-fall months.

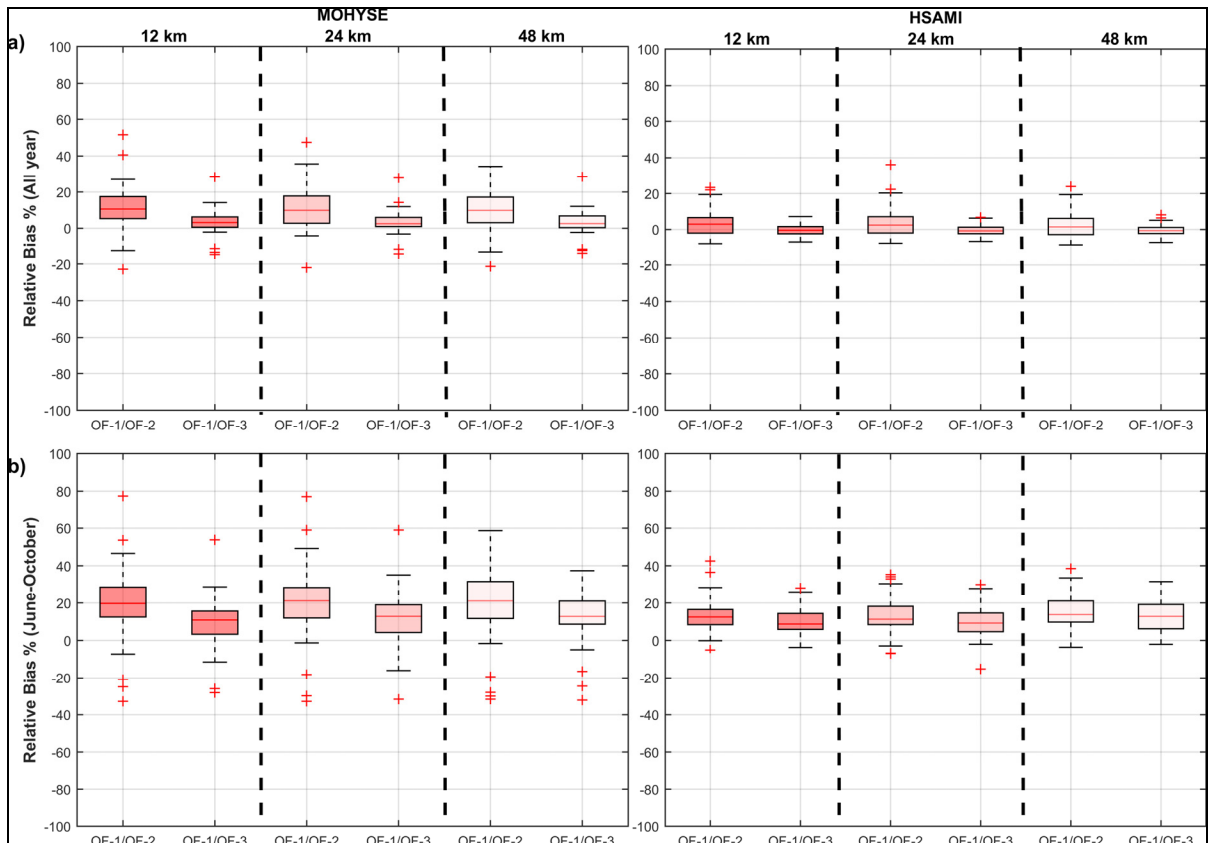


Figure 4.19 Relative biases (%) between generated streamflows with different calibration approaches. The upper panels (a) present the results obtained on the full-time series evaluations and the lower panels (b) present the results obtained on the summer-fall months

As was the case with KGE values, the relative biases presented in Figure 4.19 display similar tendencies for both models. No significant differences are observed between generated streamflows with different calibration approaches for the different climate datasets. Moreover, MOHYSE seems to display larger differences than HSAMI.

Figure 4.20 present the relative biases of four return periods. The comparisons show small differences between them as the average values between distributions are very close together. MOHYSE again shows a larger spread of values compared to HSAMI.

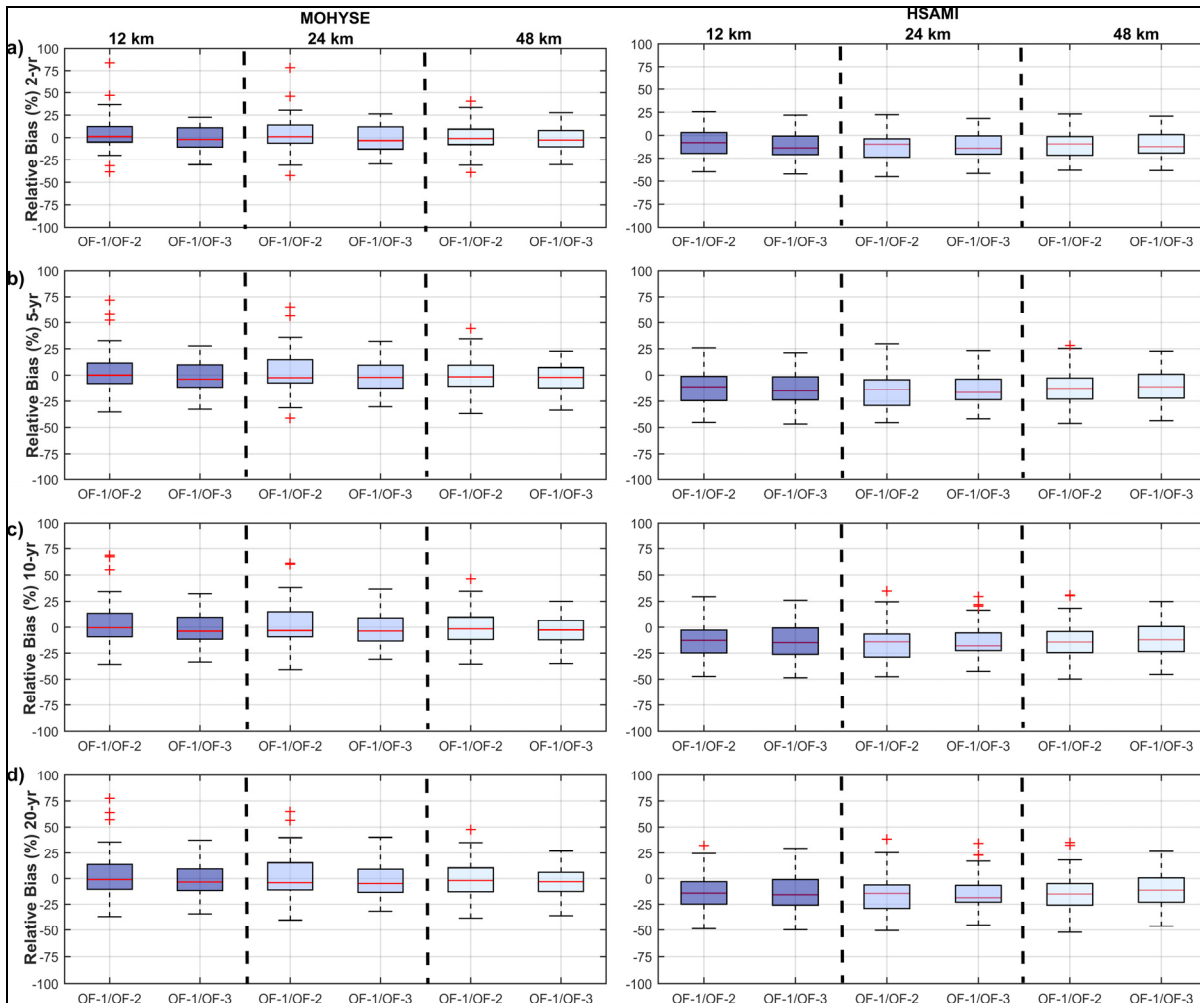


Figure 4.20 Relative biases (%) between return periods of the generated streamflows with different calibration approaches. The first panels (a) present the comparisons of 2-year return periods, the second panels (b) the comparisons of 5-year return periods, the third panels (c) the comparisons of 10-year return periods and the fourth panels (d) the comparisons of the 20-year return periods

Overall, smaller differences are observed between the generated streamflows and their flood indicators when using different calibration approaches.

CHAPTER 5

DISCUSSION

This chapter presents the discussion and interpretation of the main results presented previously. The discussion will first be oriented on the comparison of CRCM climate simulations. Then, streamflow simulations and the impact of spatial resolution on flood return periods will be discussed. For sake of clarity, the use of “increasing resolution” will refer to a refinement of the resolution, i.e. a reduction in the size of the model mesh.

5.1 Impact of spatial resolution climate outputs

The main goal of this research project was to evaluate the impact of regional climate model spatial resolution on the hydrological modelling of summer-fall floods. To do so, three specific objectives were defined. The first aimed at evaluating the impact of resolution on temperature and precipitation outputs.

The impact of CRCM spatial resolution was evaluated through the intercomparison of datasets with different resolutions for the summer and fall seasons. In order to isolate the resolution as the studied variable, the comparisons were performed between datasets issued from the same versions of the CRCM. Then, no comparisons were made between datasets issued from the CRCM4 and CRCM5. In other words, the comparisons were all made for CRCM4 and CRCM5 outputs separately.

In general, the various comparisons for CRCM4 and CRCM5 temperature demonstrate a relationship between model resolution and outputs. However, the impacts differed for the two different CRCM versions. First, for the comparisons performed between the CRCM4 datasets presented in Figure 4.1, seasonal differences were observed for the comparisons with different drivers (CGCM and ERA40c). During the summer, the CGCM comparison presented a variable hot and cold bias while a consistent hot bias was observed during the fall months. On the other hand, the ERA-40c comparison showed the opposite trend during the

fall, a cold bias over the province and a more consistent cold bias during the summer with few hot patches in the center of the province. These differences could be caused by a number of sources because the CRCM4 datasets have important differences that must be taken into account. For example, these climate simulations were performed with different drivers (CGCM and ERA40c), and, more problematically, different domains for each resolution (Quebec-15km, and North America-45km). Hence, the attribution of discrepancies in temperature values between the different CRCM4 simulations is a combination of differing spatial resolution and computational domains. It is thus impossible to specifically attribute the noted differences to a single source. The computational domain can play an important role in model outputs. For instance, when the grid points are close to the boundaries, the driver has a larger impact on the simulation. Consequently, this effect weakens as the grid points are farther from the boundaries. Recent studies (P. Roy et al., 2014) have demonstrated that the domain size and climate model driver both have large impacts on the simulation of climate variables (i.e. precipitation), which seems to correspond to the results obtained in this study.

The analysis outlined important differences in the CRCM4 simulations from both drivers. In temperature comparisons, opposite trends were observed during both seasons. Differences between 10 and 30 % were observed for precipitation seasonal relative biases, originating from the choice of driver. Therefore, it can be inferred that the driver, as well as the domain size, contribute to the differences observed in the presented comparisons. Isolating the effects of climate model resolution in such a multivariate environment is therefore challenging, especially given the lack of comparative model simulations that could help in the process. For example, having access to 15-km simulations over the North American domain or 45-km runs over the Quebec domain would help determine the sources of uncertainty and improve accuracy in the estimation of model spatial resolution impacts on climate variables. These first results highlight the need to evaluate datasets sharing common domain size and drivers. For this reason, the rest of this discussion will focus on the results obtained with the CRCM5 simulations.

The CRCM5 temperature comparisons (Figure 4.2), allow for a clearer picture to emerge with respect to the impact of spatial resolution on model outputs. The impact of spatial resolution could result in up to a 3 degrees Celsius difference in some regions. Precipitation outputs were also impacted by the spatial resolution. Figure 4.6 presented the seasonal relative biases of precipitation. It shows a clear increase in biases when increasing resolution during the summer months. The 12 km (0.11°) resolution dataset presented a consistently more humid bias than the coarser resolutions. Relative biases between 10 to 20 % were observed between the 12 km and the 24 km resolution datasets while the 12 km and 48 km comparisons reached values up to 40 % in the south of the province. In other words, summer precipitation increased with the increasing resolution. However, during the fall season this behaviour was not observed, as dry and humid patches varied in different parts of the province.

The impact of spatial resolution was also evaluated by comparing the variance ratios of climate outputs in order to evaluate changes on extremes. Both climate outputs (temperature and precipitation) showed sensitivity to the increasing spatial resolution in this regard. However, the impact was different for each climate variable. The variance ratios of the CRCM5 temperatures (see Figure 4.4) increased by approximately 10 to 15% with the increasing spatial resolution for both summer and fall. For precipitation, the ratio of the variances in Figure 4.7 also varied with the increasing resolution. Larger increase percentages are observed in the southern part of the province. This is especially true during the summer months where the variability increases by up to 50 % in some regions. Overall, the increasing resolution shows larger impacts on the variance of precipitation than for temperature. This is especially the case for the summer season. This increase in precipitation variance could be very important to trends of future flooding events. The increase in variance suggests an increase of extreme rainfall events for summer-fall months, with a likely corresponding increase in flood events. Accordingly, the impact of spatial resolution adds a layer of uncertainty for climate change impact studies concerning summer-fall floods.

5.2 Climate model-driven hydrological streamflow simulations

This section discusses the impacts of spatial resolution on streamflow simulations. As presented in the results, the differences observed for precipitation and temperature datasets resulted in streamflow differences.

5.2.1 Generation of the climate model-driven hydrological streamflows

The hydrological modelling of streamflows was performed by calibrating the hydrological models on weather observations and then feeding the different RCM climate datasets to the calibrated hydrological models. The calibration of the hydrological models on observed data is expected to add uncertainty to the obtained results due to the inevitable problems related to the quality of historical records (i.e. lack of data, biases in the measurements, etc.). Thus, the parameters obtained from the hydrological model calibration process could be biased as well. This uncertainty was then expected to be transferred to the hydrological simulations as the same parameters were used to generate the climate-driven streamflows.

In addition to the abovementioned caveat, the use of three different calibration approaches could have an influence on the streamflow simulations. This was presented by Arsenault et al. (2015) where it was shown that the objective function plays an important role on the streamflow simulations depending on how the hydrograph is targeted. Regarding extreme events simulation, it was presented that the calibration on mean hydrographs values leads to reduction in simulated extreme values. For this reason, the calibration of the hydrological models using objective functions based on mean values such as the interannual means, could lead to a less robust estimation of flooding events. In other words, the variance of the datasets is reduced when targeting mean trends. Therefore, for this study, summer-fall floods were specifically targeted in two of the objective functions.

However, for climate change impact studies, this dataset-specific calibration could not be done in the same way using climate model outputs since there are no corresponding streamflow outputs to guide the calibration.

5.2.2 Spatial resolution effects on climate model-driven hydrological streamflows

As presented in chapter 4, the KGE criterion and the relative bias were used to evaluate the impacts of the climate simulations spatial resolution on modelled streamflows. In general, both indicators were impacted by spatial resolution for both hydrological models (HSAMI and MOHYSE). Increases of up to 20 % were observed in the seasonal means of both indicators when increasing spatial resolution. These results were expected after systematic biases were observed for precipitation and temperature that were used as input for the hydrological models. The combination of colder temperatures and increasing precipitation favored the increase in the streamflow differences. These trends agreed with the results recently presented by Lucas-Picher et al. (2016). That study found that more precipitation was obtained on the finer resolution simulations of CRCM5. The added spatial resolution increased precipitation amounts in comparison to observations during the summer months (June July and August). Curry et al. (2016a, 2016b) also found similar trends when comparing CRCM4 precipitation datasets over British Columbia, for three river basins where the finer resolution presented smaller biases compared to observations for precipitation extremes represented by the 90th quantile.

Results obtained in this study showed seasonal and regional variations. The larger biases during the summer months were especially observed on the southeastern side of the province where the majority of the studied watersheds are located. The consistent humid biases combined with colder temperatures during the summer on the majority of the watersheds explain the larger biases on the local streamflow simulations. Regional differences make the extrapolation of those results to other regions very difficult. For instance, over northern Quebec, opposite trends were observed for certain grid points.

5.2.3 Flood indicators

The results presented in section 4.3 for summer-fall floods indicators revealed that the spatial resolution of the CRCM5 simulations impacted the probability of occurrences of extreme flooding events.

Figure 4.17 clearly showed the impact of resolution on floods of various return periods. Increases of around 15 % were consistently observed in the mean relative biases of both models and four flood indicators. The results also showed a systematic increase of the relative biases with increasing return periods. In other words, when the probability of occurrence was lower (i.e. the 20-year return period) the bias of the summer-fall peak flows was more biased than for a “less” extreme flood (i.e. 2-year return period). This is in line with recent studies performed in different regions of the world (Mendoza et al., 2016; Naz et al., 2016; Zhao et al., 2013). These studies presented different mean trends as the studies were performed in regions with different hydrological regimes. In spite of this, similar trends were observed on the analyses of extremes, with increases for both low and large runoff values. Overall, results in this and other studies clearly outline the impact of climate model spatial resolution on extreme floods.

5.3 Hydrological models structure and parameters impacts

The specific objectives 2 and 3 aimed to evaluate the impact of the hydrological models, differing in their structure and parameterization. Thus, two hydrological models, HSAMI and MOHYSE, were used in this study.

In general, the results presented with the KGE, relative biases and flood indicators in the section 4.3.2 did not vary much due to the choice of hydrological model and parameter set. However, it is important to recall that both hydrological models are of the same conceptual lumped category. This means that the climate simulations were spatially averaged for each

river basin. For this reason, it is not entirely possible to quantify and evaluate the impacts of hydrological model structure, since both models belong to the same general category.

Moreover, in spite of the model similarities, some differences were observed between them. HSAMI showed a generally more consistent behaviour, with tighter distributions and fewer outliers. The parameter sets also shown different influences depending on the hydrological model. The streamflow comparisons for the different calibration approaches presented in section 4.3 showed that HSAMI has larger differences when using the different parameter sets. In other words, the generated outputs were more variable depending on the objective function used. This was expected as HSAMI has more than twice the number of parameters (23 parameters) of MOHYSE (10 parameters). Thus, HSAMI can typically better fit the fixed target on the objective function. This performance is justified as HSAMI presents more degrees of freedom to adapt the parameters to represent the different hydrological processes. Unlike MOHYSE which shows less flexibility and thus has more difficulty to represent certain processes and does so with less accuracy when compared to HSAMI. In addition, HSAMI has been showed to be more robust to the different parameter sets over the province (Arsenault & Brissette, 2016; Arsenault & Brissette, 2014). This means that HSAMI was less sensible to changes on the climate inputs than MOHYSE. Therefore, more consistent distribution of results was observed with HSAMI.

5.4 Regional climate model configuration

For all the climate modelling scenarios presented in this study, the initial states inputs and internal parameters are expected to have different levels of impact on the simulated variables (Elía & Côté, 2010; Murphy et al., 2004). The number of studies related to this subject confirms that the sensitivity of the different climate model parameters and initial configurations is of big importance in the scientific community. Thus, many sources of uncertainty have been studied in order to identify their impacts (Falloon et al., 2014; Lee & Bae, 2016; Thiboult et al., 2016; Troin et al., 2016).

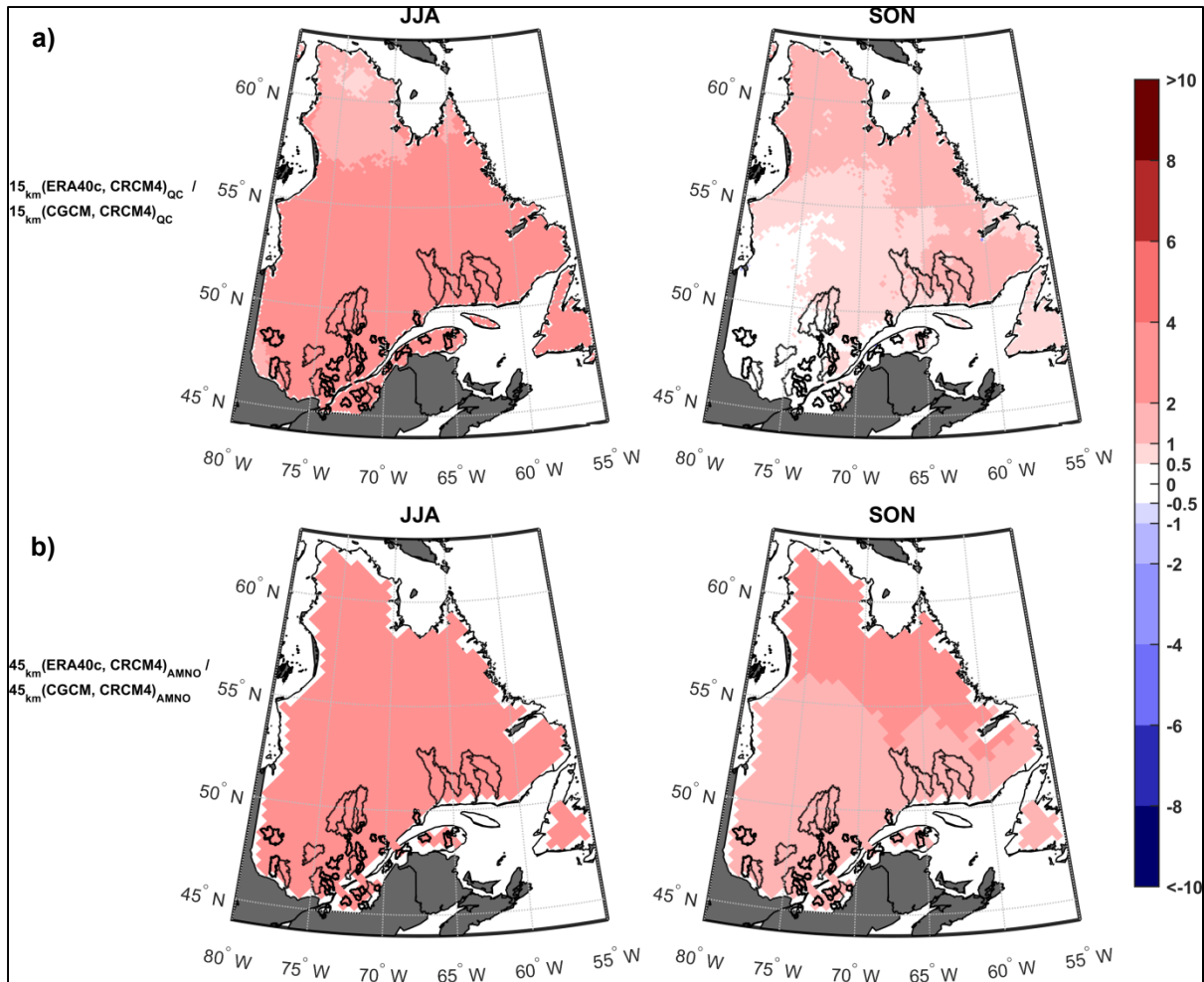


Figure 5.1 Annual daily mean bias of temperature ($^{\circ}\text{C}$) between simulations issued from CRCM4 for the summer (JJA) and fall (SON) seasons for the period 1981-2010. The upper panels (a) show the comparisons for the 15 km resolution datasets with different drivers. The lower panels (b) show the driver comparison for the 45km resolution datasets

As mentioned in section 5.1, the domain size and regional climate model driver have been shown to have an impact on the climate simulations (Curry et al., 2016a; Laprise et al., 2012). The CRCM4 climate simulations used for this study presented some of these climate model configuration differences as well as different climate model drivers. Thus, comparisons were added to evaluate the impact of the climate drivers on the temperature and precipitation simulations (see Figures 5.1 and 5.2).

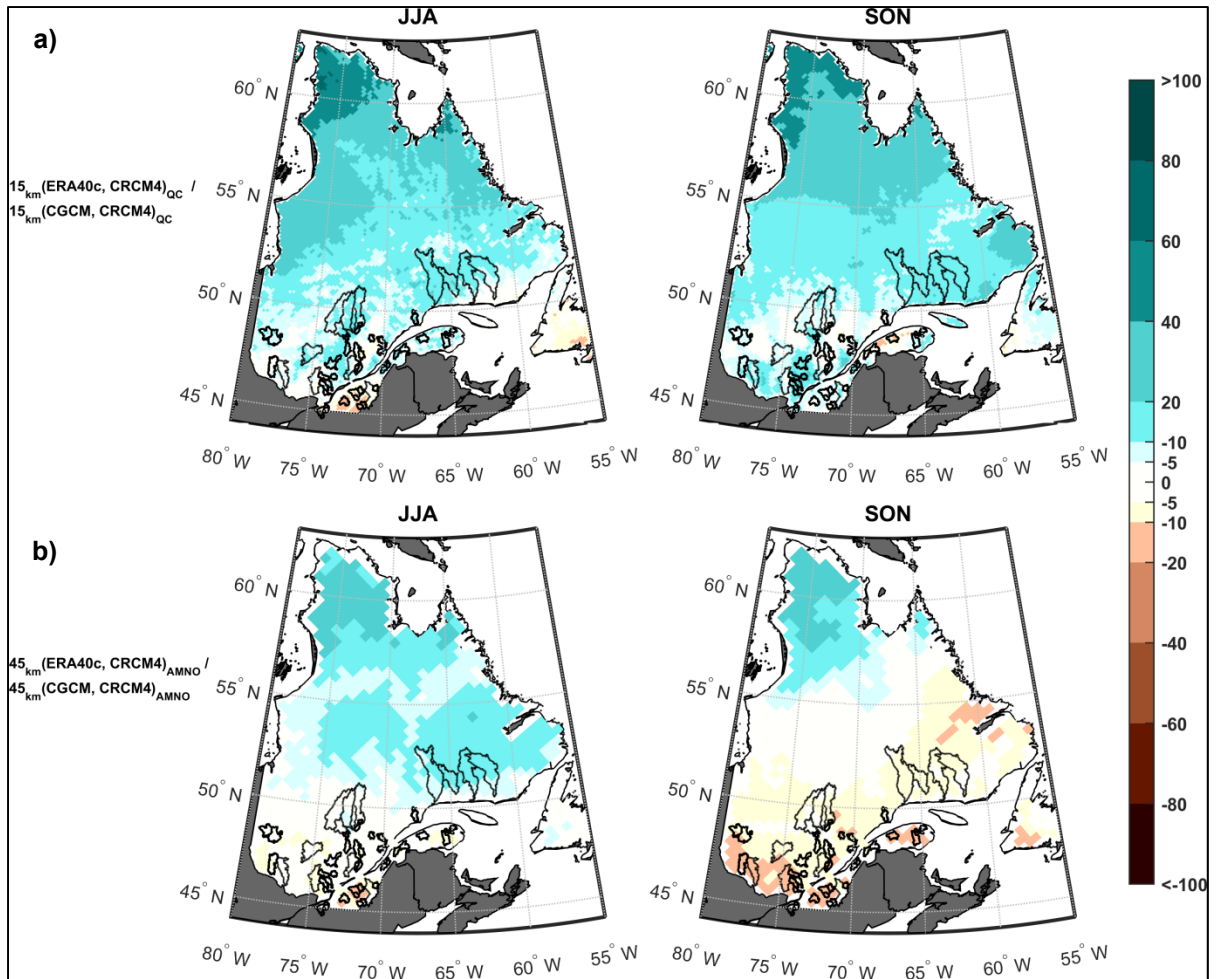


Figure 5.2 Annual daily mean relative biases (%) of precipitation (mm) between simulations issued from CRCM4 for the summer (JJA) and fall (SON) seasons for the period 1961-1990.

The upper panels (a) show the comparisons for the 15km resolution datasets. The lower panels (b) show the comparison for the 45km resolution datasets

The results show that the different drivers have behaved considerably differently when considering climate outputs, i.e. temperature and precipitation. Figure 5.1 confirms that the driver has an effect, presenting absolute biases reaching up to 4 degrees Celsius during both seasons. However, slightly larger impacts are observed during the summer months, which is especially true on the 45 km resolution comparison (lower panel). Variance analyses were also performed and confirmed that the driver impacts the results. These figures are presented in appendix II.

Likewise, the climate model driver was shown to impact precipitation outputs. The impact differs depending on the spatial resolution, with the 15 km resolution simulations appearing to be more biased depending on the climate model driver than the 45km resolution simulations during both seasons. This additional analyses confirms the decision to focus the spatial resolution analyses on the CRCM5 simulations, were the outputs share common domain and driver. These results confirm the need of further analyses of the impacts of the CRCM configuration on hydrological modelling.

5.5 Streamflow simulations and catchment size

Previously shown results confirmed the impacts of the CRCM spatial resolution on the hydrological modelling of summer-fall floods. However, this impact is likely to be different in function of the size of the catchment.

Small catchments are expected to be more strongly impacted by the spatial resolution, as the local climate trends are limited by the size of the grid of the regional climate model. This means that there are fewer grid points in a small area than in a larger area. For this reason, an additional analysis was done to explore the impact of spatial resolution as a function of catchment size. Figure 5.3 presents the relative biases between the return periods of the CRCM5 streamflows grouped by catchments smaller than 1000 km² (named *s*) and larger than 3000 km² (named *L*) for both models using the OF-2, which is the objective function targeting the summer-fall months.

Overall, a consistent difference is observed in the results for the smaller and larger catchments for the different return periods. The results confirm that the small catchments present larger bias due to the spatial resolution. In addition, the impacts are observed to systematically increase when increasing the return periods. These results were also observed on the analysis with the KGE criterion and relative biases, which can be found in the appendix III.

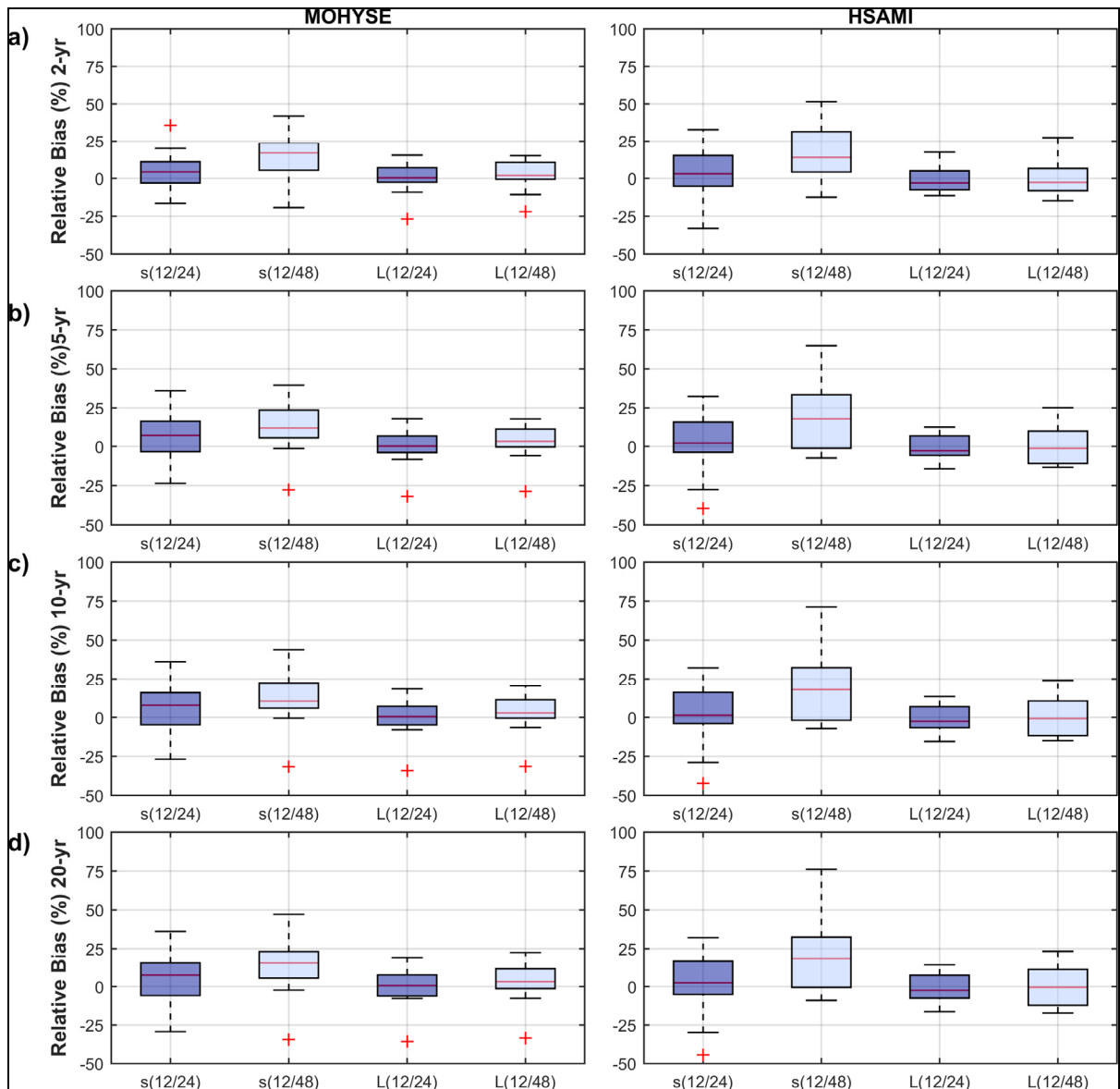


Figure 5.3 Relative biases (%) between the return periods (2, 5, 10 and 20-year) of the generated streamflows with CRCM5 outputs at different resolutions grouped by small (s) and large (L) watersheds for the OF-2. The first panels (a) present the comparisons of 2-year return periods, the second panels (b) the comparisons of 5-year return periods, the third panels (c) the comparisons of 10-year return periods and the fourth panels (d) the comparisons of the 20-year return periods

These results present evidences confirming the importance of finer spatial resolutions to analyse hydrological regimes of small catchments. The finer resolutions were observed to be of more importance for the analysis of small regions by better representing the variability of

the climate variables. This is especially the case for precipitation. In addition, when transferred to the hydrological analysis, small catchments are expected to respond differently to the increase of extreme events such as heavy rainfalls.

5.6 Limitations

Due to the scope of this project, the obtained results and analyses are subject to the following limitations. Thus, any extrapolation of the conclusions should be made with caution.

First, the results are limited to the study region. The analyses were performed over 50 watersheds in the southern part of the province of Quebec. Consequently, the results were interpreted at the local scale. Different results can be expected if the methodology was reproduced in another region with different characteristics (i.e. climate, topography, vegetation, etc.).

The climate model is also another important limitation of the methodology. The analyses were performed with two versions of the CRCM, thus the conclusions can only be applied to this regional climate model. The climate model configuration (driver, domain and resolutions) also limited the analyses. Besides, no post-processing was made to the climate simulations, adding another limitation of the analyses.

Other important limitations are related to the hydrological modelling. Two lumped hydrological models with different complexities were used only showing small differences. However, as presented in the literature, there are other types of hydrological models that could present different results, such as distributed models. As well, the methodology is limited by the choice of the calibration approaches. The use of other objective functions could impact the obtained results. Coupled with this, the parameter sets are limited by the availability and accuracy of the records of observations.

Finally, regarding the summer-fall floods analyses, the results are limited by the selected methodology. The flood distributions for the four return periods were limited by the period of 30 years and the statistical methods applied. Other extreme indicators with different statistical methods could produce different results.

CONCLUSION

The main objective of this study was to analyse the impact of spatial resolution from different climate simulations issued from two different versions of the CRCM on the hydrological modelling of summer and fall floods in southern Quebec. For this purpose, seven climate datasets were used to explore the role of spatial resolution on temperature and precipitation climate model outputs. In addition, streamflow simulations were computed and analyzed using two different hydrological models over fifty watersheds over a common reference period.

Many variables are involved in the study of the hydrologic impacts of climate change. The process to evaluate those impacts creates a modelling chain starting from the climate model and ending with the hydrological modelling. Uncertainties are added at each step of the chain, including the role of spatial resolution. For the scope of this project, only the effect of spatial resolution, hydrological model structure and parameter set were considered. The following conclusions were drawn:

The first specific objective of this work was to evaluate the impacts of the spatial resolution on the temperature and precipitation outputs. The results obtained from the analysis and comparisons of the climate outputs confirmed that spatial resolution plays an important role in the climate variables simulated by the RCMs. However, varying effects were found during the summer and fall seasons. CRCM4 simulations appeared to show more sensitivity to resolution than CRCM5 for temperature and precipitation. However, as discussed earlier, the interpretation of CRCM4 results is complicated due to the use of different simulation domains and drivers which also have an effect on the climate outputs. It is thus difficult to draw any solid conclusion.

Therefore, focusing on CRCM5 results which used the same driver and domain resulted in clearer trends. CRCM5 temperature simulations show a consistent cold bias with increasing resolution. For precipitation, a humid bias with an increasing spatial resolution was observed

during the summer months. Precipitation and temperature variance increased with increasing spatial resolution; however, a larger impact was observed for precipitation.

Concerning the hydrological modelling, HSAMI and MOHYSE presented good performances over the selected watersheds for calibration and validation periods in regards of the observed historical records. However, HSAMI showed generally better performances for the calibration and validation periods. The calibration and validation results presented that both models were impacted by the different calibration approaches. Nonetheless, HSAMI showed to be more influenced on the use of different parameter sets. This behaviour was expected due to the different number of parameters. HSAMI, a model with 23 parameters, is expected to better fit the target than MOHYSE with only 10 parameters to adjust to the observed datasets.

This research has also provided evidence showing the impact of spatial resolution in the climate driven streamflow simulations. The results showed that the larger the difference of climate model's spatial resolution, the larger the difference between simulated streamflows. This tendency was confirmed for both hydrological models and both indicators, the seasonal KGE and the seasonal relative biases. The increasing impact with increasing spatial resolution was observed to be especially true during the summer months, which could be explained by the larger biases observed in precipitation simulations during those months.

By investigating the summer-fall flood events, an increase on the summer-fall floods return periods with increasing resolution was concluded from both hydrological models. On the other hand, the hydrological models structure and the calibration approaches did not show significant impacts on the summer-fall floods. However, it is important to recall that both models are the same type. Further research is needed to evaluate other models responses.

This study has provided an insight into the spatial resolution impacts on the hydrological modelling of summer-fall floods over Quebec. The results contribute to understand the spatial resolution effects on the streamflows modelling, which could have effects on the

climate change impact studies on hydrology, emphasizing another source of uncertainty to be taken into account.

One of the main limitations on the use and production of climate variables at finer resolutions is the computational power needed to run the simulations. However, the increasing advancements in modelling and computing power means that climate models are expected to become progressively more refined. And thus, the increasing resolutions are likely to have impacts on the extreme events studies which will help to improve the current practices and to develop better techniques to estimate mean and extreme climate and hydrological events.

RECOMMENDATIONS

Thanks to the obtained results and the known limitations, the additional research possibilities are vast. Therefore, recommendations for future work are suggested.

The replication of the study in other regions with different characteristics is suggested for further research. Of particular interest would be to perform a study over a region where pluvial floods (rain-related floods) are dominant. In other words, it is suggested to perform studies in regions where the floods and hydrologic regime are not snow-related.

The use of other climate models is highly recommended to evaluate the impacts over the climate outputs. Additionally, other outputs (i.e. evaporation) of the climate models could be added on the analysis.

For the flood analyses, four flood indicators were used; however, the addition of other extreme indicators is suggested. As well, extreme low flows have become of interest for water management. Thus, the analysis of low flows is suggested for future studies.

As previously mentioned, the project was limited by the selection of two lumped models. Therefore the addition of other types of models such as the distributed and physically-based models might be considered and explored. Also, the exploration of other calibration approaches where the extreme events are the target (i.e. the return periods), could be considered for future works. Also, of special interest would be to perform studies on a several catchments with a large variety of sizes. In this way, the different impacts due to the size of the catchment could be accounted.

Finally, the development of even more refined regional climate model simulations and reanalysis simulations could represent a great tool to compare with the current simulations in order to evaluate and pursue to find the best way to model the climate and hydrological systems as accurate as possible and thus to perform better projections to the future.

APPENDIX I

REGIONAL CLIMATE MODEL DOMAINS

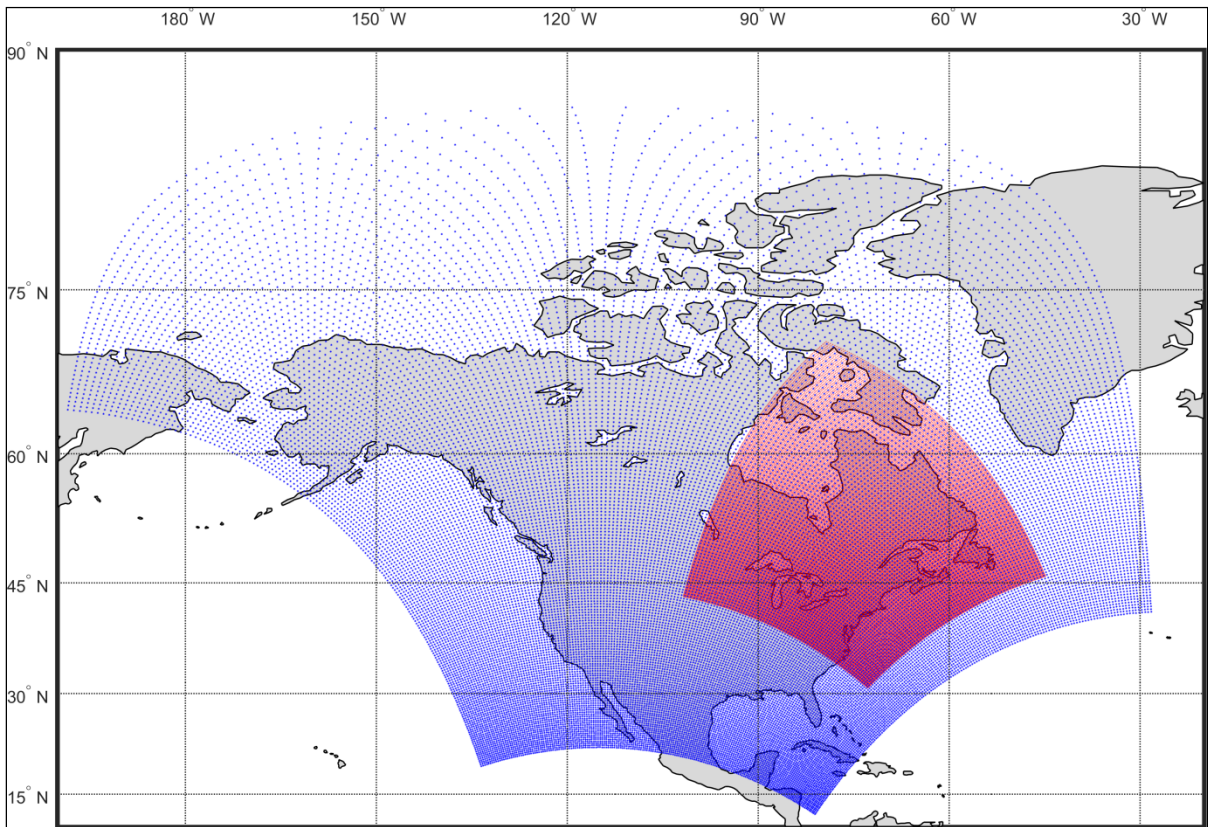


Figure-A I- 1 Computational domains of the Canadian Regional Climate Model version 4. Blue points display North American domain at 45 km. Red points display Quebec domain

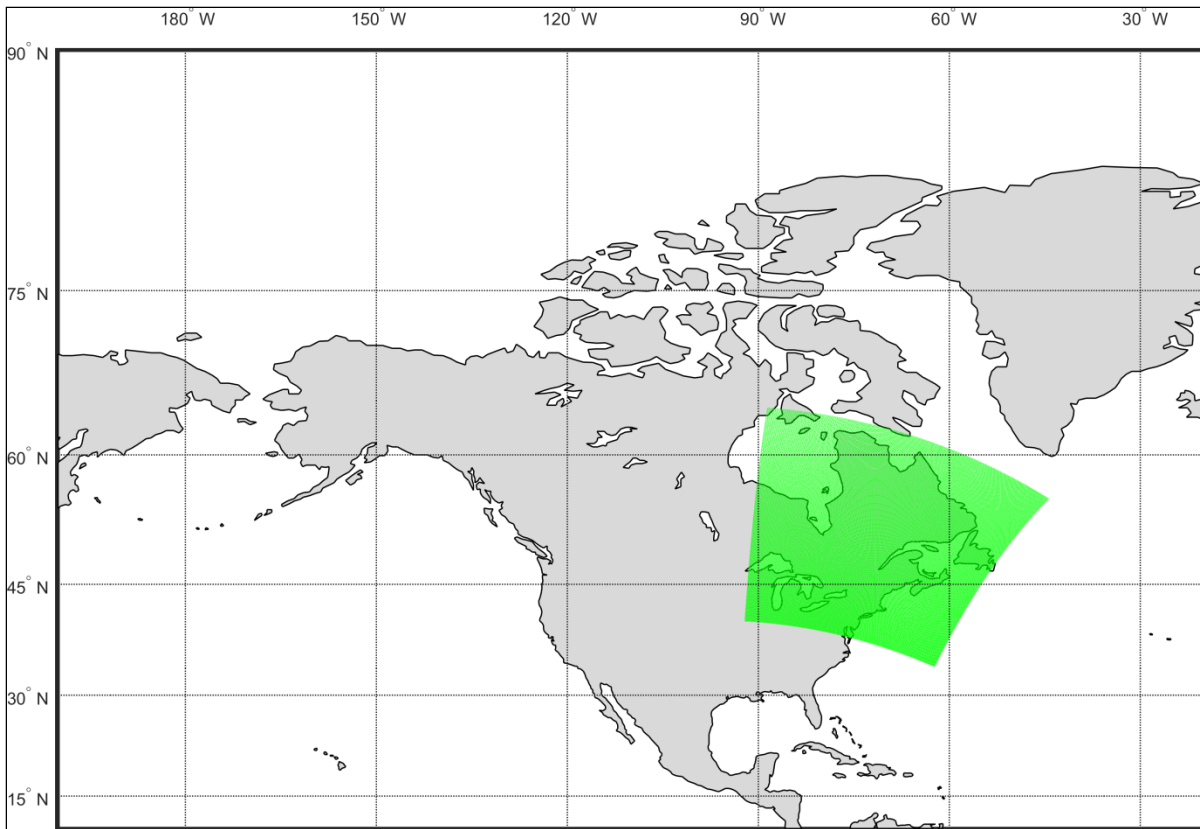


Figure-A I- 2 Computational domains of the Canadian Regional Climate Model version 5.
Green points display Quebec domain at 0.11° (≈ 12 km)

APPENDIX II

CLIMATE SIMULATIONS INTERCOMPARISON: DRIVERS

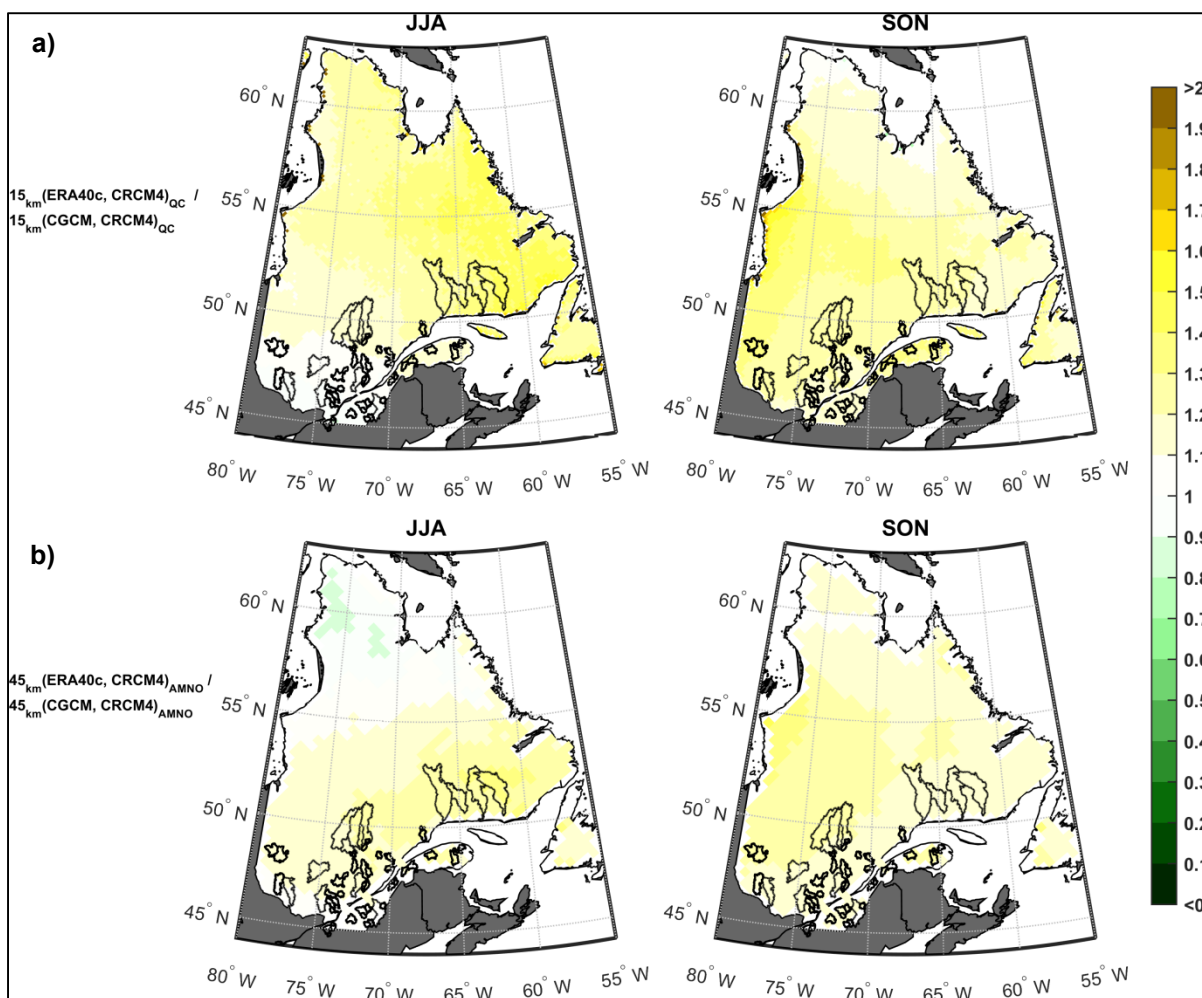


Figure-A II- 1 Ratio of annual seasonal mean temperature variances between simulations issued from CRCM4 for the summer (JJA) and fall (SON) seasons for the period 1961-1990. The upper panels (a) show the comparisons for the 15km resolution datasets. The lower panels (b) show the comparison for the 45km resolution datasets

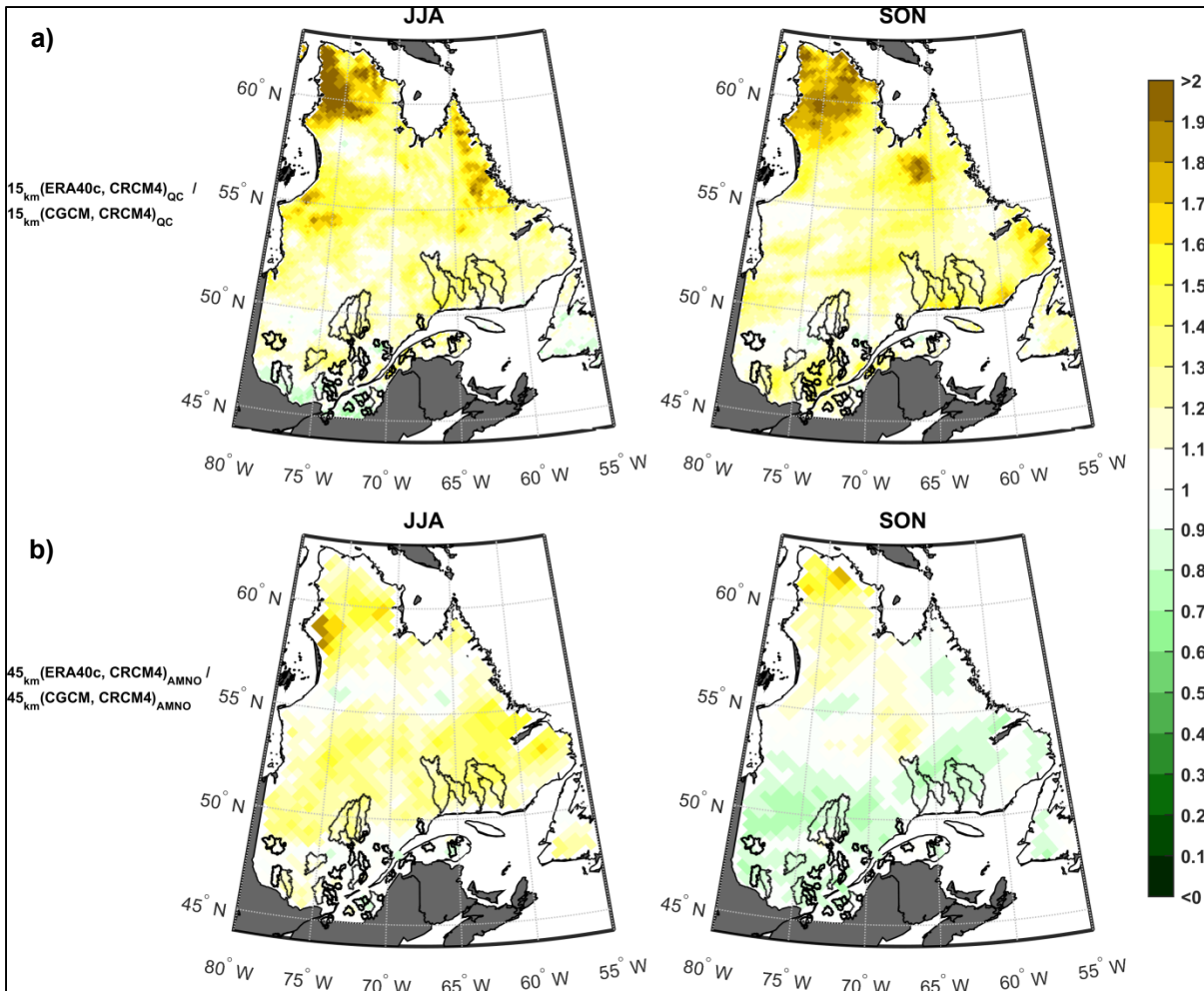


Figure-A II- 2 Ratio of annual seasonal mean temperature variances between simulations issued from CRCM4 for the summer (JJA) and fall (SON) seasons for the period 1961-1990. The upper panels (a) show the comparisons for the 15km resolution datasets. The lower panels (b) show the comparison for the 45km resolution datasets

APPENDIX III

STREAMFLOW SIMULATIONS AND CATCHMENT SIZE

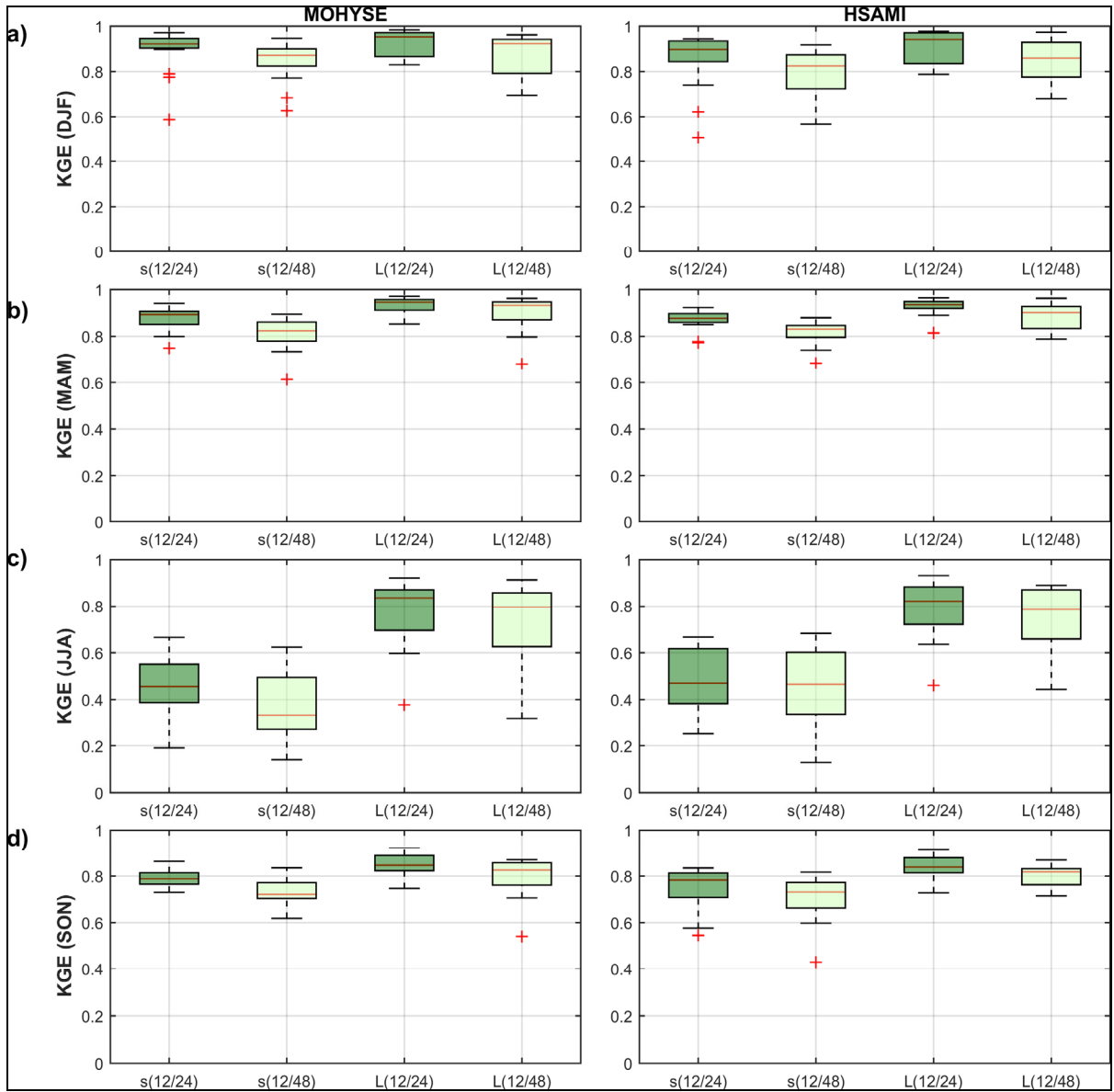


Figure-A III- 1 Seasonal KGE values between streamflows generated with CRCM5 outputs at different resolutions grouped by small (s) and large (L) watersheds for the OF-1. The first panels (a) present the results obtained for the winter, the second panels (b) the results for the spring, the third panels (c) the results for the summer and the fourth panels (d) the results for the fall

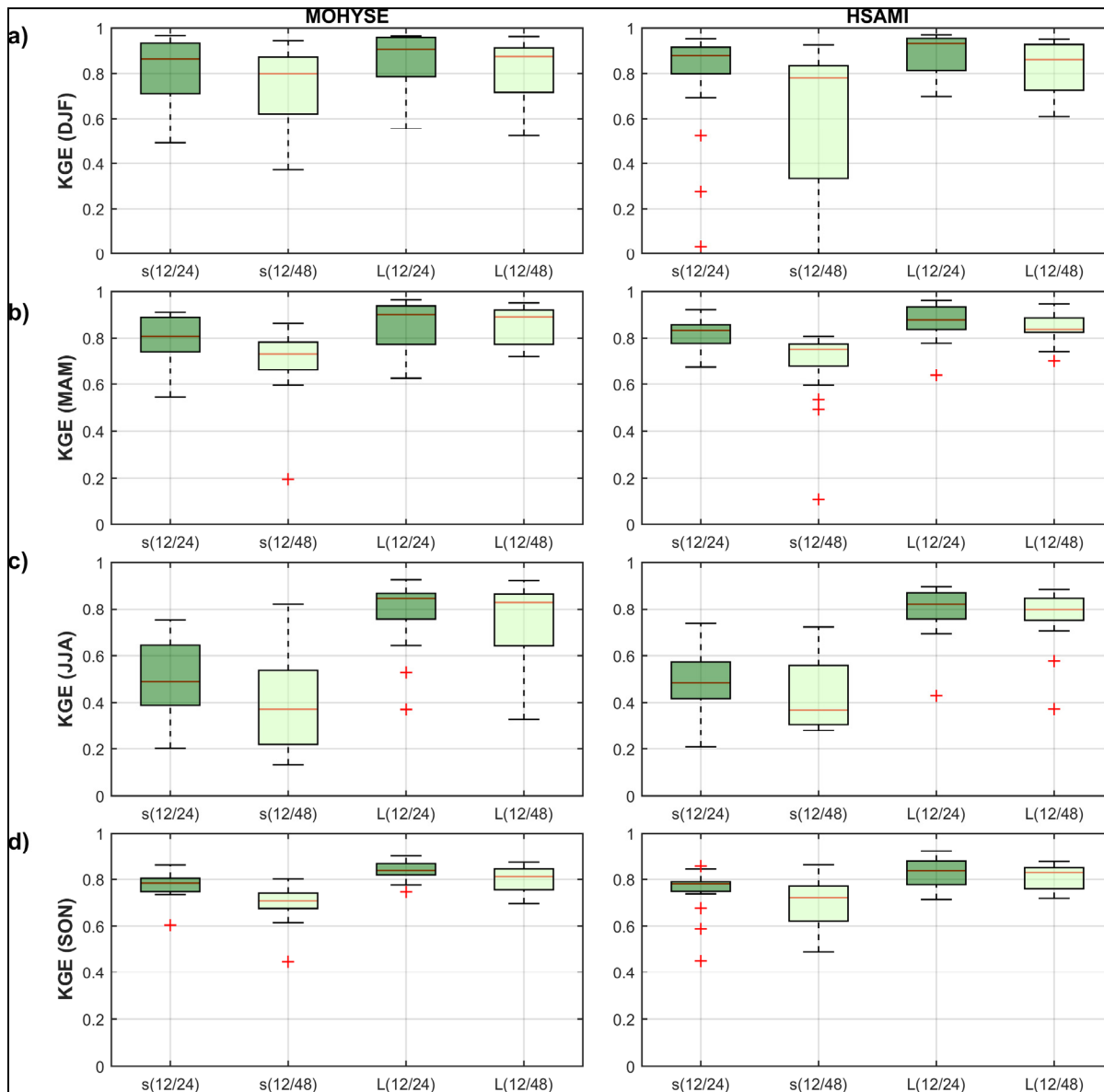


Figure-A III- 2 Seasonal KGE values between streamflows generated with CRCM5 outputs at different resolutions grouped by small (s) and large (L) watersheds for the OF-2. The first panels (a) present the results obtained for the winter, the second panels (b) the results for the spring, the third panels (c) the results for the summer and the fourth panels (d) the results for the fall

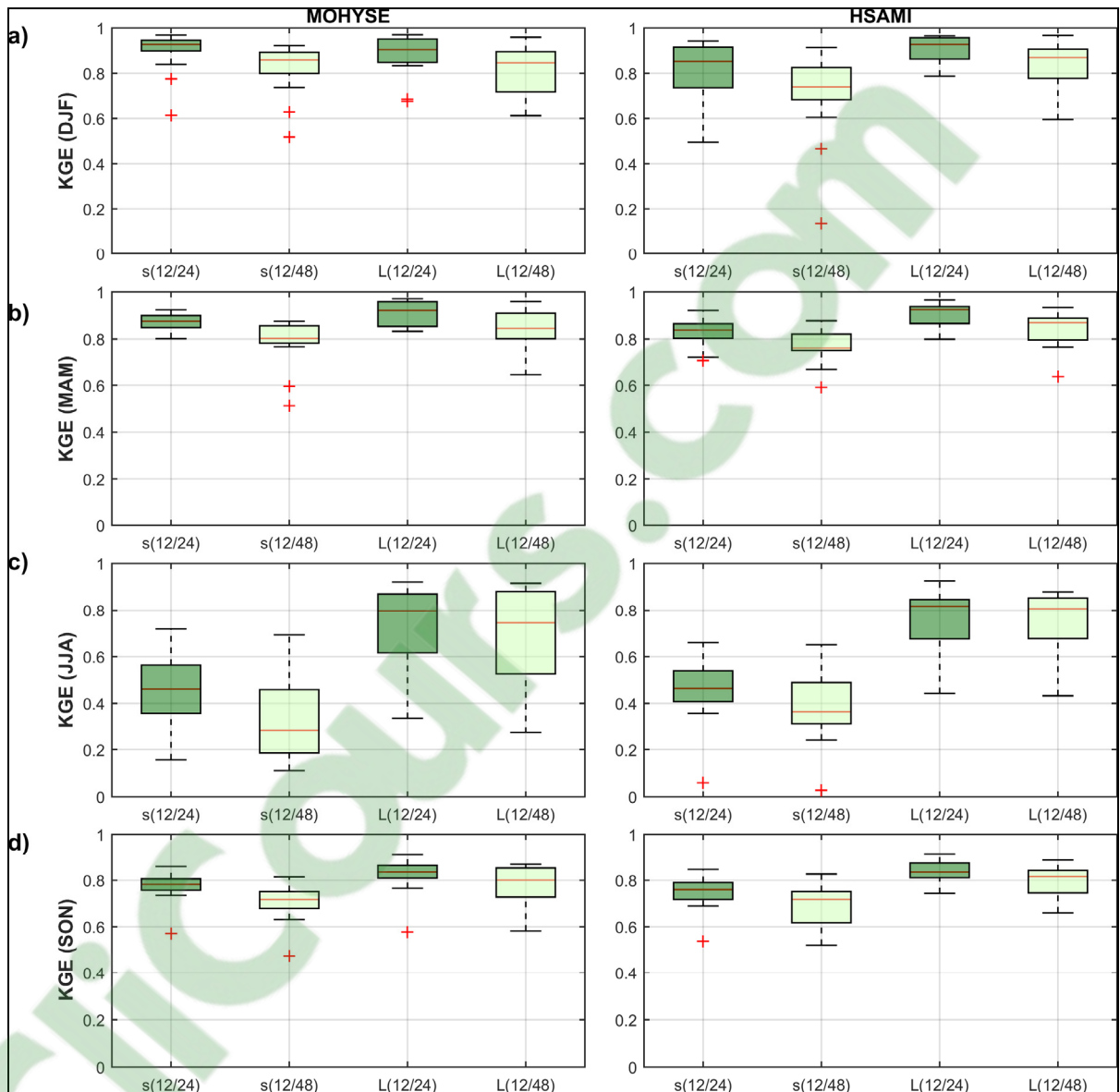


Figure-A III- 3 Seasonal KGE values between streamflows generated with CRCM5 outputs at different resolutions grouped by small (s) and large (L) watersheds for the OF-3. The first panels (a) present the results obtained for the winter, the second panels (b) the results for the spring, the third panels (c) the results for the summer and the fourth panels (d) the results for the fall

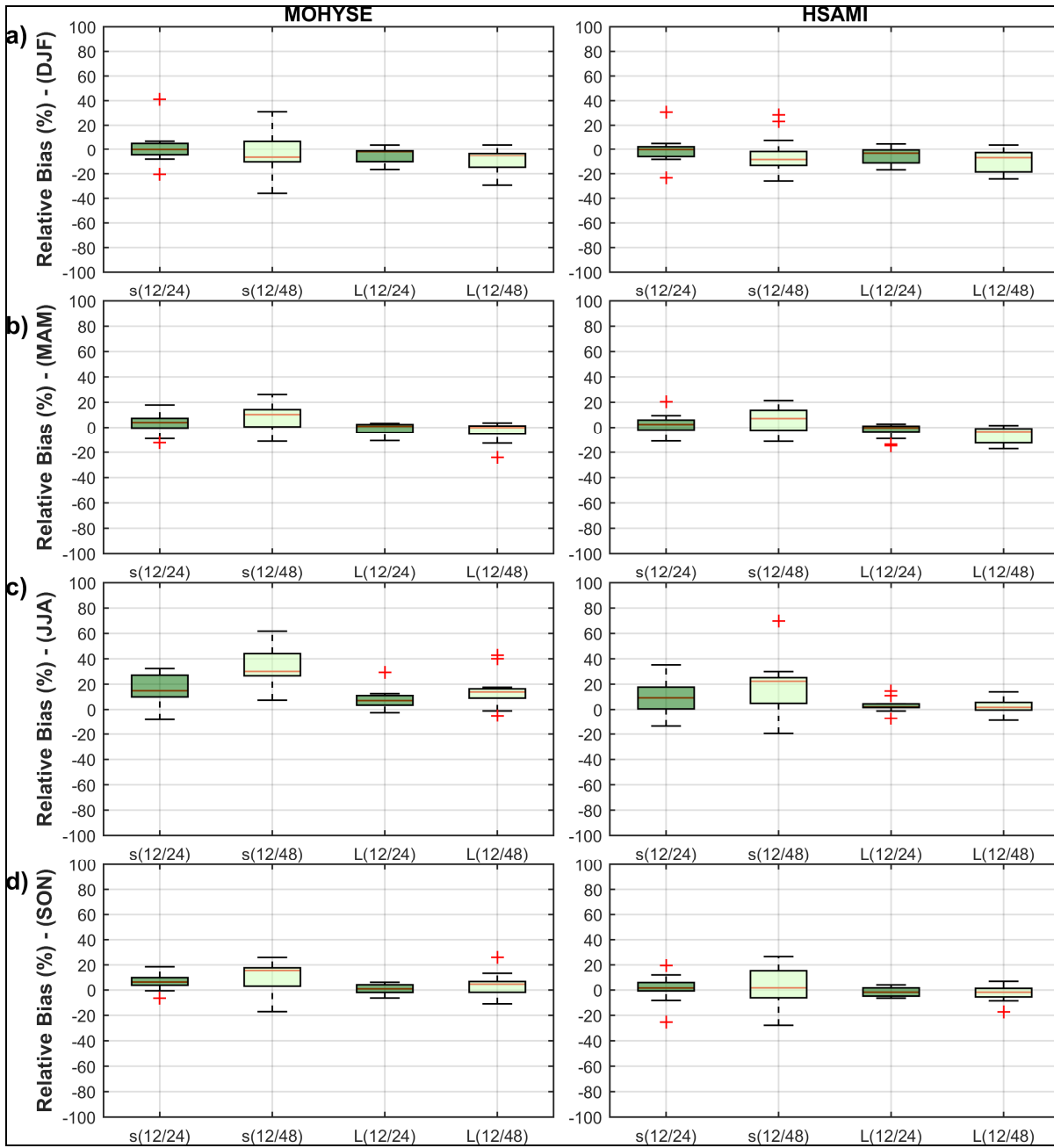


Figure-A III- 4 Seasonal relative bias (%) between streamflows generated with CRCM5 outputs at different resolutions grouped by small (s) and large (L) watersheds for the OF-1.

The first panels (a) present the results obtained for the winter, the second panels (b) the results for the spring, the third panels (c) the results for the summer and the fourth panels (d) the results for the fall

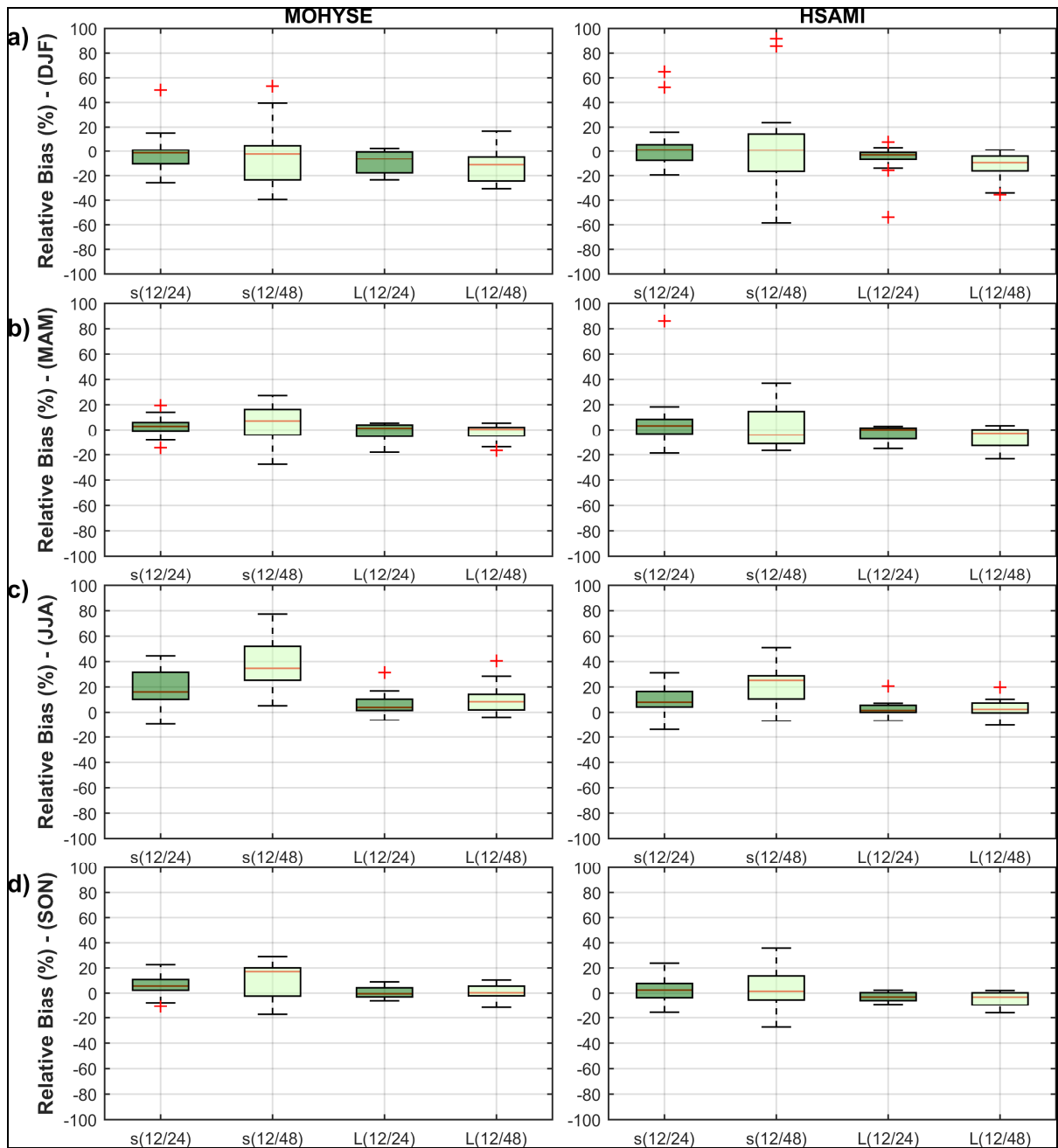


Figure-A III- 5 Seasonal relative bias (%) between streamflows generated with CRCM5 outputs at different resolutions grouped by small (s) and large (L) watersheds for the OF-2. The first panels (a) present the results obtained for the winter, the second panels (b) the results for the spring, the third panels (c) the results for the summer and the fourth panels (d) the results for the fall

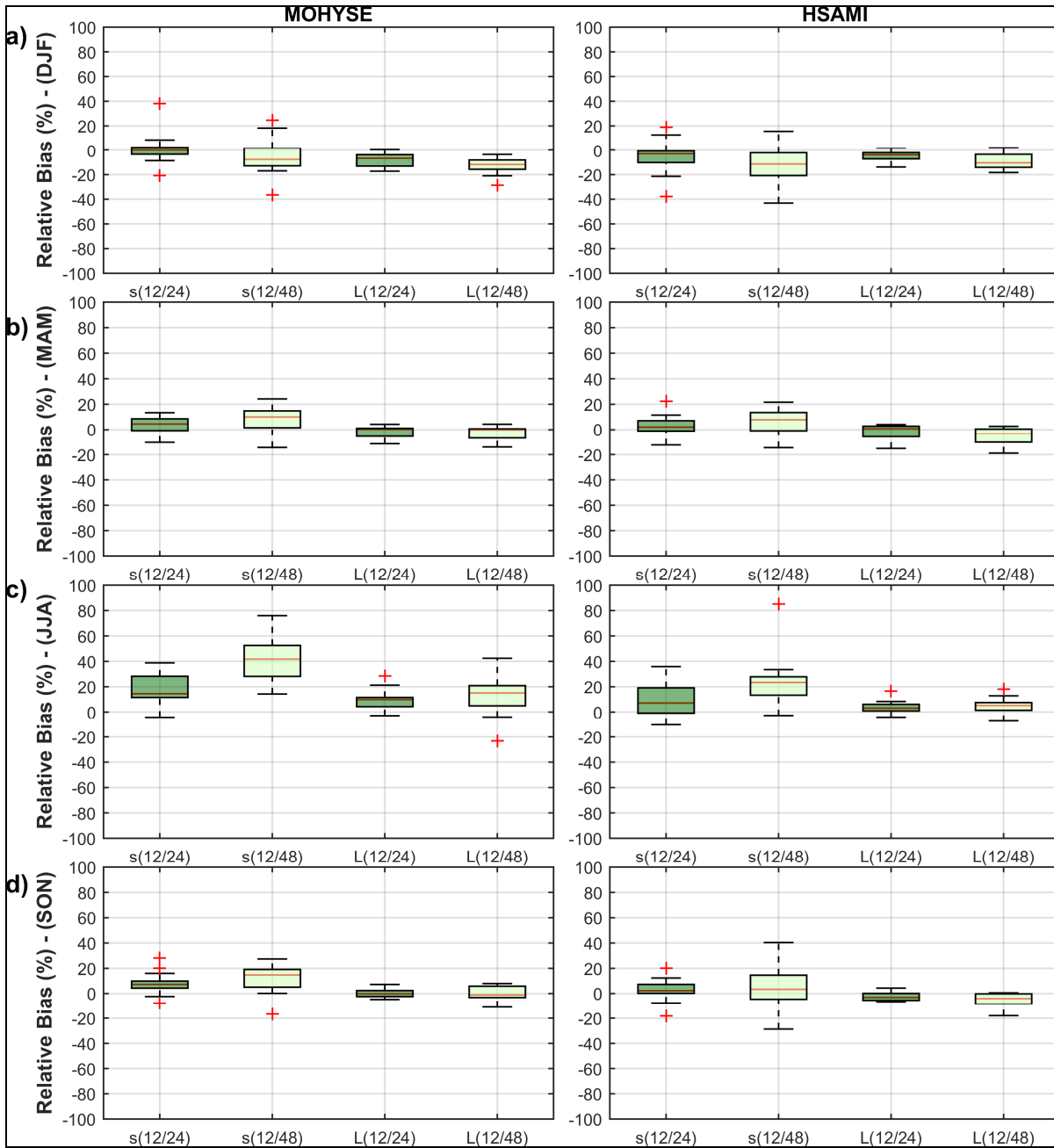


Figure-A III- 6 Seasonal relative bias (%) between streamflows generated with CRCM5 outputs at different resolutions grouped by small (s) and large (L) watersheds for the OF-3.

The first panels (a) present the results obtained for the winter, the second panels (b) the results for the spring, the third panels (c) the results for the summer and the fourth panels (d) the results for the fall

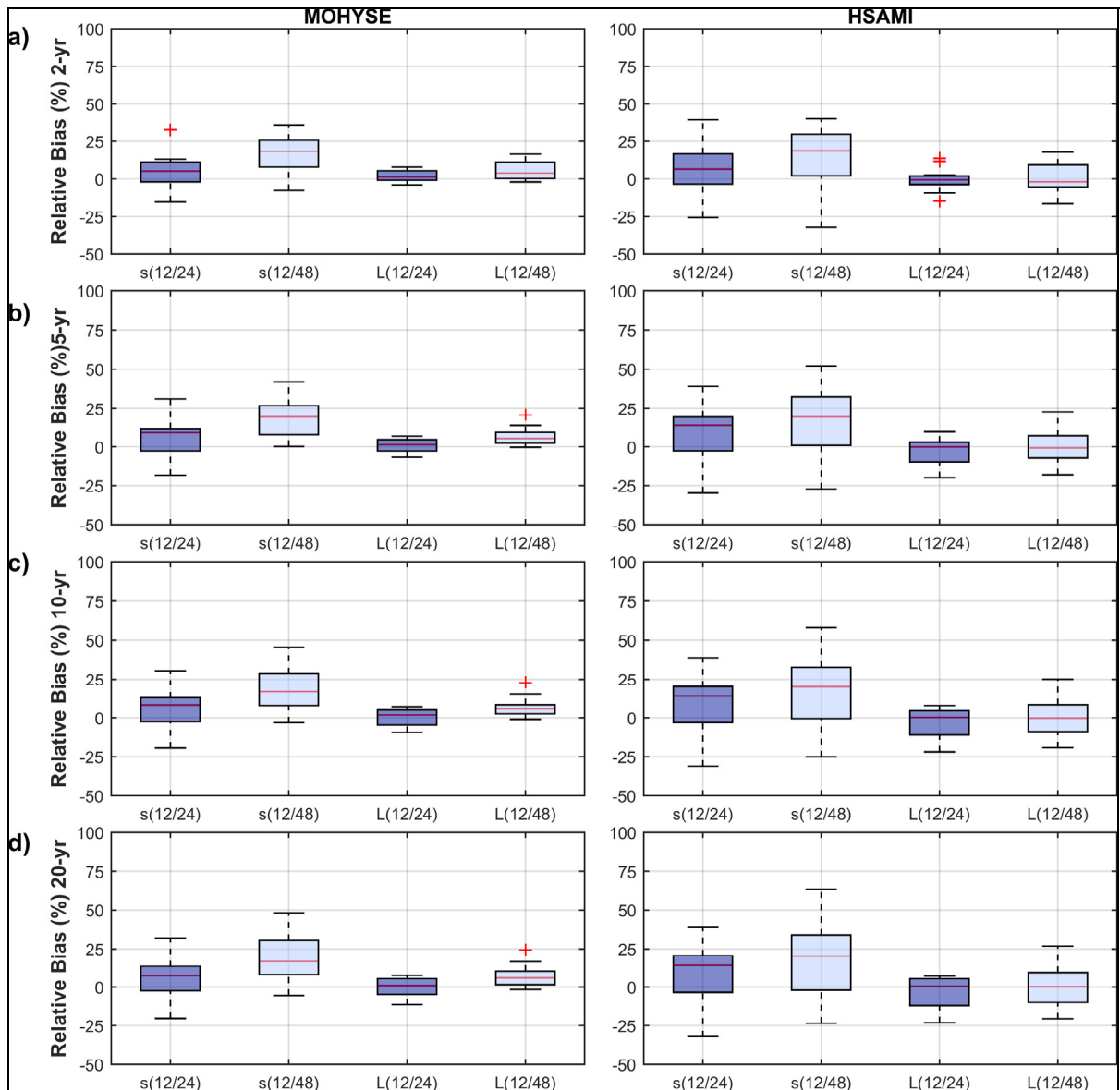


Figure-A III- 7 Relative biases (%) between the return periods (2, 5, 10 and 20-year) of the generated streamflows with CRCM5 outputs at different resolutions grouped by small (s) and large (L) watersheds for the OF-1. The first panels (a) present the comparisons of 2-year return periods, the second panels (b) the comparisons of 5-year return periods, the third panels (c) the comparisons of 10-year return periods and the fourth panels (d) the comparisons of the 20-year return periods

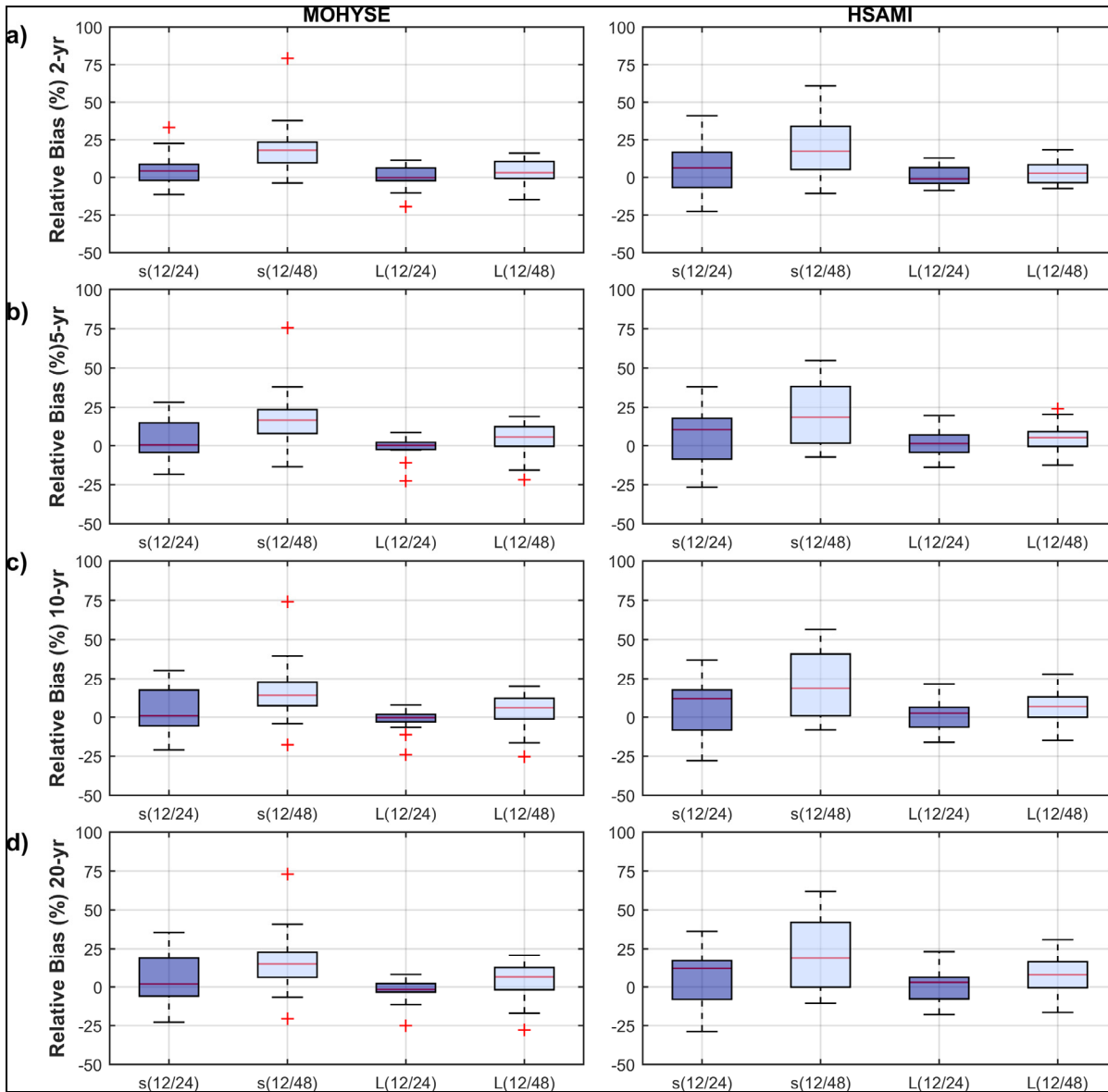


Figure-A III- 8 Relative biases (%) between the return periods (2, 5, 10 and 20-year) of the generated streamflows with CRCM5 outputs at different resolutions grouped by small (s) and large (L) watersheds for the OF-3. The first panels (a) present the comparisons of 2-year return periods, the second panels (b) the comparisons of 5-year return periods, the third panels (c) the comparisons of 10-year return periods and the fourth panels (d) the comparisons of the 20-year return periods

LIST OF BIBLIOGRAPHICAL REFERENCES

- AghaKouchak, A., Easterling, D., Hsu, K., Schubert, S., & Sorooshian, S. (2012). *Extremes in a changing climate: detection, analysis and uncertainty* (Vol. 65): Springer Science & Business Media.
- Arsenault, R. (2015). *Équifinalité, incertitude et procédures multi-modèle en prévision hydrologique aux sites non-jaugés*. Montréal: École de technologie supérieure.
- Arsenault, R., & Brissette, F. (2016). Multi-model averaging for continuous streamflow prediction in ungauged basins. *Hydrological Sciences Journal*, 61(13), 2443-2454.
- Arsenault, R., Brissette, F., Malo, J.-S., Minville, M., & Leconte, R. (2013). Structural and non-structural climate change adaptation strategies for the Péribonka water resource system. *Water Resources Management*, 27(7), 2075-2087.
- Arsenault, R., & Brissette, F. P. (2014). Continuous streamflow prediction in ungauged basins: The effects of equifinality and parameter set selection on uncertainty in regionalization approaches. *Water resources research*, 50(7), 6135-6153.
- Arsenault, R., Gatién, P., Renaud, B., Brissette, F., & Martel, J.-L. (2015). A comparative analysis of 9 multi-model averaging approaches in hydrological continuous streamflow simulation. *Journal of hydrology*, 529(Part 3), 754-767. doi:<https://doi.org/10.1016/j.jhydrol.2015.09.001>
- Arsenault, R., Poulin, A., Côté, P., & Brissette, F. (2014). Comparison of stochastic optimization algorithms in hydrological model calibration. *Journal of hydrologic engineering*, 19(7), 1374-1384.
- Bates, B., Kundzewicz, Z. W., Wu, S., & Palutikof, J. (2008). *Climate change and water: Technical paper vi*: Intergovernmental Panel on Climate Change (IPCC).
- Beck, H. E., Dijk, A. I. J. M. v., Roo, A. d., Miralles, D. G., McVicar, T. R., Schellekens, J., & Bruijnzeel, L. A. (2016). Global-scale regionalization of hydrologic model parameters. *Water resources research*, 52(5), 3599-3622. doi:10.1002/2015WR018247
- Bengtsson, L., & Shukla, J. (1988). Integration of space and in situ observations to study global climate change. *Bulletin of the American Meteorological Society*, 69(10), 1130-1143.
- Beven, K. J. (2011). *Rainfall-runoff modelling: the primer*: John Wiley & Sons.
- Boyer, C., Chaumont, D., Chartier, I., & Roy, A. G. (2010). Impact of climate change on the hydrology of St. Lawrence tributaries. *Journal of hydrology*, 384(1), 65-83. doi:<https://doi.org/10.1016/j.jhydrol.2010.01.011>

- Carter, T., Hulme, M., & Lal, M. (2007). General guidelines on the use of scenario data for climate impact and adaptation assessment.
- Caya, D., & Laprise, R. (1999). A semi-implicit semi-Lagrangian regional climate model: The Canadian RCM. *Monthly Weather Review*, 127(3), 341-362.
- Caya, D., Laprise, R., Giguère, M., Bergeron, G., Blanchet, J. P., Stocks, B. J., . . . McFarlane, N. A. (1995). Description of the Canadian Regional Climate Model. In M. J. Apps, D. T. Price, & J. Wisniewski (Eds.), *Boreal Forests and Global Change: Peer-reviewed manuscripts selected from the International Boreal Forest Research Association Conference, held in Saskatoon, Saskatchewan, Canada, September 25–30, 1994* (pp. 477-482). Dordrecht: Springer Netherlands.
- CEHQ. (2014). Plateforme de modélisation hydrologique du Québec méridional. Québec, 20 p. et annexes. Rapport technique.
- CEHQ. (2015). *Hydroclimatic Atlas of Southern Québec. The Impact of Climate Change on High, Low and Mean Flow Regimes for the 2050 horizon*. Québec, Centre d'expertise hydrique du Québec (CEHQ), 2015, 81 pp. Quebec.
- Charron, I. (2014). A Guidebook on Climate Scenarios: Using Climate Information to Guide Adaptation Research and Decisions. Ouranos. 86.
- Chebana, F., & Ouarda, T. B. M. J. (2011). Multivariate quantiles in hydrological frequency analysis. *Environmetrics*, 22(1), 63-78. doi:10.1002/env.1027
- Chen, J., Brissette, F. P., & Leconte, R. (2011). Uncertainty of downscaling method in quantifying the impact of climate change on hydrology. *Journal of hydrology*, 401(3), 190-202.
- Clavet-Gaumont, J., Sushama, L., Khaliq, M. N., Huziy, O., & Roy, R. (2013). Canadian RCM projected changes to high flows for Québec watersheds using regional frequency analysis. *International Journal of Climatology*, 33(14), 2940-2955. doi:10.1002/joc.3641
- Coppola, E., Raffaele, F., & Giorgi, F. (2016). Impact of climate change on snow melt driven runoff timing over the Alpine region. *Climate Dynamics*, 1-15.
- Côté, J., Gravel, S., Méthot, A., Patoine, A., Roch, M., & Staniforth, A. (1998). The Operational CMC–MRB Global Environmental Multiscale (GEM) Model. Part I: Design Considerations and Formulation. *Monthly Weather Review*, 126(6), 1373-1395. doi:10.1175/1520-0493(1998)126<1373:tocmge>2.0.co;2
- Curry, C. L., Tencer, B., Whan, K., Weaver, A. J., Giguère, M., & Wiebe, E. (2016a). Searching for added value in simulating climate extremes with a high-resolution regional climate model over western Canada. *Atmosphere-Ocean*, 54(4), 364-384.

- Curry, C. L., Tencer, B., Whan, K., Weaver, A. J., Giguère, M., & Wiebe, E. (2016b). Searching for Added Value in Simulating Climate Extremes with a High-Resolution Regional Climate Model over Western Canada. II: Basin-Scale Results. *Atmosphere-Ocean*, 54(4), 385-402.
- Dankers, R., & Feyen, L. (2008). Climate change impact on flood hazard in Europe: An assessment based on high-resolution climate simulations. *Journal of Geophysical Research: Atmospheres (1984–2012)*, 113(D19). doi:10.1029/2007JD009719
- Dee, D., Uppala, S., Simmons, A., Berrisford, P., Poli, P., Kobayashi, S., . . . Bauer, P. (2011). The ERA-Interim reanalysis: Configuration and performance of the data assimilation system. *Quarterly Journal of the Royal Meteorological Society*, 137(656), 553-597.
- Diaz-Nieto, J., & Wilby, R. L. (2005). A comparison of statistical downscaling and climate change factor methods: impacts on low flows in the River Thames, United Kingdom. *Climatic Change*, 69(2-3), 245-268.
- Duan, Q., Sorooshian, S., & Gupta, V. K. (1994). Optimal use of the SCE-UA global optimization method for calibrating watershed models. *Journal of hydrology*, 158(3-4), 265-284.
- Elfa, R., & Côté, H. (2010). Climate and climate change sensitivity to model configuration in the Canadian RCM over North America. *Meteorologische Zeitschrift*, 19(4), 325-339. doi:10.1127/0941-2948/2010/0469
- Falloon, P., Challinor, A., Dessai, S., Hoang, L., Johnson, J., & Koehler, A.-K. (2014). Ensembles and uncertainty in climate change impacts. *Frontiers in Environmental Science*, 2, 33.
- Field, C. B. (2012). *Managing the risks of extreme events and disasters to advance climate change adaptation: special report of the intergovernmental panel on climate change*: Cambridge University Press.
- Fortin, L.-G., Turcotte, R., Pugin, S., Cyr, J.-F., & Picard, F. (2007). Impact des changements climatiques sur les plans de gestion des lacs Saint-François et Aylmer au sud du Québec. *Canadian journal of civil engineering*, 34(8), 934-945.
- Fortin, V. (2000). Le modèle météo-apport HSAMI: historique, théorie et application. *Institut de recherche d'Hydro-Québec, Varennes*.
- Fortin, V., & Turcotte, R. (2006). Le modèle hydrologique MOHYSE. *Note de cours pour SCA7420, Département des sciences de la terre et de l'atmosphère, Université du Québec à Montréal*.
- Giorgi, F., Christensen, J., Hulme, M., Von Storch, H., Whetton, P., Jones, R., . . . Bates, B. (2001). Regional climate information-evaluation and projections. *Climate Change*

2001: *The Scientific Basis. Contribution of Working Group to the Third Assessment Report of the Intergovernmental Panel on Climate Change [Houghton, JT et al.(eds)]. Cambridge University Press, Cambridge, United Kingdom and New York, US.*

- Giorgi, F., & Gutowski, W. J. (2015). Regional Dynamical Downscaling and the CORDEX Initiative. *Annual Review of Environment and Resources*, 40(1), 467-490. doi:10.1146/annurev-environ-102014-021217
- Giorgi, F., Jones, C., & Asrar, G. R. (2009). Addressing climate information needs at the regional level: the CORDEX framework. *World Meteorological Organization (WMO) Bulletin*, 58(3), 175.
- Graham, L. P., Andréasson, J., & Carlsson, B. (2007). Assessing climate change impacts on hydrology from an ensemble of regional climate models, model scales and linking methods – a case study on the Lule River basin. *Climatic Change*, 81(1), 293-307. doi:10.1007/s10584-006-9215-2
- Grey, D., & Sadoff, C. W. (2007). Sink or Swim? Water security for growth and development. *Water Policy*, 9(6), 545-571.
- Guay, C., Minville, M., & Braun, M. (2015). A global portrait of hydrological changes at the 2050 horizon for the province of Québec. *Canadian Water Resources Journal/Revue canadienne des ressources hydriques*, 40(3), 285-302.
- Gupta, H. V., Kling, H., Yilmaz, K. K., & Martinez, G. F. (2009). Decomposition of the mean squared error and NSE performance criteria: Implications for improving hydrological modelling. *Journal of hydrology*, 377(1), 80-91.
- Hall, J., Arheimer, B., Borga, M., Brázdil, R., Claps, P., Kiss, A., . . . Lang, M. (2014). Understanding flood regime changes in Europe: A state of the art assessment. *Hydrology and Earth System Sciences*, 18(7), 2735-2772.
- Hansen, J., Sato, M., Hearty, P., Ruedy, R., Kelley, M., Masson-Delmotte, V., . . . Lo, K. W. (2016). Ice melt, sea level rise and superstorms: evidence from paleoclimate data, climate modeling, and modern observations that 2 °C global warming could be dangerous. *Atmos. Chem. Phys.*, 16(6), 3761-3812. doi:10.5194/acp-16-3761-2016
- Hansen, N., & Ostermeier, A. (1997). Convergence properties of evolution strategies with the derandomized covariance matrix adaptation: The CMA-ES. *Eufit*, 97, 650-654.
- Hartmann, D. L., Klein Tank, A. M. G., Rusticucci, M., Alexander, L. V., Brönnimann, S., Charabi, Y., . . . Zhai, P. M. (2013). Observations: Atmosphere and Surface. In T. F. Stocker, D. Qin, G.-K. Plattner, M. Tignor, S. K. Allen, J. Boschung, A. Nauels, Y. Xia, V. Bex, & P. M. Midgley (Eds.), *Climate Change 2013: The Physical Science Basis. Contribution of Working Group I to the Fifth Assessment Report of the*

Intergovernmental Panel on Climate Change (pp. 159–254). Cambridge, United Kingdom and New York, NY, USA: Cambridge University Press.

Hawkins, E., Osborne, T. M., Ho, C. K., & Challinor, A. J. (2013). Calibration and bias correction of climate projections for crop modelling: an idealised case study over Europe. *Agricultural and forest meteorology*, *170*, 19-31.

Haylock, M., Hofstra, N., Klein Tank, A., Klok, E., Jones, P., & New, M. (2008). A European daily high-resolution gridded data set of surface temperature and precipitation for 1950–2006. *Journal of Geophysical Research: Atmospheres*, *113*(D20).

Heavens, N., Ward, D., & Natalie, M. (2013). Studying and projecting climate change with earth system models. *Nature Education Knowledge*, *4*(5), 4.

Henderson-Sellers, A. (1993). An antipodean climate of uncertainty? *Climatic Change*, *25*(3-4), 203-224.

Hostetler, S. (1994). Hydrologic and atmospheric models: the (continuing) problem of discordant scales. *Climatic Change*, *27*(4), 345-350.

Huang, S., Kumar, R., Flörke, M., Yang, T., Hundecha, Y., Kraft, P., . . . Krysanova, V. (2016). Evaluation of an ensemble of regional hydrological models in 12 large-scale river basins worldwide. *Climatic Change*, *141*(3), 381-397. doi:10.1007/s10584-016-1841-8

IPCC. (2012). *Managing the Risks of Extreme Events and Disasters to Advance Climate Change Adaptation. A Special Report of Working Groups I and II of the Intergovernmental Panel on Climate Change (IPCC)* [Field, C. B., V. Barros, T. F. Stocker, D. Qin, D. J. Dokken, K. L. Ebi, M. D. Mastrandrea, K. J. Mach, G.-K. Plattner, S. K. Allen, M. Tignor, and P. M. Midgley (eds.)]. Cambridge, United Kingdom and New York, NY, USA: Cambridge University Press.

IPCC. (2013a). Annex III: Glossary. In T. F. Stocker, D. Qin, G.-K. Plattner, M. Tignor, S. K. Allen, J. Boschung, A. Nauels, Y. Xia, V. Bex, & P. M. Midgley (Eds.), *Climate Change 2013: The Physical Science Basis. Contribution of Working Group I to the Fifth Assessment Report of the Intergovernmental Panel on Climate Change* (pp. 1447–1466). Cambridge, United Kingdom and New York, NY, USA: Cambridge University Press.

IPCC. (2013b). *Climate Change 2013: The Physical Science Basis. Contribution of Working Group I to the Fifth Assessment Report of the Intergovernmental Panel on Climate Change* (T. F. Stocker, D. Qin, G.-K. Plattner, M. Tignor, S. K. Allen, J. Boschung, A. Nauels, Y. Xia, V. Bex, & P. M. Midgley Eds.). Cambridge, United Kingdom and New York, NY, USA: Cambridge University Press.

- IPCC. (2013c). Summary for Policymakers. In T. F. Stocker, D. Qin, G.-K. Plattner, M. Tignor, S. K. Allen, J. Boschung, A. Nauels, Y. Xia, V. Bex, & P. M. Midgley (Eds.), *Climate Change 2013: The Physical Science Basis. Contribution of Working Group I to the Fifth Assessment Report of the Intergovernmental Panel on Climate Change* (pp. 1–30). Cambridge, United Kingdom and New York, NY, USA: Cambridge University Press.
- Jakob Themeßl, M., Gobiet, A., & Leuprecht, A. (2011). Empirical-statistical downscaling and error correction of daily precipitation from regional climate models. *International Journal of Climatology*, *31*(10), 1530-1544.
- Jones, R., Murphy, J., & Noguer, M. (1995). Simulation of climate change over Europe using a nested regional-climate model. I: Assessment of control climate, including sensitivity to location of lateral boundaries. *Quarterly Journal of the Royal Meteorological Society*, *121*(526), 1413-1449.
- Jones, R. N. (2000). Managing uncertainty in climate change projections—issues for impact assessment. *Climatic Change*, *45*(3-4), 403-419.
- Kling, H., Fuchs, M., & Paulin, M. (2012). Runoff conditions in the upper Danube basin under an ensemble of climate change scenarios. *Journal of hydrology*, *424–425*, 264-277. doi:<https://doi.org/10.1016/j.jhydrol.2012.01.011>
- Kron, W., & Berz, G. (2007). Flood disasters and climate change: trends and options—a (re-) insurer’s view (pp. 268-273): Hamburg.
- Kundzewicz, Z. W., Kanae, S., Seneviratne, S. I., Handmer, J., Nicholls, N., Peduzzi, P., . . . Sherstyukov, B. (2013). Flood risk and climate change: global and regional perspectives. *Hydrological Sciences Journal*, *59*(1), 1-28. doi:10.1080/02626667.2013.857411
- Kundzewicz, Z. W., Kanae, S., Seneviratne, S. I., Handmer, J., Nicholls, N., Peduzzi, P., . . . Sherstyukov, B. (2014). Flood risk and climate change: global and regional perspectives. *Hydrological Sciences Journal*, *59*(1), 1-28. doi:10.1080/02626667.2013.857411
- Laprise, R. (2008). Regional climate modelling. *Journal of Computational Physics*, *227*(7), 3641-3666.
- Laprise, R., Kornic, D., Rapaić, M., Šeparović, L., Leduc, M., Nikiema, O., . . . Lucas-Picher, P. (2012). Considerations of domain size and large-scale driving for nested regional climate models: impact on internal variability and ability at developing small-scale details *Climate Change* (pp. 181-199): Springer.
- Lee, M.-H., & Bae, D.-H. (2016). Uncertainty Assessment of Future High and Low Flow Projections According to Climate Downscaling and Hydrological Models. *Procedia*

Engineering, 154(Supplement C), 617-623.
doi:<https://doi.org/10.1016/j.proeng.2016.07.560>

- Lehner, B., Döll, P., Alcamo, J., Henrichs, T., & Kaspar, F. (2006). Estimating the Impact of Global Change on Flood and Drought Risks in Europe: A Continental, Integrated Analysis. *Climatic Change*, 75(3), 273-299. doi:10.1007/s10584-006-6338-4
- Loaiciga, H. A., & Leipnik, R. B. (1999). Analysis of extreme hydrologic events with Gumbel distributions: marginal and additive cases. *Stochastic Environmental Research and Risk Assessment*, 13(4), 251-259. doi:10.1007/s004770050042
- Lucas-Picher, P., Laprise, R., & Winger, K. (2016). Evidence of added value in North American regional climate model hindcast simulations using ever-increasing horizontal resolutions. *Climate Dynamics*, 1-23. doi:10.1007/s00382-016-3227-z
- Mareuil, A., Leconte, R., Brissette, F., & Minville, M. (2007). Impacts of climate change on the frequency and severity of floods in the Châteauguay River basin, Canada. *Canadian journal of civil engineering*, 34(9), 1048-1060. doi:10.1139/107-022
- Marques, F. J., Coelho, C. A., & de Carvalho, M. (2015). On the distribution of linear combinations of independent Gumbel random variables. *Statistics and Computing*, 25(3), 683-701. doi:10.1007/s11222-014-9453-5
- Martynov, A., Laprise, R., Sushama, L., Winger, K., Šeparović, L., & Dugas, B. (2013). Reanalysis-driven climate simulation over CORDEX North America domain using the Canadian Regional Climate Model, version 5: model performance evaluation. *Climate Dynamics*, 41(11), 2973-3005. doi:10.1007/s00382-013-1778-9
- McGuffie, K., & Henderson-Sellers, A. (2001). Forty years of numerical climate modelling. *International Journal of Climatology*, 21(9), 1067-1109.
- MDDELCC. (2017). Ministère du Développement durable, de l'Environnement et de la Lutte contre les changements climatiques . Gestion intégrée des ressources en eau par bassins versants.
- Meehl, G. A., Covey, C., Taylor, K. E., Delworth, T., Stouffer, R. J., Latif, M., . . . Mitchell, J. F. (2007). The WCRP CMIP3 multimodel dataset: A new era in climate change research. *Bulletin of the American Meteorological Society*, 88(9), 1383-1394.
- Mendoza, P. A., Mizukami, N., Ikeda, K., Clark, M. P., Gutmann, E. D., Arnold, J. R., . . . Rajagopalan, B. (2016). Effects of different regional climate model resolution and forcing scales on projected hydrologic changes. *Journal of hydrology*, 541(Part B), 1003-1019. doi:<https://doi.org/10.1016/j.jhydrol.2016.08.010>
- Minville, M., Brissette, F., Krau, S., & Leconte, R. (2009). Adaptation to climate change in the management of a Canadian water-resources system exploited for hydropower. *Water Resources Management*, 23(14), 2965-2986.

- Minville, M., Brissette, F., & Leconte, R. (2008). Uncertainty of the impact of climate change on the hydrology of a nordic watershed. *Journal of hydrology*, 358(1), 70-83.
- Mizuta, R., Yoshimura, H., Murakami, H., Matsueda, M., Endo, H., Ose, T., . . . Kitoh, A. (2012). Climate Simulations Using MRI-AGCM3.2 with 20-km Grid. *Journal of the Meteorological Society of Japan. Ser. II*, 90A, 233-258. doi:10.2151/jmsj.2012-A12
- Moore, C., & Doherty, J. (2005). Role of the calibration process in reducing model predictive error. *Water resources research*, 41(5).
- Moriasi, D. N., Arnold, J. G., Van Liew, M. W., Bingner, R. L., Harmel, R. D., & Veith, T. L. (2007). Model evaluation guidelines for systematic quantification of accuracy in watershed simulations. *Transactions of the ASABE*, 50(3), 885-900.
- Moss, R. H., Edmonds, J. A., Hibbard, K. A., Manning, M. R., Rose, S. K., Van Vuuren, D. P., . . . Kram, T. (2010). The next generation of scenarios for climate change research and assessment. *Nature*, 463(7282), 747-756.
- Murphy, J. M., Sexton, D. M. H., Barnett, D. N., Jones, G. S., Webb, M. J., Collins, M., & Stainforth, D. A. (2004). Quantification of modelling uncertainties in a large ensemble of climate change simulations. *Nature*, 430, 768. doi:10.1038/nature02771 <https://www.nature.com/articles/nature02771#supplementary-information>
- Music, B., & Caya, D. (2007). Evaluation of the hydrological cycle over the Mississippi River basin as simulated by the Canadian Regional Climate Model (CRCM). *Journal of Hydrometeorology*, 8(5), 969-988.
- Music, B., & Caya, D. (2009). Investigation of the sensitivity of water cycle components simulated by the Canadian Regional Climate Model to the land surface parameterization, the lateral boundary data, and the internal variability. *Journal of Hydrometeorology*, 10(1), 3-21.
- Nash, J. E., & Sutcliffe, J. V. (1970). River flow forecasting through conceptual models part I—A discussion of principles. *Journal of hydrology*, 10(3), 282-290.
- Naz, B. S., Kao, S.-C., Ashfaq, M., Rastogi, D., Mei, R., & Bowling, L. C. (2016). Regional hydrologic response to climate change in the conterminous United States using high-resolution hydroclimate simulations. *Global and Planetary Change*, 143, 100-117. doi:<https://doi.org/10.1016/j.gloplacha.2016.06.003>
- Oyerinde, G., Hountondji, F., Lawin, A., Odofin, A., Afouda, A., & Diekkrüger, B. (2017). Improving Hydro-Climatic Projections with Bias-Correction in Sahelian Niger Basin, West Africa. *Climate*, 5(1), 8.
- Pechlivanidis, I., Jackson, B., McIntyre, N., & Wheatler, H. (2011). Catchment scale hydrological modelling: a review of model types, calibration approaches and

- uncertainty analysis methods in the context of recent developments in technology and applications. *Global NEST Journal*, 13(3), 193-214.
- Poulin, A., Brissette, F., Leconte, R., Arsenault, R., & Malo, J.-S. (2011). Uncertainty of hydrological modelling in climate change impact studies in a Canadian, snow-dominated river basin. *Journal of hydrology*, 409(3), 626-636.
- Prudhomme, C., Jakob, D., & Svensson, C. (2003). Uncertainty and climate change impact on the flood regime of small UK catchments. *Journal of hydrology*, 277(1), 1-23.
- Prudhomme, C., Reynard, N., & Crooks, S. (2002). Downscaling of global climate models for flood frequency analysis: where are we now? *Hydrological processes*, 16(6), 1137-1150.
- Quilb , R., Rousseau, A. N., Moquet, J.-S., Trinh, N. B., Dibike, Y., Gachon, P., & Chaumont, D. (2008). Assessing the effect of climate change on river flow using general circulation models and hydrological modelling—Application to the Chaudi re River, Quebec, Canada. *Canadian Water Resources Journal*, 33(1), 73-94.
- Randall, D. A., Wood, R. A., Bony, S., Colman, R., Fichet, T., Fyfe, J., . . . Srinivasan, J. (2007). Climate models and their evaluation *Climate Change 2007: The physical science basis. Contribution of Working Group I to the Fourth Assessment Report of the IPCC (FAR)* (pp. 589-662): Cambridge University Press.
- Riboust, P., & Brissette, F. (2015). Climate change impacts and uncertainties on spring flooding of Lake Champlain and the Richelieu River. *JAWRA Journal of the American Water Resources Association*, 51(3), 776-793.
- Richardson, L. (1922). Weather prediction by numerical process.
- Roy, L., Leconte, R., Brissette, F., & Marche, C. (2001). The impact of climate change on seasonal floods of a southern Quebec River Basin. *Hydrological processes*, 15(16), 3167-3179. doi:10.1002/hyp.323
- Roy, P., Gachon, P., & Laprise, R. (2014). Sensitivity of seasonal precipitation extremes to model configuration of the Canadian Regional Climate Model over eastern Canada using historical simulations. *Climate Dynamics*, 43(9-10), 2431-2453.
- Sakamoto, T. T., Komuro, Y., Nishimura, T., Ishii, M., Tatebe, H., Shioyama, H., . . . Suzuki, T. (2012). MIROC4h—a new high-resolution atmosphere-ocean coupled general circulation model. *Journal of the Meteorological Society of Japan. Ser. II*, 90(3), 325-359.
- Schneider, S. H. (1983). CO₂, climate and society: a brief overview *Social Science Research and Climate Change* (pp. 9-15): Springer.
- Schneider, S. H. (1992). Introduction to climate modeling. *SMR*, 648, 6.

- Scinocca, J., McFarlane, N., Lazare, M., Li, J., & Plummer, D. (2008). The CCCma third generation AGCM and its extension into the middle atmosphere. *Atmospheric Chemistry and Physics*, 8(23), 7055-7074.
- Singh, V. P., & Woolhiser, D. A. (2002). Mathematical modeling of watershed hydrology. *Journal of hydrologic engineering*, 7(4), 270-292.
- Solomon, S., Qin, D., Manning, M., Chen, Z., Marquis, M., Averyt, K., . . . Miller, H. (2007). Contribution of working group I to the fourth assessment report of the intergovernmental panel on climate change, 2007: Cambridge University Press, Cambridge.
- Stocker, T. F., Qin, D., Plattner, G.-K., Alexander, L. V., Allen, S. K., Bindoff, N. L., . . . Xie, S.-P. (2013). Technical Summary. In T. F. Stocker, D. Qin, G.-K. Plattner, M. Tignor, S. K. Allen, J. Boschung, A. Nauels, Y. Xia, V. Bex, & P. M. Midgley (Eds.), *Climate Change 2013: The Physical Science Basis. Contribution of Working Group I to the Fifth Assessment Report of the Intergovernmental Panel on Climate Change* (pp. 33–115). Cambridge, United Kingdom and New York, NY, USA: Cambridge University Press.
- Taylor, K. E., Stouffer, R. J., & Meehl, G. A. (2011). An Overview of CMIP5 and the Experiment Design. *Bulletin of the American Meteorological Society*, 93(4), 485-498. doi:10.1175/BAMS-D-11-00094.1
- Te Chow, V. (1988). *Applied hydrology*: Tata McGraw-Hill Education.
- Teutschbein, C., & Seibert, J. (2010). Regional climate models for hydrological impact studies at the catchment scale: a review of recent modeling strategies. *Geography Compass*, 4(7), 834-860.
- Thiboult, A., Anctil, F., & Boucher, M. A. (2016). Accounting for three sources of uncertainty in ensemble hydrological forecasting. *Hydrol. Earth Syst. Sci.*, 20(5), 1809-1825. doi:10.5194/hess-20-1809-2016
- Thirel, G., Andréassian, V., Perrin, C., Audouy, J. N., Berthet, L., Edwards, P., . . . Vaze, J. (2015). Hydrology under change: an evaluation protocol to investigate how hydrological models deal with changing catchments. *Hydrological Sciences Journal*, 60(7-8), 1184-1199. doi:10.1080/02626667.2014.967248
- Trenberth, K. E. (1992). *Climate system modeling*. Cambridge ; New York: Cambridge University Press.
- Troin, M., Poulin, A., Baraer, M., & Brissette, F. (2016). Comparing snow models under current and future climates: Uncertainties and implications for hydrological impact studies. *Journal of hydrology*, 540, 588-602. doi:<http://dx.doi.org/10.1016/j.jhydrol.2016.06.055>

- Trudel, M., Doucet-Généreux, P.-L., & Leconte, R. (2017). Assessing River Low-Flow Uncertainties Related to Hydrological Model Calibration and Structure under Climate Change Conditions. *Climate*, 5(1), 19.
- Uppala, S. M., Kållberg, P., Simmons, A., Andrae, U., Bechtold, V. d., Fiorino, M., . . . Kelly, G. (2005). The ERA-40 re-analysis. *Quarterly Journal of the Royal Meteorological Society*, 131(612), 2961-3012.
- Veijalainen, N., Lotsari, E., Alho, P., Vehviläinen, B., & Käyhkö, J. (2010). National scale assessment of climate change impacts on flooding in Finland. *Journal of hydrology*, 391(3), 333-350.
- Velázquez, J., Anctil, F., & Perrin, C. (2010). Performance and reliability of multimodel hydrological ensemble simulations based on seventeen lumped models and a thousand catchments. *Hydrology and Earth System Sciences*, 14(11), 2303-2317.
- Vormoor, K., Lawrence, D., Schlichting, L., Wilson, D., & Wong, W. K. (2016). Evidence for changes in the magnitude and frequency of observed rainfall vs. snowmelt driven floods in Norway. *Journal of hydrology*, 538(Supplement C), 33-48. doi:<https://doi.org/10.1016/j.jhydrol.2016.03.066>
- WDR. (2016). *World Disasters Report. Resilience: saving lives today, investing for tomorrow*. International Federation of Red Cross and Red Crescent Societies, Geneva, 264 pp.
- Wehner, M., Arnold, J., Knutson, T., Kunkel, K., & LeGrande, A. (2017). Droughts, floods, and hydrology.
- Wilby, R. L. (2005). Uncertainty in water resource model parameters used for climate change impact assessment. *Hydrological processes*, 19(16), 3201-3219.
- Wilby, R. L., & Dessai, S. (2010). Robust adaptation to climate change. *Weather*, 65(7), 180-185.
- Wilby, R. L., Wigley, T., Conway, D., Jones, P., Hewitson, B., Main, J., & Wilks, D. (1998). Statistical downscaling of general circulation model output: a comparison of methods. *Water resources research*, 34(11), 2995-3008.
- Yue, S., Ouarda, T. B. M. J., Bobée, B., Legendre, P., & Bruneau, P. (1999). The Gumbel mixed model for flood frequency analysis. *Journal of hydrology*, 226(1), 88-100. doi:[https://doi.org/10.1016/S0022-1694\(99\)00168-7](https://doi.org/10.1016/S0022-1694(99)00168-7)
- Zhao, F., Zhang, L., Chiew, F. H. S., Vaze, J., & Cheng, L. (2013). The effect of spatial rainfall variability on water balance modelling for south-eastern Australian catchments. *Journal of hydrology*, 493(Supplement C), 16-29. doi:<https://doi.org/10.1016/j.jhydrol.2013.04.028>